

ABSTRACT

LIANG, SHUANG. Partitioning and Extraction into Perfluorinated-Alcohol Induced Coacervates. (Under the direction of Dr. Morteza G. Khaledi).

During the past three decades, Aqueous Two Phase Systems (ATPS) have been widely utilized for extraction and separation of biological mixtures, especially for industrial large-scale downstream processes in biotechnology. Comparing to traditional water-organic solvent systems, ATPS are more environmental friendly, less toxic and cheaper. Recently, it was discovered in this laboratory that perfluorinated-alcohols and acids can induce coacervation and phase separation in the aqueous solutions of a wide range of amphiphilic molecules; including various types of surfactants (ionic, nonionic, and zwitterionic). The coacervate phase is highly enriched with the surfactant while the other aqueous phase is surfactant-poor. The goals of this thesis are to study the interactive nature of perfluorinated-Alcohol Induced Coacervate (PFAIC) systems, their ability to extract proteins, as well as development of strategies for recovery of extracted proteins from the coacervate samples through back extraction or removal of surfactant. Optical images of surfactant-rich phases were obtained by light microscopy, showing a great number of spherical shape structures in surfactant-rich phase. Different types of dyes were selected as probes to visualize the interaction between the dyes and the coacervate phases. Partition coefficients of the dyes in different PFAIC systems were determined. Both hydrophobic and electrostatic interactions play significant roles in solute extraction into coacervate phases. The partitioning patterns of two model proteins, bovine serum albumin and cytochrome c in different PFAIC systems were investigated. The studies included simple PFAIC composed of a single surfactant as well as complex PFAIC that comprised a mixture of an anionic and a cationic surfactant. The

use of both cationic and anionic surfactant based gel electrophoresis for protein recovery and separation from the coacervate phase was examined. Several strategies for removal of surfactants and recovery of the extracted proteins were investigated. These included precipitation of the cationic complex in complex PFAIC systems through evaporation of HFIP as well as lowering the temperature, dialysis, use of size-exclusion spin columns (also known as Filter-Aided Sample Preparation (FASP) method), and solubilizing and back extraction into urea. The FASP method was proved to be effective in removing the surfactants from the coacervate phases and recovery of protein samples for LC-MS analysis.

© Copyright 2013 by Shuang Liang

All Rights Reserved

Partitioning and Extraction into Perfluorinated-Alcohol Induced Coacervates

by
Shuang Liang

A thesis submitted to the Graduate Faculty of
North Carolina State University
in partial fulfillment of the
requirements for the degree of
Master of Science

Chemistry

Raleigh, North Carolina

2013

APPROVED BY:

Dr. Edmond F. Bowden

Dr. Robert M. Kelly

Dr. Morteza G. Khaledi

Committee Chair

BIOGRAPHY

I was born in Zhuzhou, China, in the year of 1986. I completed my Bachelor of Science degree in Chemistry from University of Science and Technology of China in 2009. During my junior year in college I worked in the lab of Dr. Qingxiang Guo as an undergraduate research assistant and for the first time, savored the joy of thinking like a real scientist. In the fall of 2010, I joined the Department of Chemistry here at NC State University to pursue my Master degree. Since then, with the guidance and encouragement from my advisor Dr. Morteza G. Khaledi, I dived into the world of coacervate.

ACKNOWLEDGMENTS

I would like to thank Dr. Morteza G. Khaledi for providing me the opportunity to study in his lab, especially for his guidance and encouragement throughout my graduate study, and the compassion and support he offered to me when I was going through difficult times. I am also totally obliged to Dr. Gufeng Wang and Dr. David Muddiman for their passion, support and guidance for our collaborative projects.

I thank the current and former lab members of Khaledi lab: Sam, Chris, Mahboubeh , Nathan, James who provided tremendous help and stimulating suggestions to my research, and Marissa who assisted me as an undergraduate researcher; I also would like to acknowledge the members of our department, especially Luyang Zhao and Bhanu Neupane in Wang's lab for discussion and instrument operation with microscope; Emine Gokce in Muddiman's lab for dedicating her time in problem discussion and running Mass Spec experiments; Zhixia Ye in Williams's lab for giving advice in gel electrophoresis, Le Li in Smirnov's lab for help in dialysis experiment, as well as many other friends, Luyan He, Jia Liu, Jieqi Wang, Lingjiao Qi, Junjie Zhao for their friendship and support during my graduate study. I am also very grateful to the support I received from outside the department.

I want to thank especially Simon Lappi who was working in the Nanochemistry Laser and Vibrational Spectroscopy Laboratory for his assistance with ATR-IR work.

Finally, this thesis is dedicated to my family, my parents and grandparents, whose unconditional support has sustained me through difficult moments; and to my dear husband Yesu, whose unwavering love always motivates me to accomplish this thesis.

TABLE OF CONTENTS

LIST OF TABLES	vii
LIST OF FIGURES	viii
Chapter 1	1
Introduction.....	1
Coacervation	1
Representation and Structure of Coacervates	1
Complex and Simple Coacervation	3
Coacervation in Aqueous Solution of Biopolymers	3
Polymer-based ATPS.....	4
Cloud Point Systems (CPS)	5
Protein separation by ATPS.....	5
Perfluorinated-alcohol Induced Coacervates (PFAIC)	7
Outline of the thesis	10
References.....	12
Chapter 2.....	19
Probing a Complex Perfluoro-Alcohol Induced Coacervates by Dye Extraction and Optical Microscopy: SDS-CTAB-HFIP System	19
Abstract.....	19
Introduction.....	21
Experimental Section.....	22
Materials	22
Methods.....	22

Results and Discussion	26
Chemical Composition of Complex PFAIC Phase	27
Chemical Composition of Coacervates and Partitioning Patterns	34
Microscopy Imaging	41
Conclusion	48
References	50
Supplemental Data	52
Chapter 3	54
Partitioning of Proteins in Perfluorinated Alcohols Induced Coacervates	54
Abstract	54
Introduction	55
Experimental Section	57
Materials	57
Methods	57
Results and Discussion	60
Conclusion	67
References	68
Supplemental Data	72
Chapter 4	82
Extraction of Proteins in Perfluorinated Alcohols Induced Coacervates: Strategies for Removal of Surfactants, Gel Electrophoresis, and LC-MS Analysis for Peptide Mapping ...	82
Abstract	82
Introduction	83
Materials	85

Methods.....	86
Gel Preparation for DTAB-PAGE	86
Extraction and recovery of BSA from complex coacervate	86
Extraction of proteins mixture by different PFAIC systems and examined by SDS- PAGE	87
Removal of surfactants from PFAIC phase	88
Surfactant Removal for LC-MS Analysis.....	89
Results and Discussion	91
Direct Introduction of Coacervate Sample in PAGE.....	91
The effect of HFIP on SDS-PAGE	95
Extraction of protein mixtures in ATPSs followed by FASP clean-up method	99
Membrane protein extraction by ATPSs combined with nano LC-MS/MS detection .	102
Conclusion	108
References.....	110
Supplemental Data	112

LIST OF TABLES

Table 2-1. Concentrations and standard deviations of HFIP and H ₂ O in coacervate phase at different wavenumbers.....	36
Table 2-2. Comparison of Partition coefficient of Nile Red, 6-carboxyfluorescein, Rhodamine 6G and Methylene Blue in different ATPS	39
Table 2-3. Data of quantitation analysis of total surfactant concentration	52
Table 3-1. Composition of tube 1-6 in Figure 3-4 and observation.....	61
Table 3-2. Partition coefficients and Extraction Parameters of BSA in simple PFAIC	64
Table 3-3. SDS-HCl-HFIP acid induced cloud point two phase system	77
Table 3-4. Observation of cytochrome c extraction in SDS/HCl/HFIP system	78
Table 3-5. Observation of cytochrome c extraction in CTAB-HFIP-Tris system.....	79
Table 4-1. Abundance ratio between bacteriorhodopsin and BSA calculated from the most abundant peptide peaks for each protein.....	107

LIST OF FIGURES

Figure 1-1. General schematic diagram of coacervation	2
Figure 1-2. (a)Light microscopy image of Gemini coacervate droplets; (b)Schematic drawing of the sponge phase.....	2
Figure 1-3. Light microscopy image of complex coacervate phase of 10% 1:1 SDS : CTAB, 15% v/v HFIP	8
Figure 1-4. Schematic of stabilization of cationic surfactants with fluoro-alcohols A) TFE and B)HFIP	10
Figure 2-1. Quantitation of total surfactants aggregated in coacervate phase	29
Figure 2-2. ATR-FTIR spectrum for HFIP in water (v/v)	29
Figure 2-3. ATR-FTIR spectra of coacervate phases induced by 9% (v/v) and 27% (v/v) HFIP, 100mM 1:1SDS/CTAB	30
Figure 2-4. ATR-FITR spectra of coacervate at different surfactant concentration.....	33
Figure 2-5. Calibration curve for quantitation of water concentration in coacervates on ATR-FTIR water peak around 1640cm ⁻¹	35
Figures 2-6, 2-7, 2-8, 2-9. Extraction of inorganic ions	40
Figure 2-10, 2-11, 2-12, 2-13, 2-14. Optical microscopy images of complex coacervates	43
Figure 2-15, 2-16. 3D image of a spherical micro-droplet in coacervate phase.....	44
Figure 2-(17-27). Optical microscopy images for coacervates at different compositions.....	47
Figure 2-28. Precipitation of surfactants by adding organic solvents.....	53
Figure 2-29. HFIP calibration curve v/v	53
Figure 3-1. Structure of DMMAPS	58
Figure 3-2. Scheme of preparation of complex or simple coacervate samples to extract proteins.....	58

Figure 3-3. Calibration curves of BSA in both Aq and coacervate phase made of 66.7mM total concentration of CTAB-NaOH- 25% v/v HFIP	59
Figure 3-4. Extraction of cytochrome c with different composition of SDS-CTAB HFIP	61
Figure 3-5. Extraction of cytochrome c with addition of NaOH or HCl in complex PFAIC .	63
Figure 3-6. Experimental linear relationship between 1/CF and 1/R	65
Figure 3-7. Calibration curve of BSA in Aqueous phase of 1:1 100mMSDS:100mM CTAB, 10% v/v HFIP complex coacervation	72
Figure 3-8. Calibration curve of BSA in coacervate phase of 1:1 100mM SDS:100mM CTAB, 10% v/v HFIP complex coacervation.....	72
Figure 3-9. Calibration curve of BSA in Aqueous phase of 1:1 50mMSDS:50mMCTAB, 10% v/v HFIP complex coacervation	72
Figure 3-10. Calibration curve of BSA in coacervate phase of 1:1 50mM SDS:50mM CTAB, 10% v/v HFIP complex coacervation	73
Figure 3-11. Calibration curve of BSA in Aqueous phase of 1:1 20mMSDS:20mMCTAB, 10% v/v HFIP complex coacervation	73
Figure 3-12. Calibration curve of BSA in coacervate phase of 1:1 20m MSDS:20mM CTAB, 10% v/v HFIP complex coacervation	73
Figure 3-13. Calibration curve of BSA in Aq phase of 1:1 100mMCTAB:100mM NaOH, 25% v/v HFIP simple ATPS	74
Figure 3-14. Calibration curve of BSA in coac phase of 66.7mMCTAB in 66.7mM NaOH, 25% v/v HFIP simple ATPS	74
Figure 3-15. Calibration curve of BSA in coacervate phase of 50mM CTAB in 0.195M Tris buffer with 10% v/v HFIP.....	74
Figure 3-16. Calibration curve of BSA in coacervate phase of 50mM DMMAPS in 10% v/v HFIP	75
Figure 3-17. Calibration curve of BSA in coacervate phase of 50mM SDS in 4M HCl, 10% v/v HFIP	75

Figure 3-18. Calibration curve of BSA in Aq phase of 50mM SDS in 4M HCl, 10% v/v HFIP	75
Figure 3-19 Calibration curve of BSA in Aq phase of 0.45M Na ₂ SO ₄ in 10% v/v HFIP.....	76
Figure 3-20 Calibration curve of BSA in bottom phase of 0.45M Na ₂ SO ₄ in 10% v/v HFIP	76
Figure 3-21. Emission Spectrum of BSA in coacervate phase of 50mM CTAB in 0.195M Tris buffer, 10% v/v HFIP. Excitation wavelength is 280nm.	80
Figure 3-22. Emission spectra of BSA standard solutions in the Aq phase of CTAB-HFIP-NaOH	80
Figure 3-23. Fluorescence spectra of BSA in coacervate sample and standards.....	81
Figure 4-1. Scheme of ATPS preparation, surfactant removal through FASP and analysis followed by Nano LC-MS/MS.....	90
Figure 4-2. SDS-PAGE. BSA extracted into coacervate phase of SDS/CTAB/HFIP without sample treatment.	92
Figure 4-3A. DTAB-HFIP coacervate applied to DTAB-PAGE	94
Figure 4-3B. CTAB-HFIP coacervate applied to DTAB-PAGE.....	94
Figure 4-4. SDS-PAGE, extraction of BSA and gramicidin D.....	95
Figure 4-5. SDS-PAGE to study the effect of HFIP on gel	96
Figure 4-6. Recovery of BSA from complex coacervate phase applied onto SDS-PAGE.....	97
Figure 4-7. SDS-PAGE of protein mixture extracted by 6 different ATPSs.....	101
Figure 4-8. Sample images of extracted bacteriorhodopsin in HFIP and four ATPSs	102
Figure 4-10. Example TIC for a sample where SDS is not properly removed.....	106
Figure 4-9. Total ion Chromatograms of four ATPSs, SDS/HCl/HFIP, CTAB/HFIP, Na ₂ SO ₄ /HFIP and DMMAAPS/HFIP, of extracted BSA and bacteriorhodopsin.....	104
Figure 4-11. Selected Ion Chromatograms for the most abundant BR and BSA Peptides...	106

Figure 4-12. Total Ion Chromatogram with bacteriorhodopsin identified in CTAB-HFIP extraction..... 112

Figure 4-13. Matched peptides fragments of bacteriorhodopsin digested by trypsin identified. 113

Figure 4-14. Extracted Ion Chromatograms and FTMS spectra for identified BR peptide1 113

Figure 4-15. Extracted Ion Chromatograms and FTMS spectra for identified BR peptide2 114

Figure 4-16. Extracted Ion Chromatograms and FTMS spectra for identified BR peptide3 115

Chapter 1

Introduction

Coacervation

The phenomenon of “unmixing” liquid-liquid layers in aqueous solutions of amphiphilic compounds has been observed and investigated as early as 1900s, and the word “coacervation” was firstly introduced in 1929 by Bungenberg de Jong and Kruyt[1] to describe this phenomenon in colloid systems. The word “coacervation” is derived from the Latin prefix “co” which means “together”, and “acervus” which means “a heap”. The term coacervation implies aggregation of colloidal particles which form a stable separate phase, immiscible from another liquid phase which is lean in colloids. Typically, coacervates are divided into complex and simple categories. Complex coacervates are composed of two oppositely charged surfactants[2][3] [4], polymers[5] [6], or proteins/polysaccharides[7][8], which result in formation of a coacervate phase upon electrostatic interaction . Simple coacervates are commonly made of single amphiphilic molecule or two similarly charged amphiphiles.

Representation and Structure of Coacervates

The formation of coacervates involves aggregation of amphiphilic molecules that results in phase separation in the solvent, typically water. Simple coacervation and subsequent phase separation is induced by addition of salt[9][10] or alcohol[11], changes in pH[12], or in temperature[13][14].

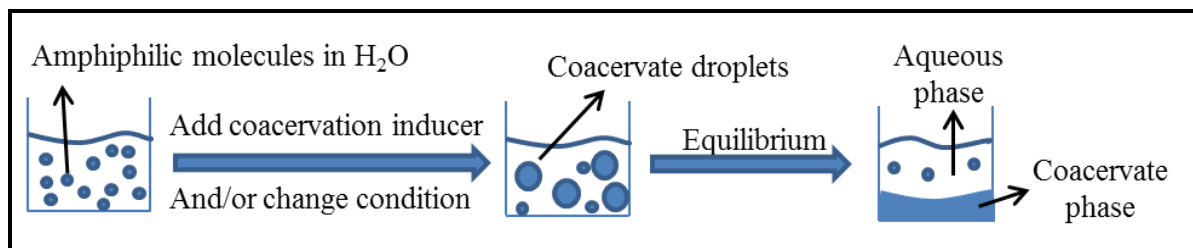
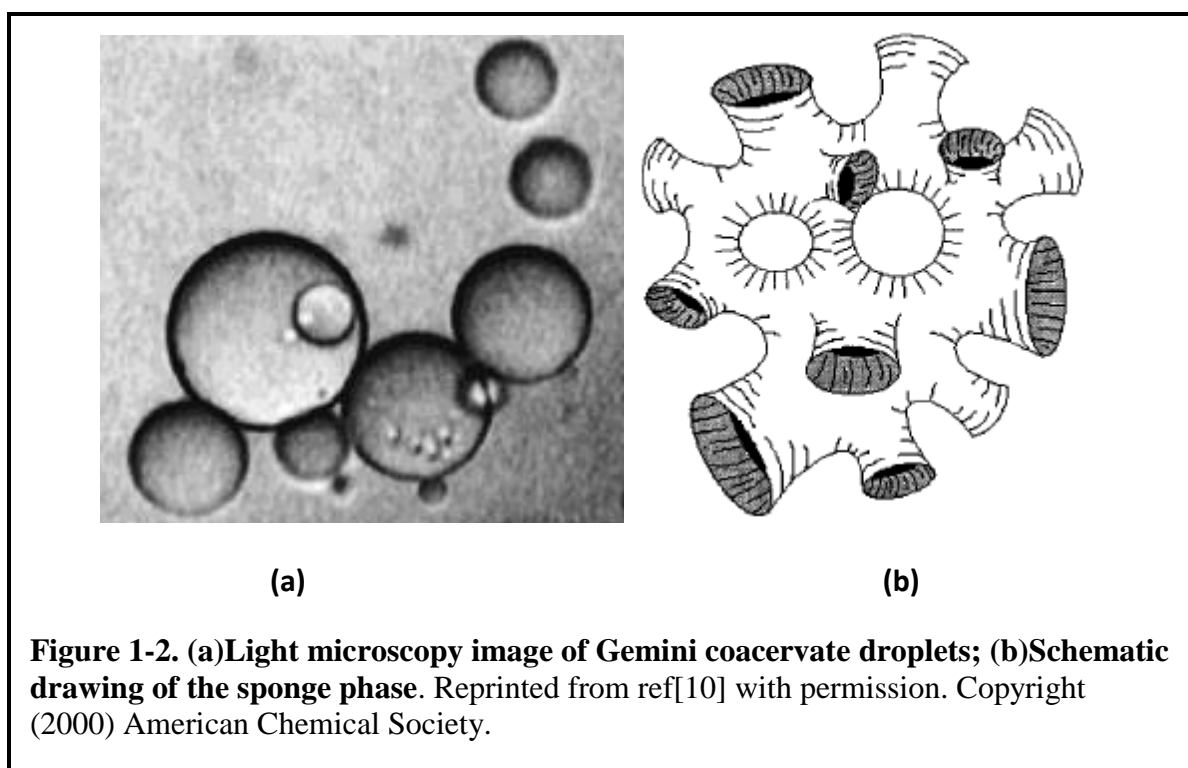


Figure 1-1. General schematic diagram of coacervation



Menger *et al.*[10] have investigated the structure of a simple coacervate phase made of a zwitterionic Gemini surfactant in water. A light microscopy picture of the simple coacervate

phase is shown in Figure 1-2a. The size of those droplets varies from 10 to 300 μm as shown in the microscopy image. The sponge-like structure in Figure 1-2b illustrates the presence of pores inside the droplets microstructure. The cryo-HRSEM experiments have been performed to detect surface structure of the coacervate droplets, showing porous morphology on the surface, ranging from 25 to 125nm, with water occupying inside the pores.

Complex and Simple Coacervation

Coacervation in Aqueous Solution of Biopolymers

One example of complex coacervation is aqueous solutions of gelatin, a protein with the isoelectric point (IEP) of between 3.8-4.4 and gum arabic, which is a mixture of glycoproteins and polysaccharides with a more acidic IEP of around 1. At pH values between the two IEP of gelatin and gum Arabic, coacervation occurs due to electrostatic interaction between the positively charged gelatin and the negatively charged gum arabic[1]. On the other hand, addition of alcohols to the aqueous gelatin solution induces simple coacervation[15]. With the addition of alcohol, hydrogen bonding interaction between water and alcohol is more favorable than water-gelatin interaction. This leads to aqueous phase separation; with one phase that is rich and the other one lean in gelatin. Both simple and complex coacervation present potential advantages in protein extraction and purification[16][17], as well as encapsulation in drug or food industry[18][19].

In addition to protein-polysaccharides coacervation, other complex coacervation such as protein-polyelectrolytes has been studied by Dubin *et. al*[20][21], using models for protein-

polyelectrolyte complex (e.g. BSA-PMA) to investigate selective phase separation by adjusting pH or ionic strength of the system. Moreover, DNA as the target macromolecule has also been reported to form complex coacervate with cationic or zwitterionic amphiphiles. For instance, the use of complexation between a cationic polymer, PDMAPS[22], and DNA is reported as a as DNA catching/releasing system. Also complexation between DNA and cationic surfactant CTAB[23] is reported for preparation of DNA gel particles.

Polymer-based ATPS

A popular ATPS is composed of mixture of aqueous solutions of polyethylene glycol (PEG) and dextran that demix in with each polymer enriched in separate aqueous phases. The upper phase is concentrated with more hydrophobic PEG and lower phase mostly consists of dextran. Less polar and more hydrophobic proteins will partition into the top PEG phase while more polar and hydrophilic proteins will prefer the lower dextran phase[24]. Water is the major component in both phases which provides low interfacial tensions[25] and a friendly environment for biomolecules[27]. Different molecular weights of PEG and dextran have an impact on partitioning behavior of molecules due to polymers hydrophobicity differences. The greater the differences of hydrophobicity between the two polymers, the easier the polymers solutions demix and form separate phases. The PEG-dextran system is one of the most commonly used ATPS that has been applied in scale up processing of biomaterials[27].

Cloud Point Systems (CPS)

Another group of ATPS is composed of nonionic or zwitterionic surfactants. Aqueous solutions of surfactants undergo phase separation upon reaching their cloud point temperature (CPT) [13][14]. At the CPT, the aqueous solutions of nonionic surfactants become cloudy and phase separation begins with the formation of small droplets. Above the CPT, two clear phases can be observed, with one phase containing high concentration of the surfactant and the other aqueous phase is mostly depleted of the surfactant. For the zwitterionic surfactants, cloud point phase separation is often occurs upon lowering the temperature. Furthermore, aqueous solutions of certain cationic or anionic surfactants can go through the cloud point separation with addition of salts or strong acids as reported by Kaler and co-workers [28] and Pérez-Bendito et.al. [29].

Protein separation by ATPS

As compared to traditional organic solvent-water extraction systems, both simple and complex coacervates systems serve as safer and more environmentally benign alternatives. Most coacervates are aqueous based and can also be categorized as Aqueous Two Phase Systems (ATPS). There are a variety of ATPS made of different types of amphiphilic molecules. [46][47]. Due to the high concentration of water in both layers, ATPS have advantages[48][49][50] in separation, extraction and purification of biological materials, providing a mild environment to maintain the bioactivity and a low interfacial tension which results in an efficient mass transfer. Moreover, ATPS methods are well adapted for large-

scale application by using currently available commercial equipment for water-organic systems.

The applications of both polymer-based ATPS and CPS for extraction and purification of biomaterials have been widely reported and reviewed [25][30][31][32]. Examples include separation and extraction of biomolecules such as DNA[33], proteins[34], cells[32], organisms, [35], etc.. The most widely reported applications of various ATPS focus on separation and extraction of proteins [16][20][21][36][37][38]. Among them, polymer-ATPS can be induced by biomolecule-polyelectrolyte aggregation, two oppositely charged polyelectrolytes, as well as weakly/asymmetrically charged polyion-colloidal systems. The phase separation can be induced under particular pH or ionic strength of solution. The net charge on proteins would be different under different pH environment, depending on their isoelectric points. The extent of proteins interactions with a given phase varies depending on the proteins charge and chemical composition of the ATPS. Thus, pH could be used to manipulate extraction selectivity. Hydrophobic interaction with the amphiphilic-rich phases is the main driving force in extracting target proteins in polymer-ATPS and CPS. Bordier[38] first used Triton X-114 to show the selectivity of cloud point system in separating hydrophobic integral membrane proteins from hydrophilic and amphiphilic proteins as the membrane proteins are primarily solubilized in the surfactant-rich phase while the water soluble proteins are mostly in the surfactant-lean phase.

A key limitation for both polymer-ATPS and CPS is poor extraction selectivity. The nonionic or zwitterionic surfactants in CPS or nonionic polymers that form ATPS have very similar solvation properties. Both systems lack charged and hydrogen bond donor groups that could

provide selective interactions with biomacromolecules, especially proteins. Several factors such as the size or molecular weight of the polymers in ATPS, concentration of the amphiphile, ionic strength, or pH could also have significant influence on protein partitioning between aqueous two-phases[40].

One successful example of protein extraction in polymer-ATPS is separation of tPA (tissue plasminogen activator) from cell components in PEG/phosphate[37]. As a very hydrophobic protein, tPA is more attracted to polymer-rich phase in PEG/phosphate in ATPS and shows high partition coefficient (100-1000) between the two phases. Both pH and NaCl were adjusted to obtain high recovery factor[37]. The molecular weight of PEG can also be optimized the partitioning. The challenge in such extraction process is the difficulty in back extraction of the hydrophobic protein from the PEG phase to another phase for tPA recovery. Addition of organic solvent and modification of pH can be used to enhance interaction of the hydrophobic protein with the water-based environment and, thus improving solubility and back extraction efficiency.

Perfluorinated-alcohol Induced Coacervates (PFAIC)

Khaledi *et al.* have recently reported that water-miscible perfluorinated alcohol and acids induce simple and complex coacervation in aqueous solutions of a wide variety of individual and mixed amphiphiles [41]. The amphiphilic molecules include cationic, anionic, zwitterionic, nonionic surfactants, phospholipids, bile salts, and polyelectrolytes. In Figure 1-3, a light microscopy image of a SDS-CTAB-HFIP coacervate phase is shown, indicating

high population of microstructure with size varying from 1-8 μm . The mechanism for formation of PFAIC is still unknown which might be different for simple and complex coacervation.

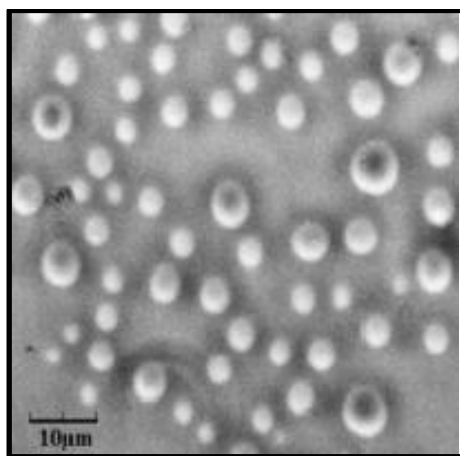


Figure 1-3. Light microscopy image of complex coacervate phase of 10% 1:1 SDS : CTAB, 15% v/v HFIP. Reprinted from ref[41] with permission. Copyright (2013) American Chemical Society.

Other types of coacervate phases and polymer-ATPS contain very high water concentration (e.g. up to 95% w/w) [10] while the PFAIC contain only about 5-35% w/w water in the coacervate phase depending on the composition of constituent components. Moreover, the coacervates are highly enriched with the perfluorinated alcohol (*coacervator*) with concentrations as high as ~40%-50% w/w (as weight percentage in coacervate phase). A

hypothesis for coacervation mechanism involves dehydration of the alkyl chains of the amphiphiles by the fluorinated groups that leads to aggregation and aqueous phase separation. As a result, the amphiphile-rich coacervates have an enriched-HFIP micro-environment where water is repelled into the amphiphile-lean aqueous phase.

Perfluorinated alcohols such as 1,1,1,3,3,3-hexafluoro-2-propanol (HFIP) have attracted much attention in investigating proteins properties because of their ability to stabilize secondary structures in proteins and peptides. At low concentrations HFIP molecules form micelle-like clusters in HFIP-water mixtures due to hydrophobic interactions between fluorine groups. [42][43]. It is believed that the HFIP clusters provide a more hydrophobic microenvironment surrounding the peptides that has a dehydration effect and subsequent enhancement of stabilization of the α helix structure in proteins and unfolded peptides[44].

Jenkins reported that aliphatic alcohols and other classes of perfluorinated reagents did not induce coacervation in mixtures of complex cationic surfactants. Thus, the presence of both the fluorine groups and the strong hydrogen bond donor hydroxyl or carboxylic groups in perfluorinated alcohols and acids would be necessary for coacervate formation. In addition to the dehydration effect of the fluorine groups, it is hypothesized that the hydroxyl group in perfluorinated alcohols would interact with the charged head groups of the surfactants and facilitates formation of coacervation and phase separation (Fig. 1-4).

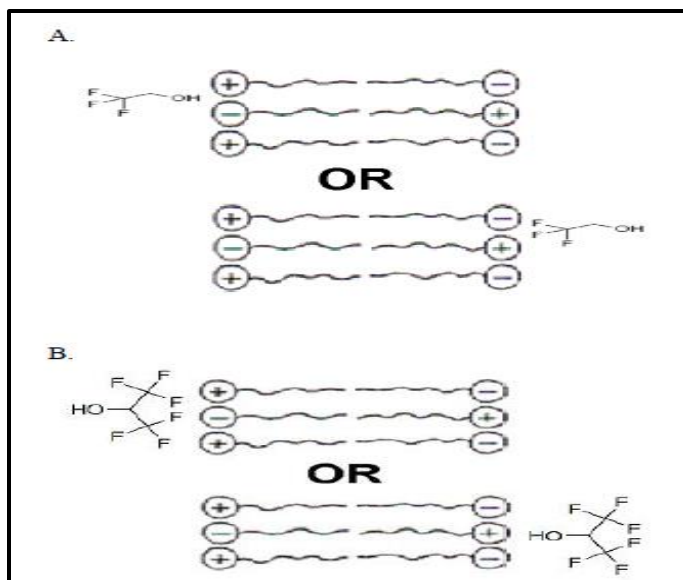


Figure 1-4. Schematic of stabilization of cationic surfactants with fluoro-alcohols A) TFE and B) HFIP. Reprinted from ref[45] with permission.

Outline of the thesis

This thesis describes the results of three research projects related to the characteristics of coacervates and applications for proteins extraction. In chapter 2, the interactive properties and structures of a complex coacervate of SDS-CTAB-HFIP were probed by both bulk experiments of dye extraction and studies involving light microscopy observation of coacervate structure using various charged and uncharged dyes as probes. Compositional analysis of the above PFAIC was also conducted to better understand the complex coacervate system.

In chapter 3, proteins partitioning patterns and extraction in complex and simple PFAIC were investigated. Several parameters (such as pH, mole fraction of the oppositely charged

surfactants in the complex system, etc) can be used to control proteins interaction with the coacervate phase. Quantitative measurements were performed to determine partition coefficients of proteins and to compare the extraction ability between different systems.

Due to the presence of both cationic and anionic surfactants in the complex coacervate phase, quick recovery of proteins is challenging. Back extraction and dialysis show low recovery efficiency in complex coacervation system. Chapter 4 presents different sample preparation methods for protein recovery in both complex and simple coacervates, which allows further separation and analysis of proteins by LC and mass spectrometry. CTAB-Gel electrophoresis was adapted for protein recovery from coacervates that were made by the cationic surfactant. In order to make the surfactant-rich coacervates compatible with mass spectrometry, surfactants have to be completely prior to LC/MS analysis. The Filter-Aided Sample Preparation method (FASP) [51] was used to successfully remove surfactants from the coacervates after proteins extraction. Gel electrophoresis and MS results implied the success of surfactants removal.

References

- [1] H. G. Bungenberg de Jong and H. R. Kruyt, "Coacervation (Partial Miscibility on Colloid Systems)," *Proc Koninkl Med Akad Watershap*, vol. 32, pp. 849–856, 1929.
- [2] Y. Nan, H. Liu, and Y. Hu, "Aqueous two-phase systems of cetyltrimethylammonium bromide and sodium dodecyl sulfonate mixtures without and with potassium chloride added," *Colloids Surfaces Physicochem. Eng. Asp.*, vol. 269, no. 1–3, pp. 101–111, Nov. 2005.
- [3] P. Weschayanwivat, O. Kunanupap, and J. F. Scamehorn, "Benzene removal from waste water using aqueous surfactant two-phase extraction with cationic and anionic surfactant mixtures," *Chemosphere*, vol. 72, no. 7, pp. 1043–1048, Jul. 2008.
- [4] T. Lu, Z. Li, J. Huang, and H. Fu, "Aqueous Surfactant Two-Phase Systems in a Mixture of Cationic Gemini and Anionic Surfactants," *Langmuir*, vol. 24, no. 19, pp. 10723–10728, Oct. 2008.
- [5] S. S. Singh, A. K. Siddhanta, R. Meena, K. Prasad, S. Bandyopadhyay, and H. B. Bohidar, "Intermolecular complexation and phase separation in aqueous solutions of oppositely charged biopolymers," *Int. J. Biol. Macromol.*, vol. 41, no. 2, pp. 185–192, Jul. 2007.
- [6] U. Sivars, K. Bergfeldt, L. Piculell, and F. Tjerneld, "Protein partitioning in weakly charged polymer-surfactant aqueous two-phase systems," *J. Chromatogr. B. Biomed. Sci. App.*, vol. 680, no. 1, pp. 43–53, 1996.

- [7] C. Schmitt, C. Sanchez, S. Desobry-Banon, and J. Hardy, "Structure and Technofunctional Properties of Protein-Polysaccharide Complexes: A Review," *Crit. Rev. Food Sci. Nutr.*, vol. 38, no. 8, pp. 689–753, Dec. 1998.
- [8] C. G. de Kruif, F. Weinbreck, and R. de Vries, "Complex coacervation of proteins and anionic polysaccharides," *Curr. Opin. Colloid Interface Sci.*, vol. 9, no. 5, pp. 340–349, Dec. 2004.
- [9] F. M. Menger and B. M. Sykes, "Anatomy of a coacervate," *Langmuir*, vol. 14, no. 15, pp. 4131–4137, 1998.
- [10] F. M. Menger, A. V. Peresyphkin, K. L. Caran, and R. P. Apkarian, "A Sponge Morphology in an Elementary Coacervate," *Langmuir*, vol. 16, no. 24, pp. 9113–9116, Nov. 2000.
- [11] B. Mohanty and H. B. Bohidar, "Systematic of alcohol-induced simple coacervation in aqueous gelatin solutions," *Biomacromolecules*, vol. 4, no. 4, pp. 1080–1086, Aug. 2003.
- [12] G. Weiß, A. Knoch, A. Laicher, F. Stanislaus, and R. Daniels, "Simple coacervation of hydroxypropyl methylcellulose phthalate (HPMCP) I. Temperature and pH dependency of coacervate formation," *Int. J. Pharm.*, vol. 124, no. 1, pp. 87–96, Sep. 1995.
- [13] W. L. Hinze and E. Pramauro, "A Critical Review of Surfactant-Mediated Phase Separations (Cloud-Point Extractions): Theory and Applications," *Crit. Rev. Anal. Chem.*, vol. 24, no. 2, pp. 133–177, Jan. 1993.

- [14] F. H. Quina and W. L. Hinze, "Surfactant-Mediated Cloud Point Extractions: An Environmentally Benign Alternative Separation Approach," *Ind. Eng. Chem. Res.*, vol. 38, no. 11, pp. 4150–4168, Nov. 1999.
- [15] B. Mohanty and H. B. Bohidar, "Systematic of alcohol-induced simple coacervation in aqueous gelatin solutions," *Biomacromolecules*, vol. 4, no. 4, pp. 1080–1086, Aug. 2003.
- [16] Y. Wang, J. Y. Gao, and P. L. Dubin, "Protein separation via polyelectrolyte coacervation: Selectivity and efficiency," *Biotechnol. Prog.*, vol. 12, no. 3, pp. 356–362, 1996.
- [17] R. A. Curtis and L. Lue, "A molecular approach to bioseparations: Protein–protein and protein–salt interactions," *Chem. Eng. Sci.*, vol. 61, no. 3, pp. 907–923, Feb. 2006.
- [18] *Microencapsulation: methods and industrial applications*, 2nd ed. New York: Taylor & Francis, 2006.
- [19] L. L. Balassa, G. O. Fanger, and O. B. Wurzburg, "Microencapsulation in the food industry," *C R C Crit. Rev. Food Technol.*, vol. 2, no. 2, pp. 245–265, Jul. 1971.
- [20] P. L. Dubin, J. Gao, and K. Mattison, "Protein Purification by Selective Phase Separation with Polyelectrolytes," *Sep. Purif. Rev.*, vol. 23, no. 1, pp. 1–16, Jan. 1994.
- [21] C. L. Cooper, P. L. Dubin, A. B. Kayitmazer, and S. Turksen, "Polyelectrolyte–protein complexes," *Curr. Opin. Colloid Interface Sci.*, vol. 10, no. 1–2, pp. 52–78, Aug. 2005.

- [22] A. Ohsugi, H. Furukawa, A. Kakugo, Y. Osada, and J. P. Gong, "Catch and Release of DNA in Coacervate-Dispersed Gels," *Macromol. Rapid Commun.*, vol. 27, no. 15, pp. 1242–1246, Aug. 2006.
- [23] M. C. Morán, M. G. Miguel, and B. Lindman, "DNA gel particles," *Soft Matter*, vol. 6, no. 14, p. 3143, 2010.
- [24] *Protein purification methods: a practical approach*. Oxford ; New York: IRL Press at Oxford University Press, 1989.
- [25] A. D. Diamond and J. T. Hsu, "Protein partitioning in PEG/dextran aqueous two-phase systems," *Aiche J.*, vol. 36, no. 7, pp. 1017–1024, Jul. 1990.
- [26] P. A. Albertsson, *Partition of cell particles and macromolecules: separation and purification of biomolecules, cell organelles, membranes, and cells in aqueous polymer two-phase systems and their use in biochemical analysis and biotechnology*, 3rd ed. New York: Wiley, 1986.
- [27] G. Johansson, "Partition of salts and their effects on partition of proteins in a dextran-poly (ethylene glycol)-water two-phase system," *Biochim. Biophys. Acta*, vol. 221, no. 2, pp. 387–390, Nov. 1970.
- [28] S. R. Raghavan, H. Edlund, and E. W. Kaler, "Cloud-Point Phenomena in Wormlike Micellar Systems Containing Cationic Surfactant and Salt," *Langmuir*, vol. 18, no. 4, pp. 1056–1064, Feb. 2002.
- [29] I. Casero, D. Sicilia, S. Rubio, and D. Pérez-Bendito, "An Acid-Induced Phase Cloud Point Separation Approach Using Anionic Surfactants for the Extraction and

Preconcentration of Organic Compounds,” *Anal. Chem.*, vol. 71, no. 20, pp. 4519–4526, Oct. 1999.

- [30] J. A. Asenjo and B. A. Andrews, “Aqueous two-phase systems for protein separation: Phase separation and applications,” *J. Chromatogr. A*, vol. 1238, pp. 1–10, May 2012.
- [31] K. S. M. S. Raghavarao, T. V. Ranganathan, N. D. Srinivas, and R. S. Barhate, “Aqueous two phase extraction-an environmentally benign technique,” *Clean Technol. Environ. Policy*, vol. 5, no. 2, pp. 136–141, Jul. 2003.
- [32] K. Vijayakumar, S. Gulati, A. J. deMello, and J. B. Edel, “Rapid cell extraction in aqueous two-phase microdroplet systems,” *Chem. Sci.*, vol. 1, no. 4, p. 447, 2010.
- [33] I. P. Trindade, M. M. Diogo, D. M. F. Prazeres, and J. C. Marcos, “Purification of plasmid DNA vectors by aqueous two-phase extraction and hydrophobic interaction chromatography,” *J. Chromatogr. A*, vol. 1082, no. 2, pp. 176–184, Aug. 2005.
- [34] T. Saitoh, H. Tani, T. Kamidate, and H. Watanabe, “Phase separation in aqueous micellar solutions of nonionic surfactants for protein separation,” *Trac Trends Anal. Chem.*, vol. 14, no. 5, pp. 213–217, 1995.
- [35] D. M. Morré and D. J. Morre, “Aqueous two-phase partition applied to the isolation of plasma membranes and Golgi apparatus from cultured mammalian cells,” *J. Chromatogr. B. Biomed. Sci. App.*, vol. 743, no. 1, pp. 377–387, 2000.
- [36] Y. Xu, M. Mazzawi, K. Chen, L. Sun, and P. L. Dubin, “Protein Purification by Polyelectrolyte Coacervation: Influence of Protein Charge Anisotropy on Selectivity,” *Biomacromolecules*, vol. 12, no. 5, pp. 1512–1522, May 2011.

- [37] C. Hodgson, B. A. Andrews, V. Riveros-Moreno, and J. A. Asenjo, "PARTITIONING AND SEPARATION OF tPA (TISSUE PLASMINOGEN ACTIVATOR) IN AQUEOUS TWO-PHASE SYSTEMS," presented at the 7th International Conference on Partitioning in ATPSs, New Orleans, USA, 1991.
- [38] C. Bordier, "Phase separation of integral membrane proteins in Triton X-114 solution," *J. Biol. Chem.*, vol. 256, no. 4, pp. 1604–1607, Feb. 1981.
- [39] V. S. Starova and S. A. Kulichenko, "Preconcentration of proteins using modified micellar phases of sodium dodecyl sulfate," *J. Anal. Chem.*, vol. 65, no. 12, pp. 1215–1220, Dec. 2010.
- [40] J. A. Asenjo and B. A. Andrews, "Aqueous two-phase systems for protein separation: A perspective," *J. Chromatogr. A*, vol. 1218, no. 49, pp. 8826–8835, Dec. 2011.
- [41] M. G. Khaledi, S. I. Jenkins, and S. Liang, "Perfluorinated Alcohols and Acids Induce Coacervation in Aqueous Solutions of Amphiphiles," *Langmuir*, vol. 29, no. 8, pp. 2458–2464, Feb. 2013.
- [42] K. Yoshida, T. Yamaguchi, T. Adachi, T. Otomo, D. Matsuo, T. Takamuku, and N. Nishi, "Structure and dynamics of hexafluoroisopropanol-water mixtures by x-ray diffraction, small-angle neutron scattering, NMR spectroscopy, and mass spectrometry," *J. Chem. Phys.*, vol. 119, p. 6132, 2003.
- [43] B. Czarnik-Matuszewicz, S. Pilorz, L. P. Zhang, and Y. Wu, "Structure of hexafluoroisopropanol–water mixture studied by FTIR-ATR spectra and selected chemometric methods," *J. Mol. Struct.*, vol. 883, pp. 195–202, 2008.

- [44] D.-P. Hong, M. Hoshino, R. Kuboi, and Y. Goto, "Clustering of Fluorine-Substituted Alcohols as a Factor Responsible for Their Marked Effects on Proteins and Peptides," *J. Am. Chem. Soc.*, vol. 121, no. 37, pp. 8427–8433, Sep. 1999.
- [45] S. I. Jenkins, "Novel Aqueous Two-Phase Systems: Characterization and Applications in Chemical Separation," PhD Dissertation, North Carolina State University, 2011.
- [46] J. X. Xiao, U. Sivars, and F. Tjerneld, "Phase behavior and protein partitioning in aqueous two-phase systems of cationic–anionic surfactant mixtures," *J. Chromatogr. B. Biomed. Sci. App.*, vol. 743, no. 1, pp. 327–338, 2000.
- [47] C.-L. Liu, Y. J. Nikas, and D. Blankschein, "Novel bioseparations using two-phase aqueous micellar systems," *Biotechnol. Bioeng.*, vol. 52, no. 2, pp. 185–192, Mar. 2000.
- [48] R. Hatti-Kaul, "Aqueous two-phase systems," *Mol. Biotechnol.*, vol. 19, no. 3, pp. 269–277, 2001.
- [49] *Partitioning in aqueous two-phase systems: theory, methods, uses, and application to biotechnology*. Orlando: Academic Press, 1985.
- [50] H.-E. Åkerlund, "Partition by Countercurrent Distribution (CCD)," in *Aqueous Two-Phase Systems*, vol. 11, New Jersey: Humana Press, pp. 55–64.
- [51] J. R. Wiśniewski, A. Zougman, N. Nagaraj, and M. Mann, "Universal sample preparation method for proteome analysis," *Nat. Methods*, vol. 6, no. 5, pp. 359–362, Apr. 2009.

Chapter 2

Probing a Complex Perfluoro-Alcohol Induced Coacervates by Dye

Extraction and Optical Microscopy: SDS-CTAB-HFIP System

Abstract

Water-miscible perfluorinated alcohols have been found to induce complex coacervation with mixed cationic and anionic surfactants in aqueous solutions[1]. 1,1,1,3,3,3-hexafluoropropanol (HFIP) is one of the most powerful inducers of coacervates in aqueous solutions of amphiphiles. The goal of this paper is to investigate the complex coacervate composed of *catanionic* amphiphiles, namely mixtures of the anionic SDS and cationic CTAB, which are the most commonly used surfactants for solubilization, denaturation/refolding, cleaning and hygiene purposes. The characterization and analysis of the novel aqueous two phase system (ATPS) have been investigated in this paper. We also studied partitioning behavior of four different dyes with negative, neutral and positive charge respectively. Partition coefficients of the model dyes were determined at different chemical compositions of coacervates, namely mole ration of SDS/CTAB, total concentration of surfactants, as well as %HFIP. The partition coefficient for the neutral and positively charged dyes were much higher in coacervate systems made of equimolar SDS-CTAB (1:1 mole ratio) than at other mole ratios at all total concentration of surfactants. The negatively charged dye has greater affinity toward the cationic-rich system made of 3:7 SDS-CTAB,

indicating strong electrostatic interaction. Partition coefficient decreases with increasing initial HFIP concentration. ATR-IR data shows that concentration of HFIP in coacervate phase only changes by 3% when increasing initial HFIP% from 9% to 27% (v/v), while water concentration increases dramatically. Moreover optical microscopy with different dyes was used to probe the microscopic structure of the coacervate and aqueous phases.

Key words: ATPS, coacervation, HFIP, SDS, CTAB, dye, microscopy.

Introduction

The applications of coacervates have been expanded to commercial encapsulation of drugs [2][3] as well as effective extraction and separation approaches [4][5]. “Coacervation” was firstly introduced by Bungenberg de Jong and Kruyt in 1929[6] to describe the mixing and aggregating phenomena of amphiphilic molecules. In their paper, the aqueous solution is separated into two immiscible liquid phases where one is rich in amphiphilic molecules and the other is poor in amphiphiles. During this process, hydrophobic, electrostatic, steric effects and hydrogen bonding interactions could contribute to formation of self-assembling structures such as micelles, vesicles, gel and coacervates[7]. However, coacervation leads to phase separation in aqueous media. [8]. Recently, we reported perfluorinated alcohols/acids induced coacervation (PFAIC), where addition of a small percentage of perfluoro-alcohol/acid can induce coacervation and liquid-liquid phase separation in the aqueous solutions of a broad range of amphiphilic molecules[1]. Among all the novel coacervation systems, complex coacervation firstly called our attention because of interesting phase changes in aqueous solutions of oppositely charged surfactants from turbid solutions (liquid-solid phases) to liquid - liquid phases separation. Generally, complex coacervation occurs in systems containing two oppositely charged amphiphiles with specific molecular structures and/or through changes in pH, ionic strength, temperature, or addition organic modifier. Usually, the complex coacervate phase is rich in both oppositely charged amphiphiles and the aqueous phase is lean in both amphiphiles. Samuel Jenkins in his dissertation[9] studied the phase diagram of coacervation SDS(sodium dodecyl sulfate)/CTAB(cetyl triammonium

bromide)/HFIP(1,1,1,3,3,3-hexafluoropropanol), indicating a wide range of %HFIP(5%-35%) to form coacervation depending on surfactant concentration and mole ratio. Both SDS and CTAB are commonly used detergents. The goal of our study is to characterize the novel ATPS and extraction mechanisms in the complex coacervates composed of two oppositely charged surfactants, the anionic SDS and the cationic CTAB. By mixing these two surfactants, white precipitation will be formed. When HFIP is added into the mixture at a certain percentage, liquid-liquid phase separation occurs. The coacervation shows high flexibility in controlling partitioning selectivity due to electrostatic interaction and hydrogen bonding groups. The self-assembled coacervate phase is found to have microstructures which will also be discussed in this chapter.

Experimental Section

Materials

Sodium dodecyl sulfate (SDS) and cetyltrimethylammonium bromide (CTAB) were purchased from Affymetrix USB Corporation, “Ultrapure” (Cleveland, OH). Dodecyltrimethylammonium bromide (DTAB), 99%, was purchased from Sigma Aldrich. 1,1,1,3,3,3-hexafluoropropanol(HFIP) , $\geq 99\%$, was purchased from TCI America.

Methods

Quantitation of total surfactant content

The total surfactant content was determined by gravimetric analysis for different composition of SDS-CTAB-HFIP system in both aqueous and coacervate phases. 100mM SDS and

100mM CTAB were mixed at mole ratios 1:1, 7:3 and 3:7 with 9%, 18%, 22.5% and 27% v/v HFIP to obtain 1.0 mL total volume of solution (i.e. 455 μ L 100mM SDS and 455 μ L 100mM CTAB and 90 μ L HFIP to make total volume of 1.0mL two phases when coacervates are formed) or total volume of a single phase. The top aqueous phase and bottom coacervate phase were separated after 24 hours equilibration at room temperature. Freeze-drying was used to dry each phase. The mass of surfactants mixture in the aqueous phase or coacervate phase was weighed individually on balance to give the mass of surfactants mixture in each phase, thus calculating distribution of surfactants between two phases.

Analysis of HFIP by Attenuated Total Reflectance-Fourier Transform Infrared (ATR-FTIR)

The crystalline germanium attachment for the ATR-FTIR (Pike Technologies Inc., MIRacle Single Reflection ATR, Madison, WI) was mounted on Bio-Rad (Hercules, CA) Digilab FTS-3000 Fourier transform infrared (FT-IR) spectrometer to perform sample analysis. The narrow band mercury-cadmium-telluride (MCT) detector was cooled by liquid nitrogen for 20min before loading sample. The instrument was purged by dry compressed air all the time during the experiment to eliminate the effect of water in air for spectra. An accumulation of 64 scans was performed to obtain average spectra at room temperature. The data was collected from 0 to 7899 cm^{-1} with a resolution of 1 cm^{-1} and the region between 700 and 1800 cm^{-1} was examined to determine HFIP concentration in coacervates. The coacervate samples of SDS-CTAB-HFIP were prepared by mixing stock solutions 100mM SDS and 100mM CTAB at mole ratio 1:1 with 9% and 27% (v/v) HFIP.

Determination of Partition Coefficients(K)

In order to understand the interactive nature of the coacervates with different chemical compositions, partition coefficients of four fluorescent dyes with different charges were determined using spectrofluorimetry. Partition Coefficient is defined as $K=C_{CA}/C_{Aq}$, where C_{CA} is the concentration of extracting molecules in coacervate phase and C_{Aq} is the corresponding concentration in top aqueous phase. The dyes included neutrally charged Nile Red, negatively charged 6-carboxyfluorescein, and positively charged Rhodamine 6G and Methylene Blue. A small, known amount of each dye was added to 1.0ml five ATPS with different stock surfactant concentrations (100 mM or 273 mM), HFIP concentration (9% or 18%), at mole ratios of (1:1, 3:7 and 7:3) SDS:CTAB, in 1.5ml microcentrifuge tubes. The ATPS containing the dyes were equilibrated for 24 hours on Thermo Scientific Labquake Shaker Rotisserie and the aqueous and coacervate phases were separated after equilibrium. The aqueous and coacervate phases for each system were separated and the concentrations of the dyes in each phase were determined using a HORIBA Scientific spectrofluorometer (FluoroMax-4, Edison, NJ). The partition coefficients were determined from the ratio of dye concentration in coacervate over that of in the corresponding aqueous phase (i.e. $K=[S]_{CA}/[S]_{aq}$). With the exception of one case, all four dyes interacted strongly with all coacervates (i.e. $K \gg 1$) and consequently were enriched in the coacervate phase. Thus, the coacervate phases had to be diluted by a factor of $\times 200$ with 100mM SDS prior to fluorescence measurements.

The excitation and emission wavelengths for the dyes, Nile Red, 6-carboxylfluorecein, Rhodamine 6G and Methylene Blue were 564/642nm, 450/511nm, 531/553nm, 650/673nm

respectively. The calibration curve for aqueous phase was made by preparing standards in blank aqueous phase for each of the dye at each of the water-HFIP composition. The calibration standards for coacervate phase were prepared in 995 μ l of 100mM SDS with addition of 5 μ l of blank coacervate aliquots. The separated coacervate sample was diluted 200 folds, namely 5 μ l of coacervate sample dissolved in 995 μ l of 100mM SDS solution. The separated aqueous sample was measured directly.

Potassium dichromate and copper (II) sulfate were used to observe interaction between colored non-hydrophobic ions and coacervate phase only by electrostatic interaction. Stock solution of 100mM of SDS and CTAB were mixed to prepare 1.0ml quantity of SDS/CTAB (90mM total surfactants concentration) at mole ratios 1:1, 3:7, 7:3 and final HFIP concentration of 9% v/v for study of the partitioning behavior of $\text{Cr}_2\text{O}_7^{2-}$ and Cu^{2+} into the complex coacervates.

Optical microscopy

The 2D images of the coacervate phases were taken by light microscopy under dark field condenser. An upright Nikon Eclipse 80i microscope was used for bright-field, dark-field and fluorescence imaging. The samples were excited with a mercury lamp (X-Cite 120Q) in the epi-mode with proper wavelength filters for different dyes applied in the excitation and emission channels. The signals were collected with a 100 \times Nikon Apo TIRF/1.49 oil immersion lens. An Andor iXon 897 camera (512 \times 512 imaging array, 16 \times 16 μ m pixel size) was used to record the fluorescence images. Dark-field images were obtained with the same microscope. The illumination light was focused onto the sample with an oil immersion

dark-field condenser (numerical aperture NA = 1.20-1.43). The amplification of this objective is 100 times, so actual size of pixel is $16\ \mu\text{m} / 100 = 160\ \text{nm}$.

3D imaging by confocal microscopy

Optical images at different z-axis of the sample were collected by using homebuilt confocal setup to make 3D imaging. Fluorescein isothiocyanate (FITC) was used to obtain fluorescence images under confocal microscopy. The excitation wavelength (488 nm) was provided from an air-cooled, wavelength-tunable Ar⁺ laser. The excitation beam were expanded and focused by a high numerical aperture (1.4) microscope objective (100 \times and oil immersion). Fluorescence signal was collected using the same objective. Sample scanning in the XYZ directions was achieved by using a piezo-stage (PI Nano, Physik Instrumente) mounted on a manual XY translational stage. The precision of the piezo-stage was 1.0 nm. The excitation laser power at the objective back aperture was $\sim 15\ \mu\text{W}$. The integration time and pixel size were 1 millisecond and 50 nm, respectively. The collected data were converted to images using ImageJ program.

Results and Discussion

The complex PFAIC induced by HFIP was investigated by both bulk experiments and microscopic studies. HFIP is a solvent miscible with water (100g/100mL at 25 °C) and forms micelle – like cluster structures in water. The interaction between HFIP and water decreases and HFIP clustering becomes more favorable with increasing the concentration of HFIP[10][11], due to the hydrogen bonding between HFIP molecules and hydrophobic

interaction between fluorine groups. The mechanism for fluoroalcohol induced coacervation is unknown. In surfactant solutions above critical micelle concentration, HFIP might be able to penetrate into structures like micelle, vesicle, bilayer, and lamellar. Many factors could have an impact on the formation of PFAIC such as mole ratio of cationic and anionic surfactants in complex coacervates, the percentage of HFIP, concentration of surfactants, chain length of surfactants, the pH, and others.

Chemical Composition of Complex PFAIC Phase

As mentioned earlier, the coacervate phase is highly enriched with the surfactants. The total amount of surfactant in complex coacervates of SDS-CTAB-HFIP was determined by gravimetric method. Figure2-1 shows the weight percentages of total surfactant in the coacervate phases relative to the total initial amount at different surfactant mole ratios and %HFIP. The SDS-CTAB at equimolar ratio (1:1) would form PFAIC at various HFIP from 9% to 27%. In fact, an earlier study in this laboratory has shown that the cationic surfactants of alkyl sulfates – trimethyl ammonium ion (i.e. SDS, CTAB, and their analogs with different chain lengths) can form stable coacervates over a wide range of HFIP% (v/v), starting as low as 5% and with the upper range in ~30%-35%, depending on surfactants chain lengths, mole ratio, and concentration. When percentage of HFIP is above the upper limit, only one liquid phase is present. At 7:3 SDS-CTAB (100 mM total concentration), coacervate is formed at HFIP concentrations of only below 18% v/v/ and at 3:7 SDS/CTAB coacervation occurs only at 9% HFIP. Earlier studies by Jenkins showed coacervate formation at HFIP concentration above 9% for the 3:7 SDS-CTAB, however at a much higher total surfactant concentration of 273mM[9]. It seems that at lower concentrations (e.g.

100 mM), the excess CTAB in the 3:7 SDS-CTAB can help dissolve the coacervate which leads to the formation of a single phase at 18% HFIP. This is not the case for the 7:3 SDS-CTAB system that forms coacervate at 18% HFIP. Apparently, SDS with the shorter chain than CTAB does not have the same solubilizing power, thus coacervate formation is still observed at 7:3 SDS-CTAB and 18% HFIP. We further examined the effect of chain length by testing 3:7 SDS-DTAB (100 mM) and observed that coacervate is formed at 18% HFIP. This provides additional support for the hypothesis that at lower total surfactant concentration and higher HFIP%, the excess of the longer chain CTAB can prevent formation of two phases. At the 1:1 mole ratio SDS-CTAB, about 80% of the initial amount of the total surfactant is assembled in the coacervate phase at %HFIP of 9% and 18%. The amount of surfactant in the coacervate phase decreases to below 60% of the initial amount when 27% of HFIP is used to induce coacervation. Thus, the surfactants are transferred from the bottom phase to the top aqueous phase with an increase in HFIP concentration. The 3:7 and 7:3 SDS-CTAB- 9%HFIP coacervates have about 55% and 30% surfactants relative to the total (initial) amount of surfactants respectively, which are much smaller than the 80% in 1:1. Naturally, at the 1:1 mole ratio, greater amount of the cationic complex is formed that results in a larger amount of surfactants entering into the coacervate phase. It is not clear, however, why the amount of surfactant in the 3:7 SDS-CTAB coacervate is so much greater than at 7:3 ratio. One possibility is that CTAB can form simple coacervate by itself at around neutral pH, thus in the 3:7 SDS-CTAB, there is a possibility of formation of both complex and simple coacervates. This can only be verified by determining the amount of each surfactant in both phases.

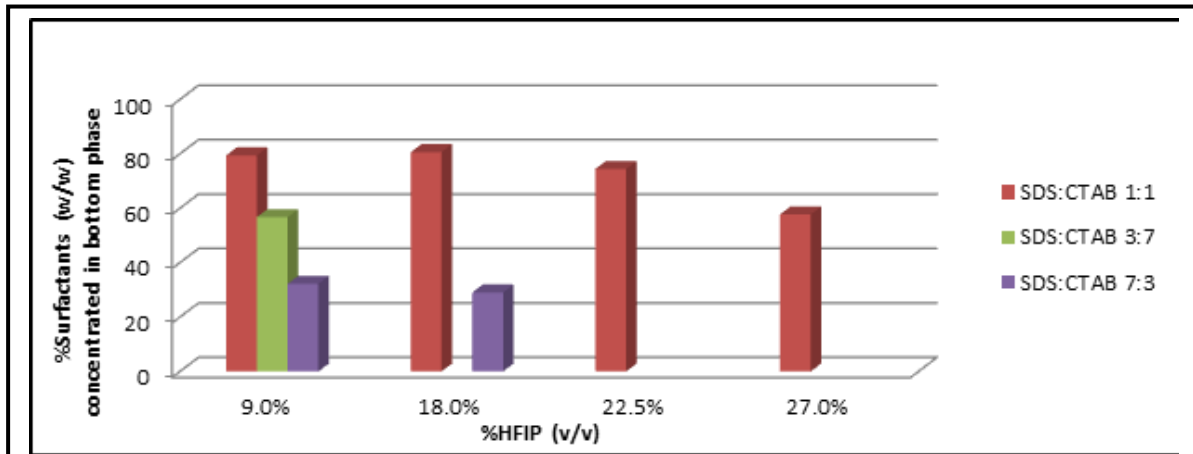


Figure 2-1. Quantitation of total surfactants aggregated in coacervate phase

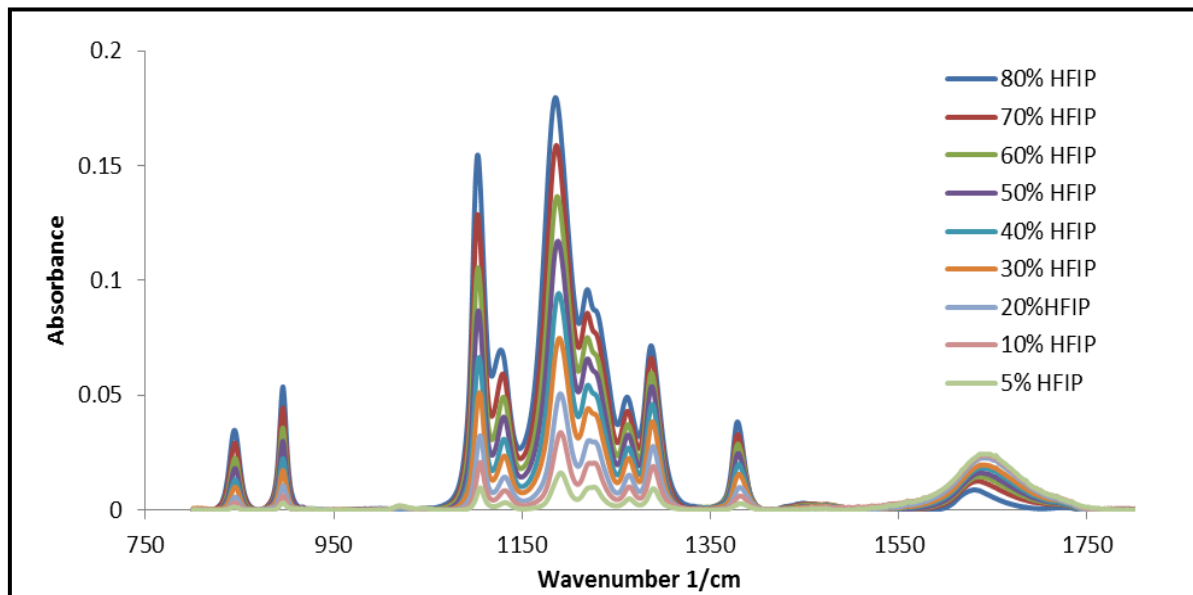
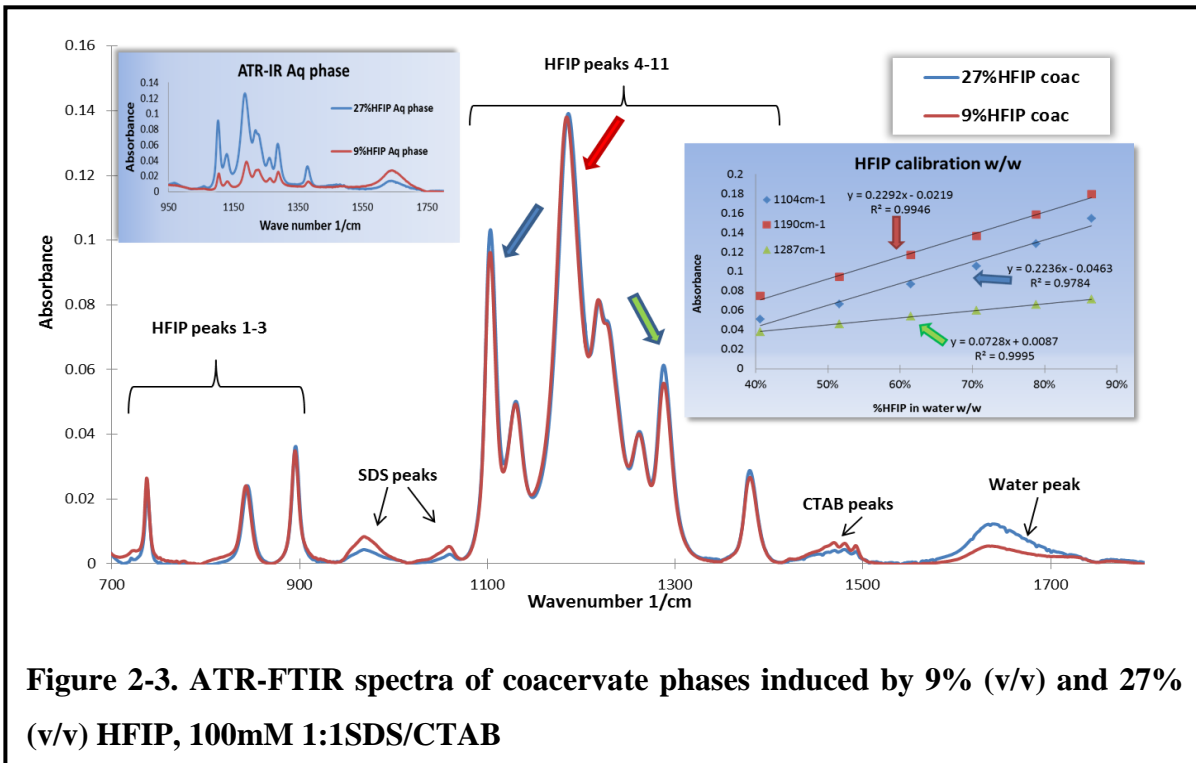


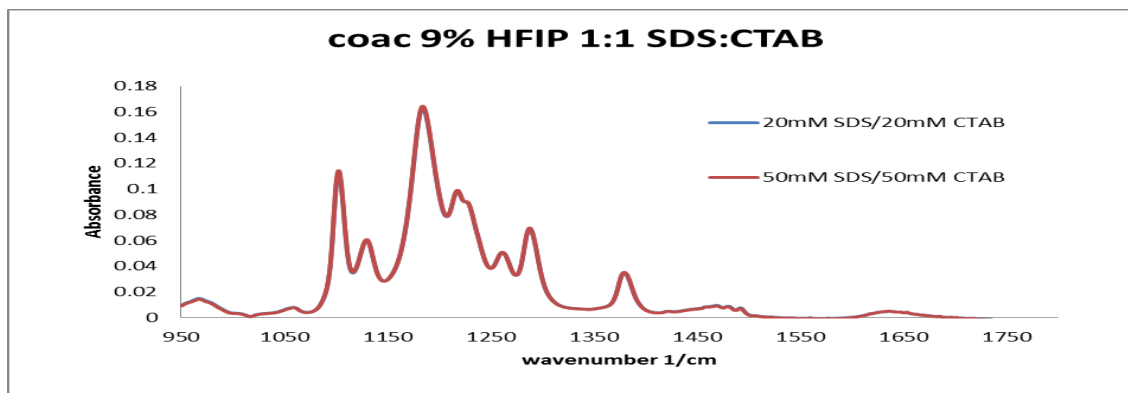
Figure 2-2. ATR-FTIR spectrum for HFIP in water (v/v)



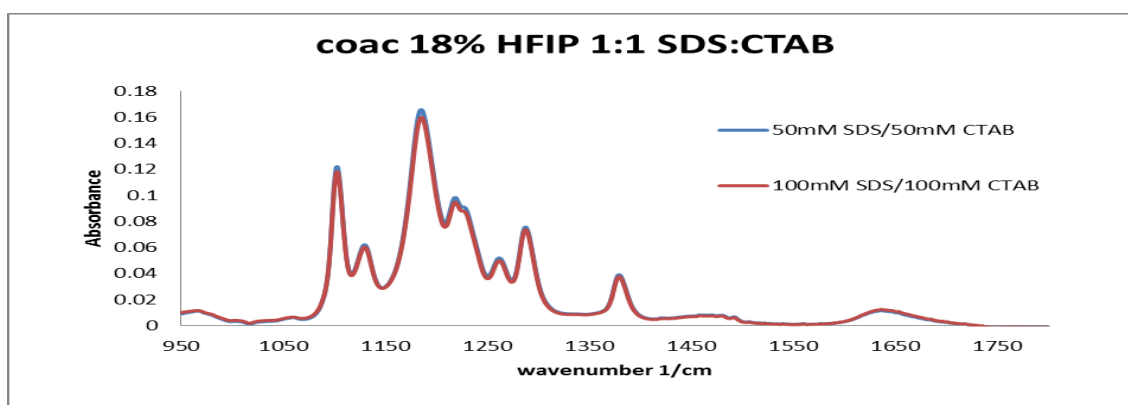
ATR-IR was used to determine the HFIP content in the 100mM 1:1 SDS/CTAB coacervate and aqueous phases at different concentrations of HFIP. Calibration curves were built based on standard mixtures of HFIP in water. The IR fingerprint region of HFIP fell between 750cm^{-1} and 1500cm^{-1} . The most intensive peaks at 1104cm^{-1} and 1190cm^{-1} and 1287cm^{-1} were selected to calculate the average concentration of HFIP in the aqueous and coacervate phases. Moreover, it was found that the peak around 1640cm^{-1} represents water peak. As shown in Figure 2-2, the water peak at 80% HFIP has lowest absorbance while at 5%, it has the highest reading around 1640cm^{-1} . Peak shifts were observed as shown in Figure 2-2, including peaks for HFIP and water. For example, there is a peak shift of 6cm^{-1} for the most

intense HFIP peak from 1191cm^{-1} to 1185cm^{-1} , and there is a peak shift of 11 wavenumbers for H_2O from 1641cm^{-1} to 1630cm^{-1} , indicating changes in OH group related intermolecular interaction due to environment differences from the aqueous-rich 5%HFIP to aqueous-poor at 80%HFIP. This peak shift follows the same trend as FTIR-ATR spectra of HFIP-water mixtures in Czarnik- Matusiewicz's paper[11]. Based on their theoretical calculation, the aggregates of HFIP, especially (dimers and trimmers), are more favorable in higher concentration of HFIP solution. Thus, the hydrogen bonding between HFIP and water is replaced by enhanced hydrogen bonding between HFIP-HFIP. Goto and his coworkers[12] examined the clustering of HFIP measured by solution small angle X-ray scattering, showing maximum formation of micelle-like HFIP clusters at about 30%(v/v). The hydrophobic $-\text{CF}_3$ groups interact through hydrophobic interaction that is a driving force for formation of micelle-like microstructures with dehydrated local environments. While fluorine groups are oriented away from bulk water, the hydroxyl groups are exposed to the aqueous media and interacting through hydrogen bonding. The intra- and inter- molecular interactions between HFIP and water molecules at different HFIP concentrations influence the vibrational energy for HFIP and H_2O , which leads to peak shift to a smaller wavenumbers. Figure 2-3 shows the overlaid IR spectra of the coacervate phases at 9%HFIP and 27%HFIP. The HFIP spectral bands are nearly indistinguishable which indicates the HFIP concentration in the coacervate phase remains constant. The concentration of HFIP in the coacervate phase at total 9% HFIP (as determined from 1104cm^{-1} peak) was 52.2% (v/v) (equivalent to 62.4% w/w) and at total 27% HFIP, the HFIP coacervate concentration was 55.0% (v/v) (or 65.0% w/w). The spectra in Figure 2-3 reveal that the concentration of water in the coacervate phase

is lower and concentration of surfactants (both SDS and CTAB) is higher at 9% HFIP than that at 27% HFIP. In other word, with an increase in HFIP concentration, surfactants in the coacervate phase are removed (and transferred to the top aqueous phase) and are replaced with water. This trend was also observed for the complex coacervates induced by TFE[1][9]. Figures 2-4A and 4B illustrate the effect of total surfactant concentration on the amount of HFIP extracted into the coacervate phase. In Fig. 2-4A and 2-4B, the PFAIC phases were prepared at 20mM and 50mM of surfactants and at 9% and 18% v/v HFIP. As can be seen from the superimposed ATR-FTIR spectra of coacervate phases, the concentration of surfactants doesn't affect the concentration of HFIP included in coacervate phases. Moreover, a non-linear calibration plot was created to determine the concentration of water in the 100mM 1:1 SDS/CTAB coacervate phases at two 9% (v/v) and 27% (v/v) HFIP using the water peak at around 1640cm^{-1} (Figure 2-5). The water contents in the coacervates induced by 9% (v/v) and 27% (v/v) HFIP were 6.9% and 21.2% w/w. The reason to report in w/w is to keep consistent unit to compare the content of HFIP, water and surfactants since so far we can only measure weight percentage of surfactants in coacervate phase.



(A)



(B)

Figure 2-4. ATR-FITR spectra of coacervate at different surfactant concentration
 (A) ATR-FTIR spectra of coacervate phases of 1:1 SDS/CTAB made at different surfactant concentrations (20mM and 50mM) and HFIP (9% v/v); (B) ATR-FTIR spectra of coacervate phases of 1:1 SDS/CTAB made at different surfactant concentrations (50mM and 100mM) and HFIP (18% v/v)

Chemical Composition of Coacervates and Partitioning Patterns

Hydrophobic effect is an important driving force for solute partitioning into coacervates. For charged solutes, electrostatic interaction would also play a significant role. Partition coefficients of solutes into coacervates depend on structural properties of solutes and chemical composition of coacervates as defined by the type, concentration, and mole ratio of constituent surfactants as well as type and concentration of the perfluorinated-alcohol or acid coacervator. We examined partitioning behavior of four dyes in complex coacervates of SDS-CTAB-HFIP with different composition. The dyes included the neutrally charged Nile Red (NR), negatively charged 6-carboxyfluorescein (6-CF), and two positively charged dyes; Rhodamine 6G (R6G) and Methylene Blue (MB). The partition coefficients of Nile Red, Rhodamine 6G and Methylene Blue in equimolar (1:1) SDS-CTAB at 9% HFIP, are significantly higher than those in unequal mole ratios of SDS and CTAB (Table 2-2). This might indicate that the 1:1 coacervate phase is more hydrophobic than those made of nonstoichiometric mole ratios and favorably extracts neutral or positively charged dyes. An increase in HFIP from 9% to 18% leads to a significant decrease in partition coefficients for all four dyes. As shown earlier, the concentration of HFIP in the coacervate phase remains nearly unchanged with an increase in total HFIP, however the concentration in the aqueous – rich phase increases that results in reducing of the aqueous phase hydrophobicity and subsequent decrease in partition coefficients. An increase in total surfactant concentration from 100 mM to 273 mM resulted in a decrease in partition coefficients. The reason behind this is not totally clear. One possible cause could be a change in the volume of the coacervate and aqueous phases.

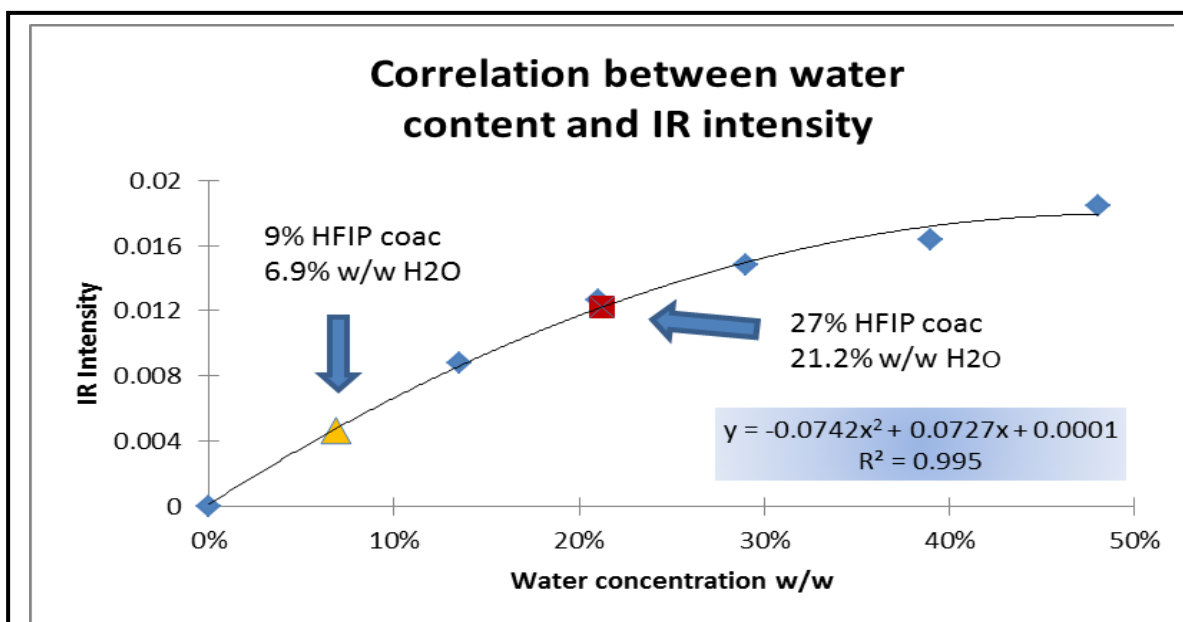


Figure 2-5. Calibration curve for quantitation of water concentration in coacervates on ATR-FTIR water peak around 1640cm⁻¹. The filled triangle corresponds the signal to water content in the coacervate phase of 100mM 1:1 SDS/CTAB induced by 9 v/v %HFIP; The filled square corresponds the signal to water content in the coacervate phase of 100mM1:1 SDS/CTAB induced by 27% v/v HFIP. The calibration fit was a second degree polynomial.

Table 2-1. Concentrations and standard deviations of HFIP and H₂O in coacervate phase at different wavenumbers

SAMPLE	HFIP v/v in coacervate \pm STD	HFIP w/w in coacervate \pm STD	Average HFIP w/w of three wavenumbers	H ₂ O w/w in coacervate
100mM 1:1 SDS/CTAB 9% (v/v) HFIP	52.2 \pm 1.6%(1104cm-1)	62.4 \pm 1.5%(1104cm-1)	64.6 \pm 3.4%	6.9 \pm 1.2%
	59.2 \pm 1.3%(1190cm-1)	68.8 \pm 1.2%(1190cm-1)		
	52.6 \pm 2.4%(1287cm-1)	62.6 \pm 2.2%(1287cm-1)		
100mM 1:1 SDS/CTAB 27% (v/v) HFIP	55.0 \pm 1.8%(1104cm-1)	65.0 \pm 1.7%(1104cm-1)	67.4 \pm 2.7%	21.2 \pm 0.4%
	58.4 \pm 2.1%(1190cm-1)	68.0 \pm 1.9%(1190cm-1)		
	60.0 \pm 2.7%(1287cm-1)	69.3 \pm 2.4%(1287cm-1)		

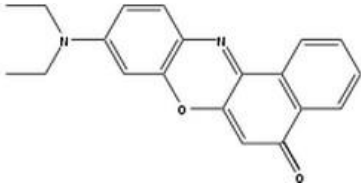
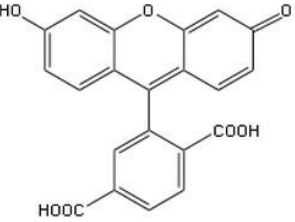
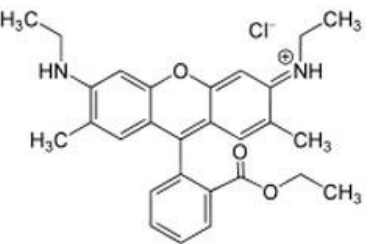
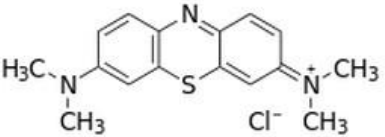
The volume of the coacervate phase increases linearly with an increase in total surfactant concentration. Thus, the volume of the aqueous – rich phase decreases if the total solution

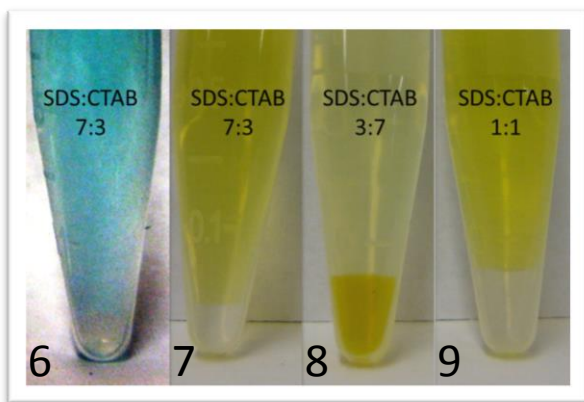
volume (i.e. volume of the aqueous plus coacervate phases) is kept constant. As a result, the solute concentration in coacervate phase decreases, and solute concentration increases in the aqueous-rich phase which leads to subsequent decrease in partition coefficient. However, this volume change effect should impact partition coefficients of all solutes to the same extent, which is not the case here. As can be seen in Table 1, K values decreased by a factor of ~2-4 for the neutral and cationic dyes and to a smaller extent (~ 1.3 x) for the anionic 6-CF.

The partitioning trends in coacervates made of different surfactant mole fractions were also investigated. The two oppositely charged surfactants form a catanionic complex through electrostatic and hydrophobic interactions. In systems with non-stoichiometric mole ratios, one of the two surfactants would be in excess. It is not clear how the surfactant in excess mole fraction is distributed between the two phases. One can envision two scenarios; the first would involve the excess surfactant to remain in the coacervate phase that leads to a “charged coacervate” phase, resulting in a less hydrophobic phase than the phase made of stoichiometric (1:1) mole ratio. Another case would involve transfer of all or some of the excess surfactant to the aqueous-rich phase and formation of micelles in that phase that would compete with the coacervate phase for interaction with solutes. Either scenario would lead to smaller partition coefficients for uncharged solutes in non-stoichiometric systems as compared to that in the 1:1 stoichiometric coacervate, which is evident from the partition coefficient of NR in Table 1. However, the partition coefficient of the solutes with an opposite charge to that of the surfactant in excess will increase in the first scenario where the coacervate is charged. The results of partition coefficients of the charged dyes in coacervates with different mole ratios suggest that the former case is more likely. As can be seen the

partition coefficients of the two positively charged solutes (R6G and MB) are greater in the anionic -rich 7:3 SDS-CTAB than in the cationic-rich 3:7 system. The negatively charged 6CF interacts very strongly with the cationic - rich 3:7 than the anionic 7:3 coacervate. The much smaller K value ($K \sim 0.3$) for 6CF in the anionic-rich phase might indicate the presence of electrostatic repulsion. In fact, this is the only case where $K < 1$ that shows a solute interaction with the aqueous - rich phase is stronger than that with coacervate. It is not clear why this possible electrostatic repulsion effect is not observed for the cationic dyes (R6G and MB) in the cationic-rich 3:7 SDS-CTAB. Likewise, the impact of the presumed “electrostatic attraction” of the positively charged solutes to the anionic-rich 7:3 SDS-CTAB has not been nearly as much as that for 6CF with the 3:7 system. This might be due to differences in CTAB and SDS in interacting with the coacervates. As described previously, HFIP can induce simple coacervate in solutions of CTAB at around neutral pH to basic solutions, while SDS would undergo coacervation only in highly acidic solutions of a strong acid (e.g. $\sim 4M$ HCl). The light microscopy images (shown below) suggest that there are different structures between 3:7 SDS/CTAB and 7:3 SDS/CTAB. With the excess of CTAB, a large number of droplets microstructures exist while there are very few droplets in the 7:3 SDS/CTAB coacervate phase. Note that the hydrophobicities of the four dyes are quite different from one another, which would have a significant effect on how they interact with the coacervates.

Table 2-2. Comparison of Partition coefficient of Nile Red, 6-carboxyfluorescein, Rhodamine 6G and Methylene Blue in different ATPS

Dye structure	Mole ratio SDS:CTAB	% HFIP (v/v)	Partition coefficient(K)	RSD
	3:7 100mM	9%	81.8	2.9%
	7:3 100mM	9%	92.0	3.5%
	1:1 100mM	9%	4.2×10^4	7.9%
	1:1 100mM	18%	170.6	11.8%
	1:1 274mM	9%	1.9×10^4	14.0%
	3:7 100mM	9%	416.2	9.6%
	7:3 100mM	9%	0.31	0.5%
	1:1 100mM	9%	28.0	17.5%
	1:1 100mM	18%	8.6	10.2%
	1:1 274mM	9%	21.8	34.1%
	3:7 100mM	9%	60.1	7.9%
	7:3 100mM	9%	104.1	6.1%
	1:1 100mM	9%	3.7×10^5	15.4%
	1:1 100mM	18%	125.8	2.6%
	1:1 274mM	9%	1.6×10^5	30.0%
	3:7 100mM	9%	19.3	10.9%
	7:3 100mM	9%	32.6	3.6%
	1:1 100mM	9%	5.7×10^3	7.9%
	1:1 100mM	18%	56.2	17.9%
	1:1 274mM	9%	1.4×10^3	17.9%



Figures 2-6, 2-7, 2-8, 2-9. Extraction of inorganic ions. CuSO_4 (6) and $\text{K}_2\text{Cr}_2\text{O}_7$ (7-8) extracted by 100 mM, 7:3, 3:7 and 1:1 SDS/CTAB with 9%(v/v) HFIP.

In order to examine the impact of electrostatic interactions in the absence of hydrophobic effects, we determined the partition coefficients of two inorganic substances, potassium dichromate and copper sulfate. The partitioning of the yellow colored dichromate ion, $\text{Cr}_2\text{O}_7^{2-}$ and blue colored Cu^{2+} ion can be visually monitored (Figures 2-6, 2-7, 2-8, 2-9). As shown in Figures 2-6 to 2-9, the negatively charged dichromate ion is concentrated in the cationic – rich coacervate (3:7 SDS-CTAB) while it remains almost entirely in the top aqueous phases of the 1:1 or 7:3 SDS/CTAB coacervates. A similar experiment for extraction of Cu^{2+} ions was performed in the anionic-rich coacervate, 7:3 SDS-CTAB. The aqua-copper (II) complex stays in the top aqueous phase which suggests that there is little or no electrostatic interaction between the “excess” anionic SDS and cationic aqua copper(II).

However, it is not clear whether there is excess SDS in the 7:3 coacervate phase. It is possible that composition of coacervate phase is not simply adjusted by surfactant ratio.

Figures 2-10 and 2-11 show the light microscopy images of the 100mM 1:1SDS/CTAB complex coacervate phase in the presence of 10% v/v HFIP under dark field and bright field respectively. Spherical structures or droplets are observed with the diameter varying from 1 to 5 μ m. The fluorescence images (Figs 2-12, 2-13, 2-14) also visualize how different probe dyes of MB, NR, and 6-CF interact with the micro-droplets. It is dark inside droplets and bright outside the droplets as shown in Figure 2-12 and Figure 2-13 above for the positively charged dye-Methylene Blue and neutrally charged dye-Nile Red. It suggests that the cationic MB and neutrally charged NR dye are predominantly localized outside of the droplets, while the negatively charged 6-CF is more localized inside the micro-spheres as shown in Figure 2-14. The composition of the droplets and the outside “bulk” phase within the coacervate phase is not known. The images illustrate the coacervate phases after 24 hours of equilibration.

Microscopy Imaging

The size of the droplets increases initially with time as they coalesce, however, the coacervate phase does not become a single uniform phase even after 4 months. The ATR-IR results show that there is 50%-60% v/v HFIP in the complex coacervate phase, thus it is very likely that the bulk phase (outside of the micro-spheres) is a large pool of HFIP and water as solvent in coacervate phases. The micro-spheres would then be a large assembly of surfactants. As shown above, only the negatively charged dye 6-CF was observed to partition

inside the droplet structures while the neutral or positively charged dyes always stayed in “bulk” phase outside the assembly droplets. One hypothesis is involves pKa shift of HFIP to more acidic values in the presence of excess CTAB, which produces negatively charged FIP⁻ ions. However FIP⁻¹ can be ion paired by counter ion such as Na⁺ or CTA⁺. The solution should be neutrally charged. When excess of CTAB is present in solution (100mM 3:7, SDS-CTAB), CTA⁺ may form aggregates with FIP⁻ based on electrostatic attraction and hydrophobic interaction. Given that fact that concentration of HFIP (v/v 9%, 857mM) is much higher than surfactant concentration, the most possible scenario would be partial ionization of HFIP and most remain in protonated form considering that HFIP is a weak acid with pKa 9.3. Thus the most possible source of “free” anion would mainly come from free SDS. The low partition coefficient in 7:3 SDS-CTAB can be explained by repulsion between negatively charged 6-carboxyfluorecein with free anionic ions in the coacervate phase.

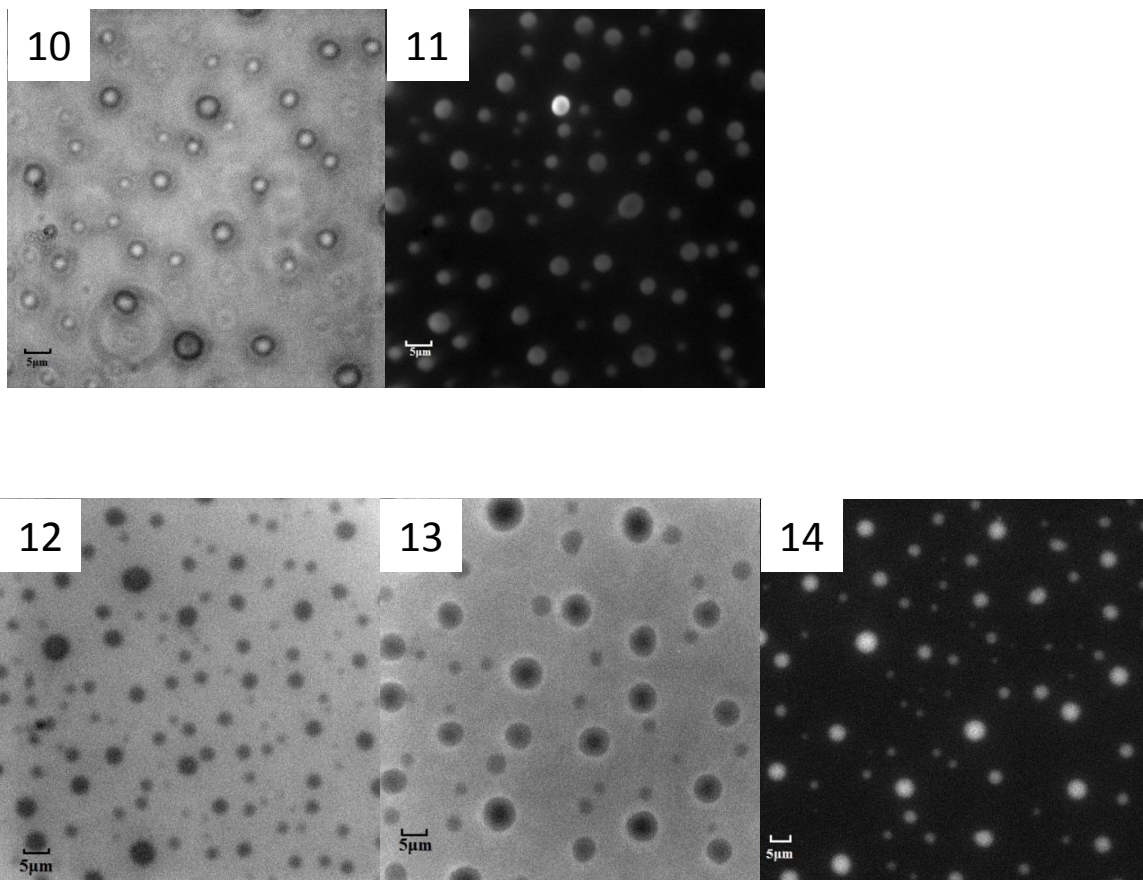
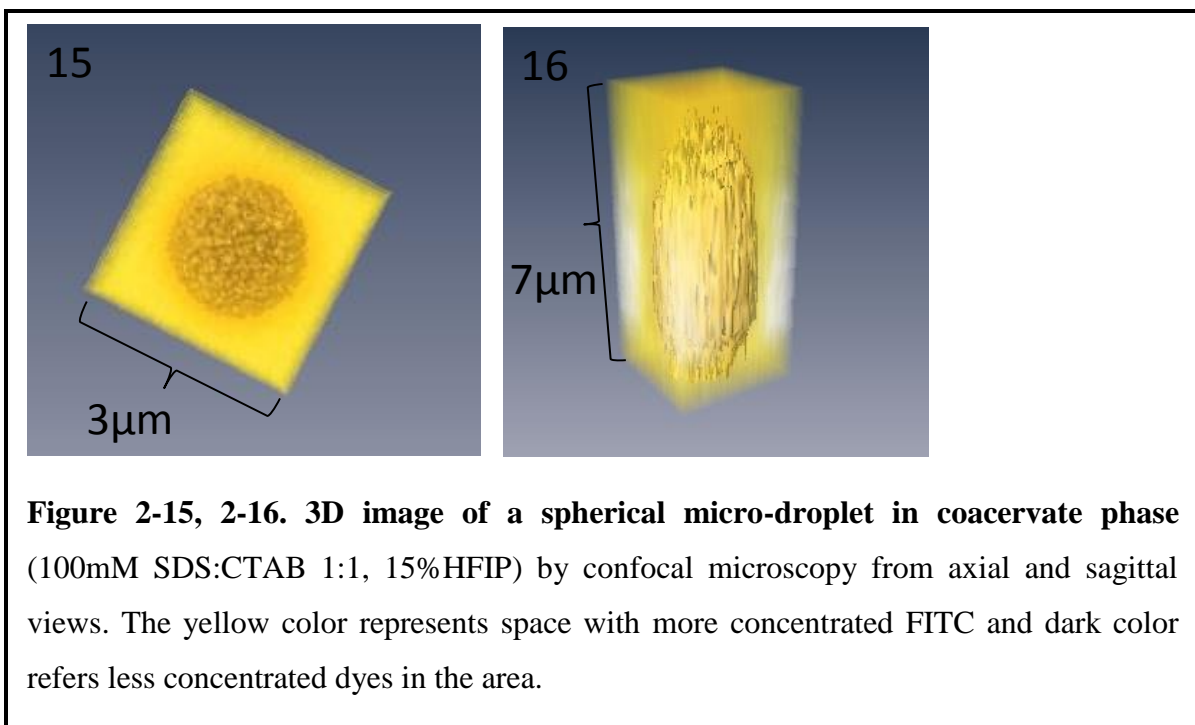


Figure 2-10, 2-11, 2-12, 2-13, 2-14. Optical microscopy images of complex coacervates.

All of the samples were equilibrated for 24 hours and separated. The microscopy images of the separated coacervate phase were taken by light microscope. Fig 2-10. Bright field image of coacervate phase of 100mM 1:1SDS/CTAB, 9%HFIP; Fig 2-11, the same as of Fig 2-9 except taken under dark field; Fig 2-12, fluorescence image of 100mM 1:1SDS/CTAB, 9%HFIP with methylene blue in coacervate phase; Fig 2-13, 100mM 1:1SDS/CTAB, 9%HFIP with Nile Red in coacervate phase; Fig 2-14, 100mM 1:1SDS/CTAB, 9%HFIP with 6-carboxyfluorescein in coacervate phase.



In addition to electrostatic attraction/repulsion, the hydrophobicity also serves as a driving force to extract 6-CF into the 1:1 SDS-CTAB droplets in the coacervate phase. The variation of K of dyes in 1:1 SDS-CTAB coacervates may also come from difference hydrophobicity between 6-carboxyfluorecein and Methylene Blue, Rhodamine 6G or Nile Red. Therefore, partitioning from top aqueous phase to bottom coacervate phase for 6-CF might be different, comparing to neutral or positively charged dyes in bulk experiments. However, the presence of SDS and CTAB in complex coacervate phase could contribute to extraction significantly, but it is still unclear how hydrophobic interaction competes with electrostatic interaction

when changing the mole ratio. The second step of partitioning between the outside of the sphere structure and inside sphere structure shows a strong connection with charge.

Figure 2-15 and 2-16 show 3D images of one typical sphere structure in complex coacervate phase (1:1 SDS-CTAB in the presence of 15% v/v HFIP) obtained by confocal laser scanning microscopy. The focal plane starts from zero to 7.5 μ m with increments of 500nm. The 3D image was created by overlaying focal planes at different layers. From axial view, one droplet was selected arbitrarily to study 3D structure. Rod-like structure was shown and the concentration of fluorescein isothiocyanate (FITC) was rich outside the droplet structure and poor inside. FITC is a fluorescein derivative with an isothiocyanate group replacing a hydrogen atom on the bottom ring with negative charge. However, at a higher percentage of HFIP, the environment of coacervate phase is different. As discussed before, there might be more water in coacervate phase while maintaining the concentration of HFIP. It is hard to compare and draw a conclusion why FITC didn't go in the droplets at 15%HFIP while 6-CF was more concentrated inside the droplet. Figures 2-15 and 2-16 here are to show the structure of a droplet from a three dimensional angle. It is still unclear what factor determines the extraction of negatively charged dye into the rod-like structure. It could be the result of competition or collaboration between hydrophobic/hydrophilic effect and electrostatic effect inside and outside the droplet structure. The sagittal view shows that the length of the rod-like structure is about 7 μ m, and the maximum diameter is about 2 μ m shown in axial view.

Figures 2-17 through 2-27 show a series of images of coacervate phases from different samples. It is clear that the coacervate phase of 3:7 SDS-CTAB has many more droplet structures than 1:1 SDS-CTAB, and the 1:1 has more droplets than the 7:3 SDS-CTAB

coacervate. After equilibration for 4 months or 6 days, the 3:7 or 1:1 SDS-CTAB coacervate samples appear to be stable and tends to maintain the droplets structure. However, with the excess of SDS, the coacervate phase of 7:3-SDS-CTAB shows aggregates with different morphology than the other two complex coacervate systems. As discussed before, the partition coefficient, K , of 6-CF is only 0.31 in the 7:3 SDS/CTAB 9% HFIP coacervate, which means the negatively charged 6-CF is not favorable in the bottom coacervate phase due to the presence of “free” SDS and/or potential “FIP⁻ - ions”. The microscope is able to trace nM level of fluorescence dye in samples. Even though most of 6-CF stays in the aqueous phase, any 6-CF remaining in the coacervate phase partitions into droplet structure as shown in Figure 2-22. Note that the “droplets” in 7:3 SDS-CTAB could be completely different than the “droplet” in 1:1 or 3:7 SDS-CTAB phases. This is also confirmed by the results shown in Figure 2-20 for 7:3 SDS-CTAB after a long equilibration time. The number of droplets decreases and can hardly be found. It is still unknown why it behaves differently with different mole ratio and what the chemical composition and structure are inside and outside those droplets. Figure 2-26 shows the image of 100 mM 1:1 SDS/CTAB 18% HFIP, with large liquid bubbles formed. The concentration of HFIP is supposed to stay similar as 9% as indicated by the ATR-IR results. The changes are the increased water concentration and the decreased surfactant concentration. The environment becomes more polar and less hydrophobic. Figure 2-27 is the bottom phase of simple coacervation CTAB-HFIP at neutral pH controlled by Tris buffer. There are aggregates in CTAB-HFIP coacervation with size less than 1 μm , due to interaction between FIP⁻ at controlled neutral pH and cationic CTA⁺ ion.

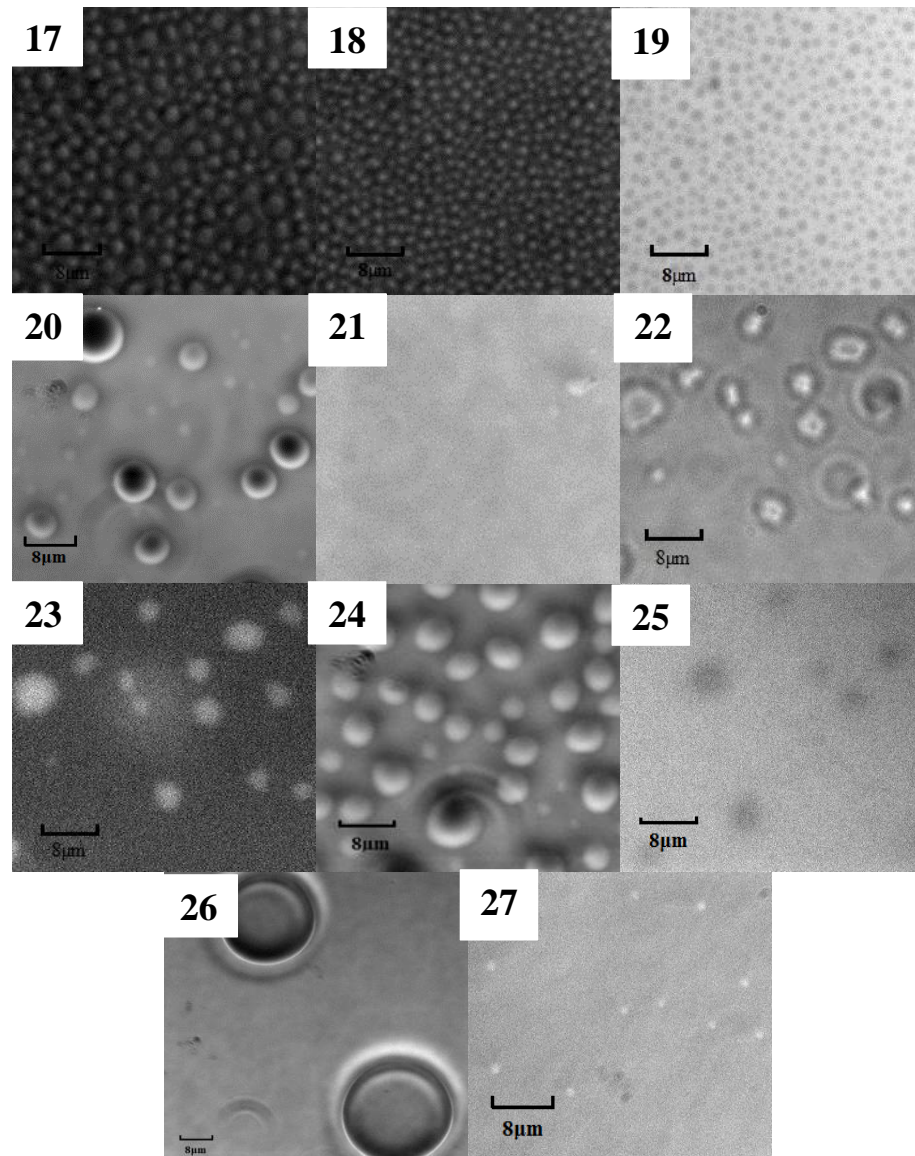


Figure 2-(17-27). Optical microscopy images for coacervates at different compositions. All fluorescence images are with 6-CF. Figs17-19, 100mM 3:7 SDS/CTAB, 9% v/vHFIP, equilibrated for (Fig. 17) 4 months, (Fig. 18) 30min,(Fig. 19) 30min(fluorescence); Figs 20-22, 100mM7:3 SDS/CTAB, 9% v/v HFIP, equilibrated for (Fig. 20)4 months, (Fig. 21)30min, (Fig. 22) 30min, fluorescence; Figures 23-25, 100mM 1:1 SDS/CTAB, 9% v/v HFIP, equilibrated for (Fig. 23)6days, (Fig. 24)2days, (Fig. 25)2days fluorescence; Figure 26, 100mM 1:1 SDS/CTAB, 18% v/ HFIP, equilibrated for 30min; Figure 27, 100mM CTAB, 9% in0.5M Tris, pH7, equilibrated for 30min.

Conclusion

The complex coacervate system SDS-CTAB-HFIP was investigated by different methods. When increasing the percentage of HFIP (v/v), the surfactant concentration in coacervate phases decreases. At the same time, more water molecules are driven into the coacervate phase to replace surfactants. Water content goes up from 6% to 21% w/w in the coacervate phase with %HFIP changing from 9% to 27%. However, the concentration of HFIP in coacervate phase only increases from 64.6% to 67.4% w/w when the initial %HFIP changed from 9% to 27%. At a fixed %HFIP, the total surfactant concentration doesn't affect %HFIP in coacervate phase. HFIP clusters could create hydrophobic local environment. Water is repelled from the PFAIC coacervate phases (6-21% w/w in coacervate phase). This is significantly different from other coacervate systems (such as CPS) that have as much as 95% w/w water[13]. Highly concentrated HFIP coacervate phases extract dyes by hydrophobic and/or electrostatic interaction, resulting in partition coefficients ranging from 0.31 to as high as 10^5 for small dye molecules. In partition coefficient measurements of four dyes with different charges, only negatively charged 6-CF has the highest K value in the cationic-rich 3:7 SDS/CTAB. For the other three dyes, the highest K values are from 1:1 anionic: cationic surfactant ratio coacervation. Hydrophobic effect is one of the major driving forces for dye extraction, especially for neutral and positively charged dyes. Other than hydrophobic interaction, electrostatic interaction between "free" CTA^+ and negative 6-CF shows the highest partition coefficient. A hypothesis was evolved that CTA^+ ions could interact with the conjugated base of weak acid HFIP, the FIP^- ions, facilitating coacervate formation. The microscopy image of the simple coacervate CTAB-HFIP at neutral pH shows

microscopic structures in the coacervate phase, indicating the cluster or aggregation structure, which might be composed by CTA^+Br^- and HFIP/FIP^- molecules. Moreover, the excess of CTAB in 3:7 SDS-CTAB coacervate results in a much larger population of droplets than 7:3 SDS-CTAB. It is possible that the microstructure and packing of surfactants/HFIP are different between the 7:3 and 3:7 mole ratios. It is not clear now why 7:3SDS/CTAB coacervate phase shows different microstructure comparing to 1:1 or 3:7 SDS/CTAB. We are not sure the actual ratio between SDS and CTAB in the coacervate phase yet. Further elemental study such as measurement of total nitrogen content and total sulfur content may help us to understand more about the mystery of coacervates.

References

- [1] M. G. Khaledi, S. I. Jenkins, and S. Liang, “Perfluorinated Alcohols and Acids Induce Coacervation in Aqueous Solutions of Amphiphiles,” *Langmuir*, vol. 29, no. 8, pp. 2458–2464, Feb. 2013.
- [2] *Biomedical applications of microencapsulation*. Boca Raton, Fla: CRC Press, 1984.
- [3] *Handbook of pharmaceutical controlled release technology*. New York: Marcel Dekker, 2000.
- [4] F. H. Quina and W. L. Hinze, “Surfactant-Mediated Cloud Point Extractions: An Environmentally Benign Alternative Separation Approach,” *Industrial & Engineering Chemistry Research*, vol. 38, no. 11, pp. 4150–4168, Nov. 1999.
- [5] W. L. Hinze and E. Pramauro, “A Critical Review of Surfactant-Mediated Phase Separations (Cloud-Point Extractions): Theory and Applications,” *Critical Reviews in Analytical Chemistry*, vol. 24, no. 2, pp. 133–177, Jan. 1993.
- [6] H. G. Bungenberg de Jong and H. R. Kruyt, “Coacervation (Partial Miscibility on Colloid Systems),” *Proc. Koninkl. Med. Akad. Wetenschap*, vol. 32, pp. 849–856, 1929.
- [7] F. M. Menger, “Remembrances of Self-Assemblies Past,” *Langmuir*, vol. 27, no. 9, pp. 5176–5183, May 2011.
- [8] E. Kizilay, A. B. Kayitmazer, and P. L. Dubin, “Complexation and coacervation of polyelectrolytes with oppositely charged colloids,” *Advances in Colloid and Interface Science*, vol. 167, no. 1–2, pp. 24–37, Sep. 2011.

- [9] S. I. Jenkins, "Novel Aqueous Two-Phase Systems: Characterization and Applications in Chemical Separation," North Carolina State University.
- [10] K. Yoshida, T. Yamaguchi, T. Adachi, T. Otomo, D. Matsuo, T. Takamuku, and N. Nishi, "Structure and dynamics of hexafluoroisopropanol-water mixtures by x-ray diffraction, small-angle neutron scattering, NMR spectroscopy, and mass spectrometry," *The Journal of chemical physics*, vol. 119, p. 6132, 2003.
- [11] B. Czarnik-Matuszewicz, S. Pilorz, L. P. Zhang, and Y. Wu, "Structure of hexafluoroisopropanol–water mixture studied by FTIR-ATR spectra and selected chemometric methods," *Journal of Molecular Structure*, vol. 883, pp. 195–202, 2008.
- [12] D. P. Hong, M. Hoshino, R. Kuboi, and Y. Goto, "Clustering of fluorine-substituted alcohols as a factor responsible for their marked effects on proteins and peptides," *Journal of the American Chemical Society*, vol. 121, no. 37, pp. 8427–8433, 1999.
- [13] F. M. Menger, A. V. Peresykin, K. L. Caran, and R. P. Apkarian, "A Sponge Morphology in an Elementary Coacervate," *Langmuir*, vol. 16, no. 24, pp. 9113–9116, Nov. 2000.

Supplemental Data

Table 2-3. Data of quantitation analysis of total surfactant concentration

A-K is the separated coacervate phase. A'-K' is the separated aqueous phase.

Tube #	Composition SDS:CTAB v/v %HFIP	Mass of surf in each phase	Sum of surfactant mass	Theo total surf mass*	% surf goes into coac phase (devided by exp value)
A	100mM 1:1 9%	0.0258	0.0325	0.0297	79.4
A'		0.0067			
B	100mM 1:1 13.5%	0.0244	0.0303	0.0282	80.5
B'		0.0059			
C	100mM 1:1 18%	0.0229	0.0284	0.0268	80.6
C'		0.0055			
D	100mM 1:1 22.5%	0.0192	0.0258	0.0253	74.4
D'		0.0066			
E	100mM 1:1 27%	0.0150	0.0260	0.0238	57.7
E'		0.0110			
F	100mM 3:7 9%	0.0187	0.0330	0.0311	56.7
F'		0.0143			
G	100mM 3:7 18%	0.0309	0.0309	0.0280	One phase
G'		One phase			
H	100mM 3:7 27%	0.0255	0.0255	0.0249	One phase
H'		One phase			
I	100mM 7:3 9%	0.0094	0.0292	0.0284	32.2
I'		0.0198			
J	100mM 7:3 18%	0.0076	0.0262	0.0255	29.0
J'		0.0186			
K	100mM 7:3 27%	0.0236	0.0236	0.0227	One phase
K'		One phase			

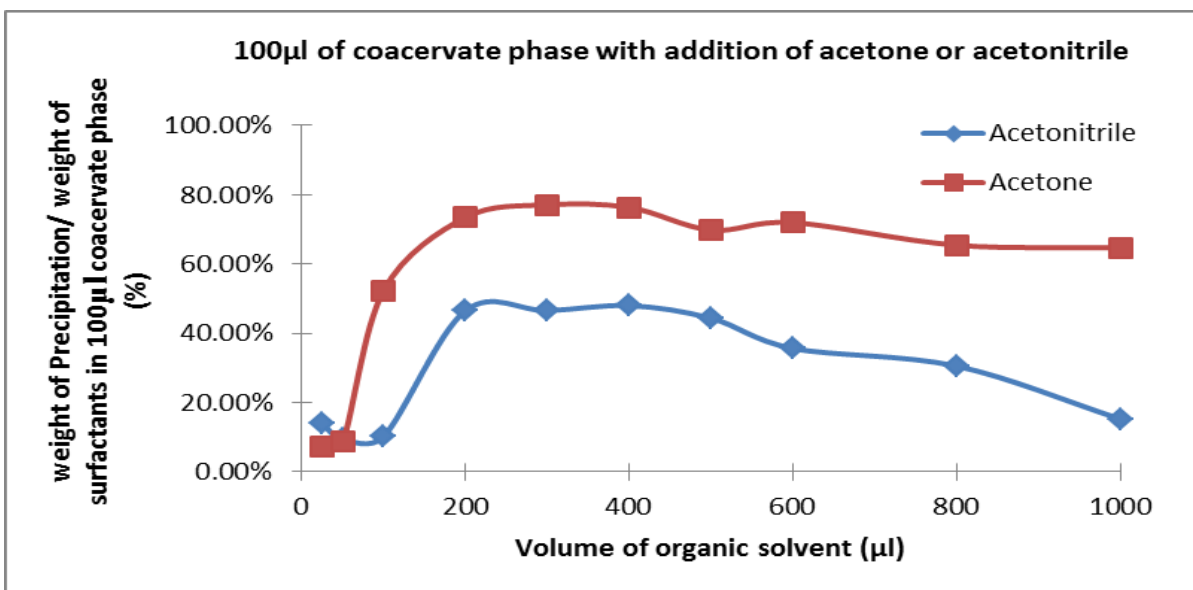


Figure 2-28. Precipitation of surfactants by adding organic solvents. 100µl of coacervate was coacervate phase of 1:1 100mM SDS:100mM CTAB with 27% v/v HFIP.

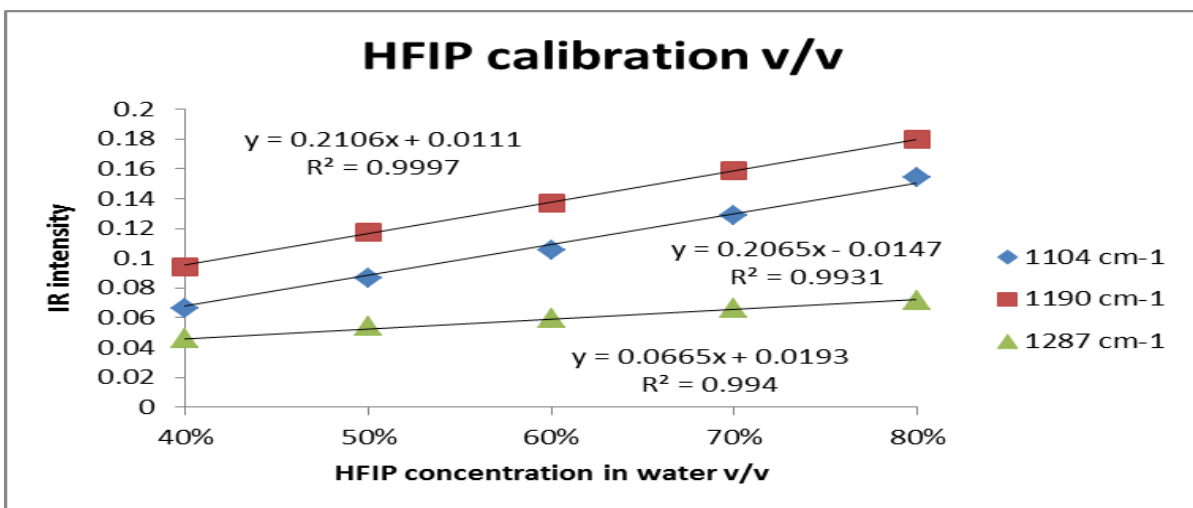


Figure 2-29. HFIP calibration curve v/v

Chapter 3

Partitioning of Proteins in Perfluorinated Alcohols Induced Coacervates

Abstract

Capabilities of aqueous-based two phase systems of simple and complex Perfluorinated Alcohol Induced Coacervates (PFAIC) for extraction of model proteins are investigated. The simple PFAIC systems include: cationic CTAB/HFIP (at neutral or basic pH), anionic SDS/HCl/HFIP, zwitterionic 3-(N,N-dimethylmyristylammonio) propane sulfonate (DMMAPS)/HFIP. In addition to coacervates, phase separation in aqueous mixture of water-HFIP was induced through addition of a Kosmotropic salt, Na₂SO₄. This allows a comparison between proteins partitioning into HFIP phase in the absence of surfactants.

Key words: PFAIC, ATPS, Extraction, Protein, surfactant

Introduction

During the past three decades, the use of aqueous two-phase systems (ATPS) for the extraction, pre-concentration and separation of biological mixtures, such as DNA, proteins and cells has grown rapidly[1][2][3][4]. The traditional ATPS includes polymer-based aqueous phase separation, biopolymer –based coacervation, as well as Cloud Point Systems (CPS) that involve nonionic or zwitterionic surfactants. Comparing to water-organic extraction systems, the ATPS are more environmentally friendly, less toxic, more compatible with biomolecules. [5][6]. The phase separation mechanism include polymer-based phase separation such as PEG-Dextran[7], and coacervates composed of different types of amphiphiles, e.g. biomacromolecules such as protein-protein/salt[8], cloud point systems(CPS)[9], polyelectrolytes such as polyelectrolyte-protein coacervation[10], charged surfactants such as Gemini-anionic surfactants[11], and others [12][13][14][15]. However, for the separation and extraction of small organic compounds, polymer-mediated phase separation has limited extraction selectivity. The cloud point coacervation occurs at a transition temperature where the surfactant solution becomes cloudy and subsequently undergoes phase transition from one liquid phase to two separate aqueous-based phases, where one phase is enriched in surfactant and the other one is surfactant-lean. A popular application of the cloud point systems is separation of hydrophilic and hydrophobic proteins, where the former is concentrated in the surfactant-lean phase, while membrane proteins are primarily extracted in the surfactant – rich coacervate phase[16][17][18]. Typically, the cloud point systems are composed of nonionic or zwitterionic surfactants [9]. A limited number of surfactants have Cloud Point Temperature (CPT) near or below ambient temperatures.

Surfactants with high CPT are not compatible for extraction of thermally labile biological compounds. This would limit the number of useful surfactants. In addition, there is little difference in solvation ability and interactive properties of various nonionic or zwitterionic surfactants that primarily comprise CPS. The nonionic or zwitterionic surfactants are neutrally charged, which limit their ability to engage in electrostatic interactions with biological molecules.

We have recently reported that perfluorinated alcohols, such as trifluoroethanol (TFE) and hexafluoroisopropanol (HFIP), and perfluorinated acids like trifluoroacetic acid (TFA), pentafluoropropionic acid (PFPA), and heptafluorobutyric acid (HFBA) can induce simple and complex coacervation in aqueous solutions of single as well as mixed oppositely charged amphiphiles with a wide range of molecular structure and over a wide range of concentrations and mole fractions[19] . The Perfluorinated Induced Alcohol / Acid Coacervates (PFAIC) can also be considered as ATPS even though the concentration of water in the coacervate phase is not as high as polymer-based ATPS or CPS. An important characteristic of PFAIC is that they can be prepared with a wide range of single and mixed amphiphilic compounds. The flexibility of adjusting the chemical composition of coacervates can be advantageous in providing a range of selectivity in extraction. In this chapter, partitioning and extraction patterns of two sample proteins, an acidic and a basic protein into different types of complex and simple coacervates with different types of surfactants have been examined.

Experimental Section

Materials

Anionic surfactant Sodium Dodecyl Sulfate (SDS, $C_{12}H_{25}OSO_3Na^+$) and cationic surfactant cetyltrimethylammonium bromide (CTAB, $CH_3(CH_2)_{15}N^+(CH_3)_3Br^-$) were purchased from Affymetrix USB corporation, “Ultrapure” (Cleveland, OH). 1,1,1,3,3,3-hexafluoropropanol(HFIP) , $\geq 99\%$, was purchased from TCI America. The zwitterionic surfactant 3-(N,N-dimethylmyristylammonio) propane sulfonate (DMMAPS) and sodium sulfate were purchased from Sigma Aldrich. Hydrochloric acid certified ACS plus, was purchased from Fisher Chemicals. Bovine serum albumin, Fraction V and cytochrome c Type IV from bovine heart were purchased from Sigma.

Methods

Sample preparation

The coacervate sample was prepared by mixing one or two concentrated stock solutions of SDS, CTAB, DMMAPS (Fig. 3-1), Na_2SO_4 , hydrochloric acid, Tris buffer, and sodium hydroxide with HFIP. Stock solutions of the model soluble protein, BSA, was first prepared in water and the protein was then extracted into coacervates for determination of partition coefficients. All samples were mixed by vortexing for 2min and centrifuged at 14,000g for 30min. Subsequently the two liquid phases were separated carefully. To measure the concentration of BSA in both phases, blank coacervates were prepared to do background subtraction in fluorescence measurements. The bottom coacervate was diluted with 1-propanol to adjust the fluorescence signal within the linear calibration range.

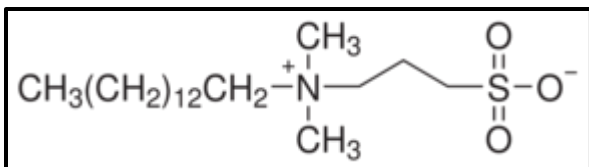


Figure 3-1. Structure of DMMAAPS

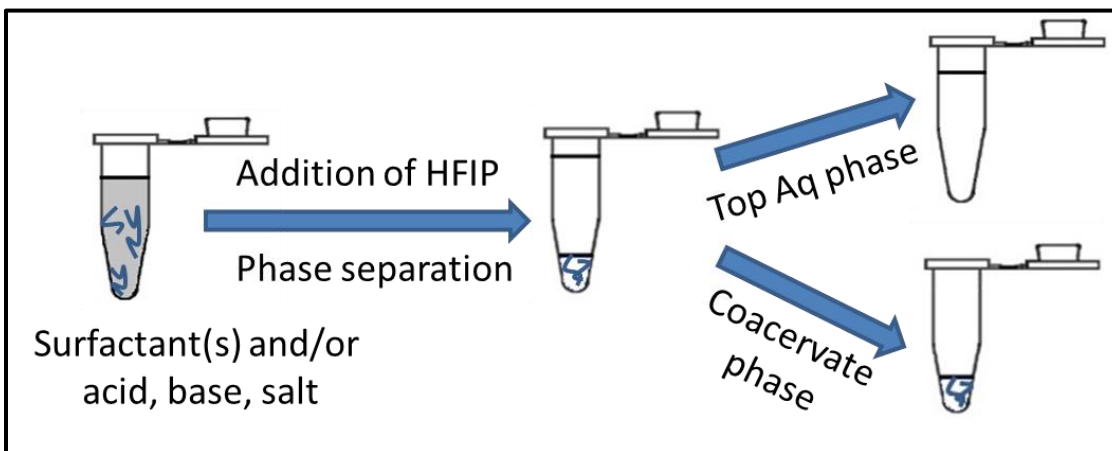


Figure 3-2. Scheme of preparation of complex or simple coacervate samples to extract proteins

The illustration of how to prepare simple or complex coacervate is shown below in Figure3-2. The bottom coacervate phase has much smaller volume than aqueous phase which provides pre-concentration and selective extraction simultaneously. The preparation is simple and fast with high extraction capability.

Determination of protein concentration

The protein concentration was determined by using fluorescence measurements. The emission spectra of BSA in different ATPS were obtained using HORIBA Scientific FluoroMax-4 spectrofluorometer to determine the concentration of the protein. The data was collected and analyzed by FluorEssence software. For each PFAIC system, a separate calibration curve was determined. The excitation wavelength for BSA was 280nm and emission wavelength was 328nm. All measurements were carried out with sample placed in a 1cm quartz cuvette.

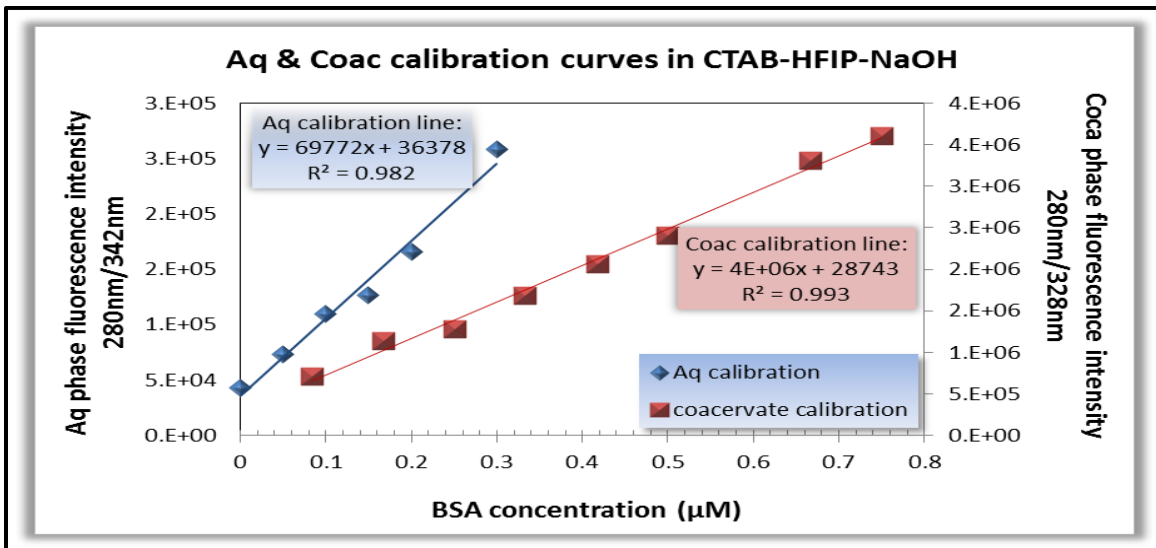


Figure 3-3. Calibration curves of BSA in both Aq and coacervate phase made of 66.7mM total concentration of CTAB-NaOH- 25% v/v HFIP

Results and Discussion

Partitioning behavior and extraction of proteins into the complex PFAIC of SDS-CTAB-HFIP can be controlled by adjusting the chemical composition of the phase as defined by surfactants concentration and mole ratio, pH, and concentration of HFIP. Figure 3-4 shows six images of partitioning of cytochrome c into the SDS-CTAB-HFIP coacervates with different surfactant mole ratios and HFIP concentration. The composition of the surfactant-rich phase was varied in SDS:CTAB mole ratio that included a cationic-rich (3:7 SDS-CTAB), an equimolar (1:1) and an anionic-rich (7:3) phase at two different HFIP concentrations. At one composition, there was no coacervation. Cytochrome c is a water soluble protein with a pI~10 that can be visually observed by its red color that is due to the presence of a heme group, which is a highly-conjugated ring system covalently bonded to protein structure.

With the exception of one composition (3:7 SDS-CTAB and 20% HFIP, tube 5 in Fig 3-4), coacervation was observed at other compositions. The images clearly show the presence of a coacervate bottom phase and a surfactant-lean aqueous top phase. The most striking observation is the strong interaction of the positively charged Cyt C protein with the anionic-rich (7:3 SDS-CTAB with 10% HFIP, tube 3 and at 20% HFIP, tube 6). This clearly shows the strong impact of electrostatic interaction on proteins partitioning and extraction patterns. At other compositions, the protein either precipitated at the interface or interacted to a smaller extent with the coacervate phase. For example, Tube 1 (1:1 SDS-CTAB, 10% HFIP) illustrates that the protein has remained in the top phase with little interaction with the

coacervate phase. This is apparently due to protein precipitation at the interface. Increasing the HFIP to 20% solubilized the protein and there is some interaction with the coacervate phase as evident from the colorful bottom phase in tube 4.

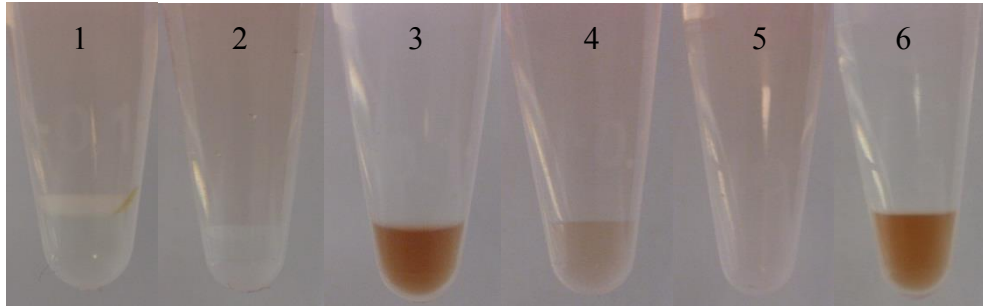


Figure 3-4. Extraction of cytochrome c with different composition of SDS-CTAB HFIP

Table 3-1. Composition of tube 1-6 in Figure 3-4 and observation

#Tube	Total concentration of surfactants	Mole ratio SDS:CTAB	% HFIP	Observation
1	90mM	1:1	10	Precipitation
2	90mM	3:7	10	Less precipitation
3	90mM	7:3	10	Two phases
4	80mM	1:1	20	Clear two phase
5	80mM	3:7	20	Clear one phase
6	80mM	7:3	20	Clear two phase

The net charge of proteins has a significant effect on their extent of interaction with the coacervate phase. Thus, selectivity of protein distribution between the top Aq phase and bottom coacervate phase could be controlled by adjusting the pH of the media. For example, consider the near complete extraction of the positively charged Cyt C into the anionic-rich 7:3 SDS-CTAB-HFIP coacervate in tube 3. Addition of NaOH leads to back extraction of the negatively charged protein into the top aqueous phase (Fig 3-5). On the other hand, addition of HCl enhances the Cyt C interaction with the coacervate phase (Fig 3-5). Another interesting observation is the effect of addition of NaOH to tube 5 in Fig 4. As mentioned earlier, the 3:7 SDS-CTAB mixture with 20% HFIP does not form coacervate. However, addition of NaOH to this mixture results in coacervate formation and concomitant partitioning of the negatively charged Cyt C with the cationic-rich coacervate phase (Fig. 3-5). In addition to the complex coacervate system, we have also discovered that perfluorinated alcohols can induce simple coacervation in aqueous solutions of individual surfactants. For example, HFIP can induce coacervation and phase separation in aqueous solutions of CTAB at pH values at or above neutral; i.e. with the addition of a buffer (e.g. Tris or Phosphate) or with simple addition of NaOH. A hypothesis is that at around neutral and basic pH values, HFIP begins to deprotonate and forms negatively charged FIP⁻ ions, which interacts electrostatically with cationic CTA⁺ ions. The underlying reason of how electrostatic complexation leads to coacervation and phase separation remains unknown.

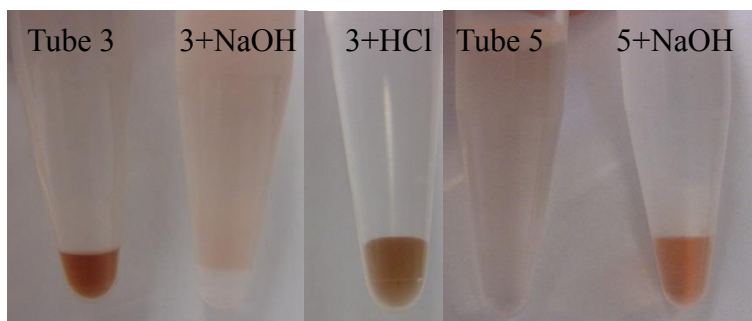


Figure 3-5. Extraction of cytochrome c with addition of NaOH or HCl in complex PFAIC: tube3, SDS/CTAB =7:3, 10% v/v HFIP, addition of 100 μ l 1.0M NaOH or 100 μ l 5.0M HCl into total volume of 1.0ml coacervates. Coacervate formation in SDS/CTAB=3:7, 20%HFIP (tube 5) with addition of 100 μ l 1.0M NaOH

In another set of experiments, we investigated the partitioning behavior of an acidic protein, bovine serum albumin (BSA, pI=4.7) in one complex and three simple PFAIC as well as the two phase Aq (Na₂SO₄)-HFIP systems. To measure protein's partition coefficients in the selected coacervate phases the concentration of protein in each of the two phases was determined by fluorescence spectroscopy. Bovine serum albumin has tryptophan and tyrosine residues which can be excited at 280nm. Fluorescence signal was measured at 330 nm. Due to high enrichment of BSA in the coacervate phases, the protein samples from the coacervate phase had to be diluted at least 15 times prior to fluorescence measurements. Separate calibration curves have been built for each of the aqueous and coacervate phases (See Figs 7-20 in the supplemental section).The partition coefficients of BSA in different phases are listed in Table 3-2. Equations 1, 2, 3 and 4 were used to determine extraction efficiency R

(%), partition coefficient K, capacity factor CF, and enrichment factor EF. Equation 5 shows the relationship between extraction efficiency and capacity factor (CF):

$$\text{Equation 1: } R(\%) = \frac{C_{CA} V_{CA}}{C_0 V_0}$$

$$\text{Equation 2: } K = \frac{C_{CA}}{C_{Aq}}$$

$$\text{Equation 3: CF (capacity factor)} = \frac{C_{CA} \times V_{CA}}{C_{Aq} \times V_{Aq}}$$

$$\text{Equation 4: } EF = \frac{C_{CA}}{C_{initial}} = \frac{1 + \frac{V_{CA}}{V_{Aq}}}{1 + \frac{V_{CA}}{K \times V_{Aq}}}$$

$$\text{Equation 5: } \frac{1}{R} = \frac{1}{CF} + 1$$

Table 3-2. Partition coefficients and Extraction Parameters of BSA in simple PFAIC

Types of ATPS	Composition of ATPS	V_{CA}/V_{Aq}	R(%)	K	CF	EF
SDS-CTAB-HFIP	45mM 1:1 SDS/CTAB, 10% v/v HFIP	0.020	58.6%	69.3	1.4	29.6
CTAB-HFIP	66.7mM CTAB and NaOH, 25% v/v HFIP	0.153	95.9%	87.6	13.5	6.98
CTAB-HFIP	50mM CTAB, 10% v/v HFIP, 0.195M Tris	0.063	87.0%	104.4	6.7	14.5
SDS-HCl-HFIP	50mM SDS, 4M HCl, 10% v/v HFIP	0.062	73.1%	37.8	2.3	12.1
DMMAPS-HFIP	50mM DMMAPS, 10% v/v HFIP	0.073	83.5%	69.4	5.1	12.3
Na ₂ SO ₄ -HFIP	0.45M Na ₂ SO ₄ , 10% v/v HFIP	0.072	69.4%	36.8	2.6	10.8

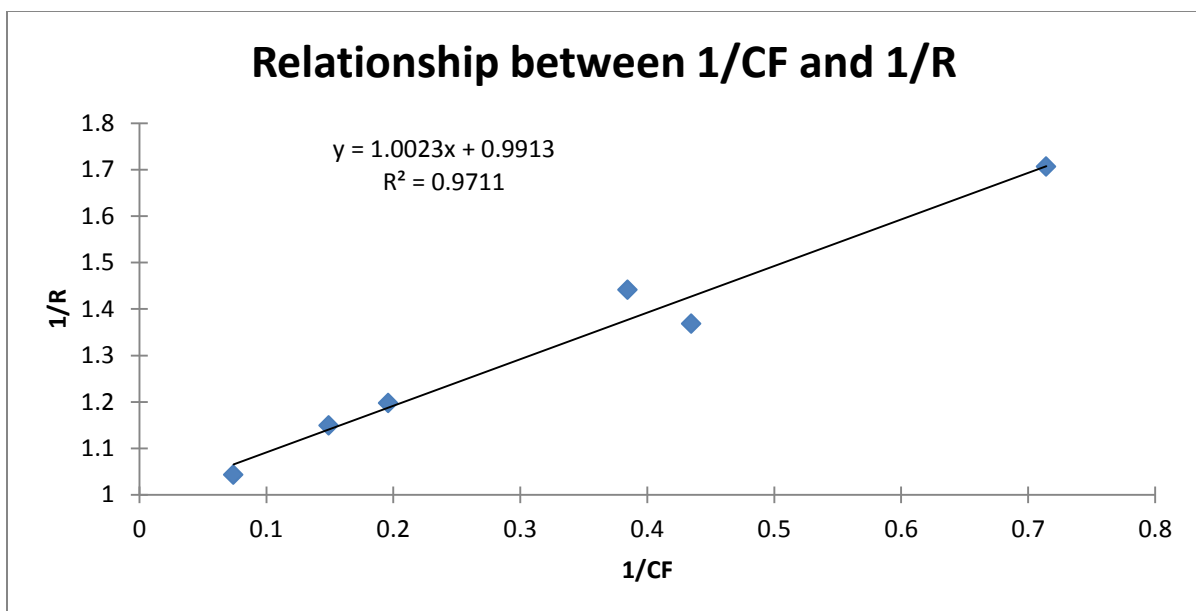


Figure 3-6. Experimental linear relationship between 1/CF and 1/R

Where C_{CA} is concentration of protein in coacervate phase and V_{CA} is volume of coacervate phase. C_0 and V_0 are the total concentration of protein and volume of ATPS. C_{Aq} is concentration of protein in aqueous phase. The extraction efficiency of BSA in complex and simple ATPS varies from 58.6% to 95.9% and K ranges from 36.8 to 104.4 that indicates strong interaction between the hydrophilic, soluble protein and all the coacervates as well as the two phase Aq-HFIP system. The other interesting result is the extraction efficiency that depends on partition coefficient as well as the volume phase ratio. Typically, in liquid – liquid extraction (such as water-organic systems), one have control over the volume of the extracting phase. Thus, one can achieve extraction efficiencies near 100% when partition coefficients are within 40-100 by adjusting the volume phase ratio around or greater than

one. However for coacervate systems, there is little control over the volume of the coacervate phase, thus the extraction efficiencies are smaller than 100%. The smaller volumes of coacervate phases combined with high partition coefficients is beneficial in achieving high pre-concentration or enrichment factors (see table 3-2). Capacity Factor (CF) is a newly defined concept that incorporates the phase volume ratio effect and is a measure of solute affinity for the coacervate phase. CF varies from 1.4 to 13.6 and the volume ratio differs from 0.02 to 0.153. CF shows strong capability of coacervate phase in extracting and containing protein molecules within a relatively small volume, e.g. more than half of the protein concentrated in one fiftieth of the total volume. The correlation between $1/CF$ and $1/R$ shows linear relationship as shown in Figure3-6, reflecting the theoretical correlation as shown in Eq.5. The overall trend in BSA interaction can be rationalized on the basis of electrostatic effects. For example, the strong interaction between BSA that carries a net negative charge at $pH > 5$ with CTAB coacervates is indicative of the favorable electrostatic attraction. On the other hand, the protein interaction with other coacervate phases that are not charged is much smaller. Nonetheless, partition coefficients in these phases range from ~40-70, which still shows strong interactions with the coacervate or HFIP phase. Clearly, hydrophobic and other types of interactions (like H-bonding) also play important roles. Interestingly, BSA partition coefficient into the complex SDS-CTAB-HFIP coacervate is the same as that into the simple coacervate made of zwitterionic surfactant DMMAPS, which may suggest that these phases have very similar hydrophobicity. An advantage of simple coacervates over complex systems is the feasibility of removal of surfactant following the extraction process as discussed in Chapter 4. The SDS-HCl-HFIP coacervate is essentially a

nonionic system, which apparently provides the same interactive properties as Aq(Na₂SO₄)-HFIP in extracting BSA. It has been reported by D. Pérez-Bendito et al. [13] that addition of a strong acid such as HCl could induce cloud point separation with surfactants, such as SDS. We have found that HFIP could decrease the cloud point temperature.

Conclusion

Complex PFAIC systems have shown flexibility in controlling extraction selectivity by adjustment of chemical composition of the phase as defined by mole ratio between anionic and cationic surfactant, concentration of HFIP, or by altering the solution pH. The alternative of using simple coacervates composed of a single surfactant could be equally powerful with significant degree of flexibility of changing the composition through selection of different surfactant types. The simple PFAIC systems have the advantage of simplicity, especially feasibility of recovery of protein from the coacervate phase, which is the subject of investigation presented in Chapter 4.

References

- [1] H. Everberg, U. Sivars, C. Emanuelsson, C. Persson, A.-K. Englund, L. Haneskog, P. Lipniunas, M. Jönstam-Karlsson, and F. Tjerneld, "Protein pre-fractionation in detergent-polymer aqueous two-phase systems for facilitated proteomic studies of membrane proteins," *Journal of Chromatography A*, vol. 1029, no. 1–2, pp. 113–124, Mar. 2004.
- [2] U. Sivars and F. Tjerneld, "Mechanisms of phase behaviour and protein partitioning in detergent/polymer aqueous two-phase systems for purification of integral membrane proteins¹¹This work was carried out in the Swedish Center for Bioseparation.," *Biochimica et Biophysica Acta (BBA) - General Subjects*, vol. 1474, no. 2, pp. 133–146, Apr. 2000.
- [3] F. H. Quina and W. L. Hinze, "Surfactant-Mediated Cloud Point Extractions: An Environmentally Benign Alternative Separation Approach," *Industrial & Engineering Chemistry Research*, vol. 38, no. 11, pp. 4150–4168, Nov. 1999.
- [4] W. L. Hinze and E. Pramauro, "A Critical Review of Surfactant-Mediated Phase Separations (Cloud-Point Extractions): Theory and Applications," *Critical Reviews in Analytical Chemistry*, vol. 24, no. 2, pp. 133–177, Jan. 1993.
- [5] K. S. M. S. Raghavarao, T. V. Ranganathan, N. D. Srinivas, and R. S. Barhate, "Aqueous two phase extraction-an environmentally benign technique," *Clean Technologies and Environmental Policy*, vol. 5, no. 2, pp. 136–141, Jul. 2003.

- [6] F. H. Quina and W. L. Hinze, "Surfactant-Mediated Cloud Point Extractions: An Environmentally Benign Alternative Separation Approach," *Industrial & Engineering Chemistry Research*, vol. 38, no. 11, pp. 4150–4168, Nov. 1999.
- [7] A. Zaslavsky, N. Gulyaeva, and B. Zaslavsky, "Peptides partitioning in an aqueous dextran–polyethylene glycol two-phase system," *Journal of Chromatography B: Biomedical Sciences and Applications*, vol. 743, no. 1, pp. 271–279, 2000.
- [8] R. A. Curtis and L. Lue, "A molecular approach to bioseparations: Protein–protein and protein–salt interactions," *Chemical Engineering Science*, vol. 61, no. 3, pp. 907–923, Feb. 2006.
- [9] W. L. Hinze and E. Pramauro, "A Critical Review of Surfactant-Mediated Phase Separations (Cloud-Point Extractions): Theory and Applications," *Critical Reviews in Analytical Chemistry*, vol. 24, no. 2, pp. 133–177, Jan. 1993.
- [10] C. L. Cooper, P. L. Dubin, A. B. Kayitmazer, and S. Turksen, "Polyelectrolyte–protein complexes," *Current Opinion in Colloid & Interface Science*, vol. 10, no. 1–2, pp. 52–78, Aug. 2005.
- [11] T. Lu, Z. Li, J. Huang, and H. Fu, "Aqueous Surfactant Two-Phase Systems in a Mixture of Cationic Gemini and Anionic Surfactants," *Langmuir*, vol. 24, no. 19, pp. 10723–10728, Oct. 2008.
- [12] R. Chollakup, W. Smitthipong, C. D. Eisenbach, and M. Tirrell, "Phase Behavior and Coacervation of Aqueous Poly(acrylic acid)–Poly(allylamine) Solutions," *Macromolecules*, vol. 43, no. 5, pp. 2518–2528, Mar. 2010.

- [13] I. Casero, D. Sicilia, S. Rubio, and D. Pérez-Bendito, "An Acid-Induced Phase Cloud Point Separation Approach Using Anionic Surfactants for the Extraction and Preconcentration of Organic Compounds," *Analytical Chemistry*, vol. 71, no. 20, pp. 4519–4526, Oct. 1999.
- [14] B. Mohanty and H. B. Bohidar, "Systematic of Alcohol-Induced Simple Coacervation in Aqueous Gelatin Solutions," *Biomacromolecules*, vol. 4, no. 4, pp. 1080–1086, Jul. 2003.
- [15] P. Weschayanwivat, O. Kunanupap, and J. F. Scamehorn, "Benzene removal from waste water using aqueous surfactant two-phase extraction with cationic and anionic surfactant mixtures," *Chemosphere*, vol. 72, no. 7, pp. 1043–1048, Jul. 2008.
- [16] D. M. Morré and D. J. Morre, "Aqueous two-phase partition applied to the isolation of plasma membranes and Golgi apparatus from cultured mammalian cells," *Journal of Chromatography B: Biomedical Sciences and Applications*, vol. 743, no. 1, pp. 377–387, 2000.
- [17] S. Luche, V. Santoni, and T. Rabilloud, "Evaluation of nonionic and zwitterionic detergents as membrane protein solubilizers in two-dimensional electrophoresis," *PROTEOMICS*, vol. 3, no. 3, pp. 249–253, Mar. 2003.
- [18] A. De Palma, A. Roveri, M. Zaccarin, L. Benazzi, S. Daminelli, G. Pantano, M. Buttarello, F. Ursini, M. Gion, and P. L. Mauri, "Extraction methods of red blood cell membrane proteins for Multidimensional Protein Identification Technology (MudPIT) analysis," *Journal of Chromatography A*, vol. 1217, no. 33, pp. 5328–5336, Aug. 2010.

- [19] M. G. Khaledi, S. I. Jenkins, and S. Liang, "Perfluorinated Alcohols and Acids Induce Coacervation in Aqueous Solutions of Amphiphiles," *Langmuir*, vol. 29, no. 8, pp. 2458–2464, Feb. 2013.
- [20] I. Casero, D. Sicilia, S. Rubio, and D. Pérez-Bendito, "An Acid-Induced Phase Cloud Point Separation Approach Using Anionic Surfactants for the Extraction and Preconcentration of Organic Compounds," *Analytical Chemistry*, vol. 71, no. 20, pp. 4519–4526, Oct. 1999.

Supplemental Data

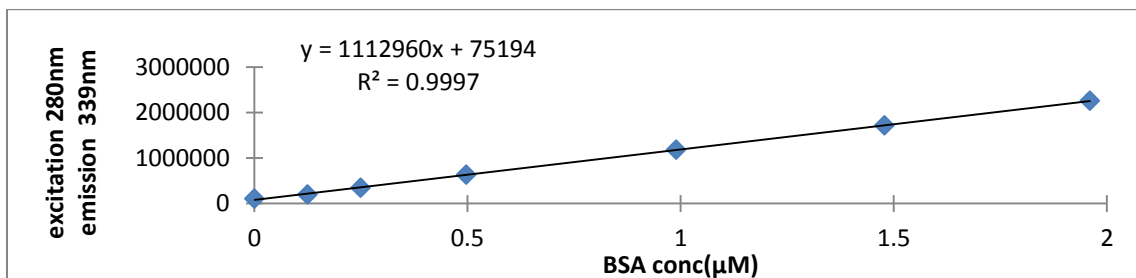


Figure 3-7. Calibration curve of BSA in Aqueous phase of 1:1 100mMSDS:100mM CTAB, 10% v/v HFIP complex coacervation

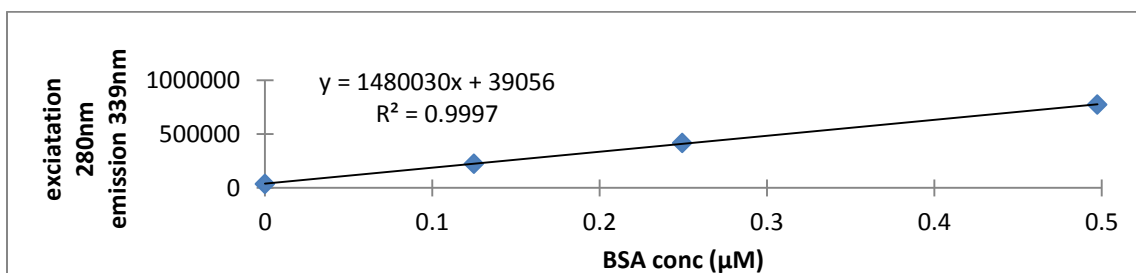


Figure 3-8. Calibration curve of BSA in coacervate phase of 1:1 100mM SDS:100mM CTAB, 10% v/v HFIP complex coacervation

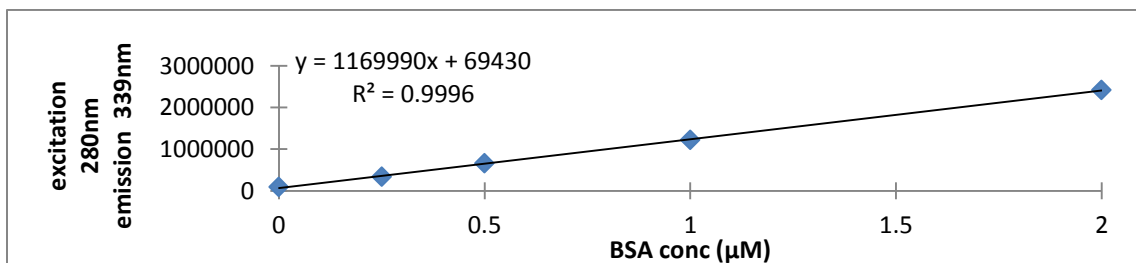


Figure 3-9. Calibration curve of BSA in Aqueous phase of 1:1 50mMSDS:50mMCTAB, 10% v/v HFIP complex coacervation

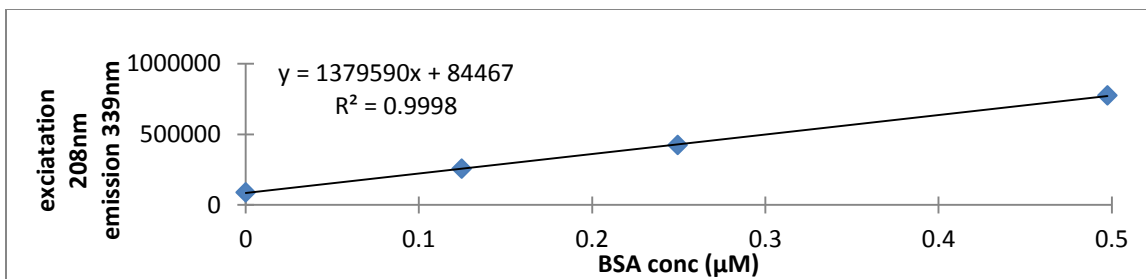


Figure 3-10. Calibration curve of BSA in coacervate phase of 1:1 50mM SDS:50mM CTAB, 10% v/v HFIP complex coacervation

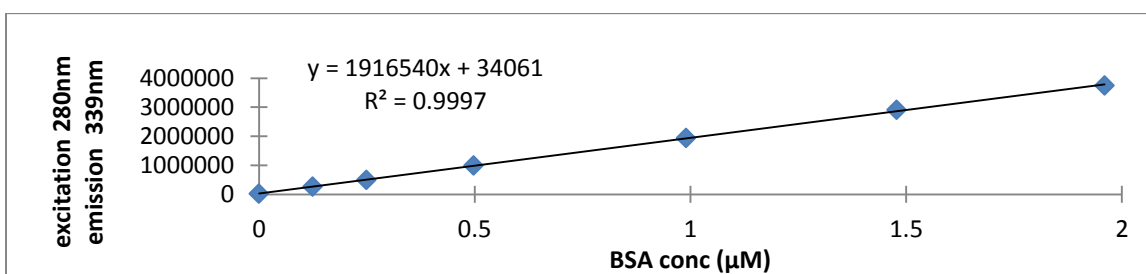


Figure 3-11. Calibration curve of BSA in Aqueous phase of 1:1 20mMSDS:20mMCTAB, 10% v/v HFIP complex coacervation

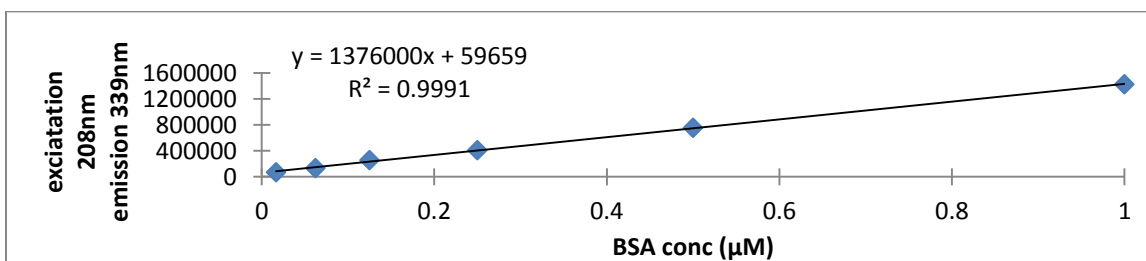


Figure 3-12. Calibration curve of BSA in coacervate phase of 1:1 20m MSDS:20mM CTAB, 10% v/v HFIP complex coacervation

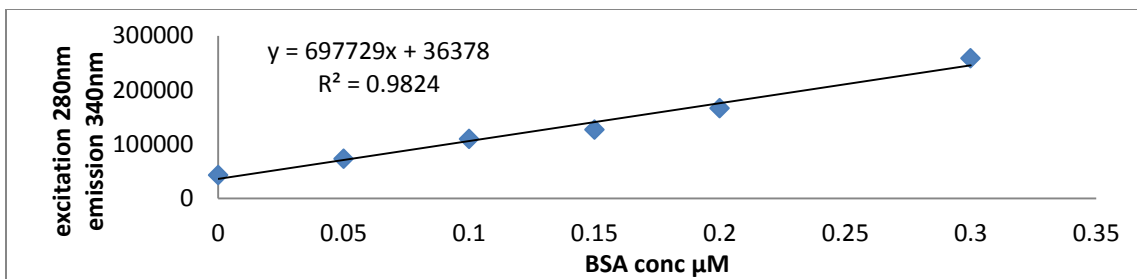


Figure 3-13. Calibration curve of BSA in Aq phase of 1:1 100mMCTAB:100mM NaOH, 25% v/v HFIP simple ATPS

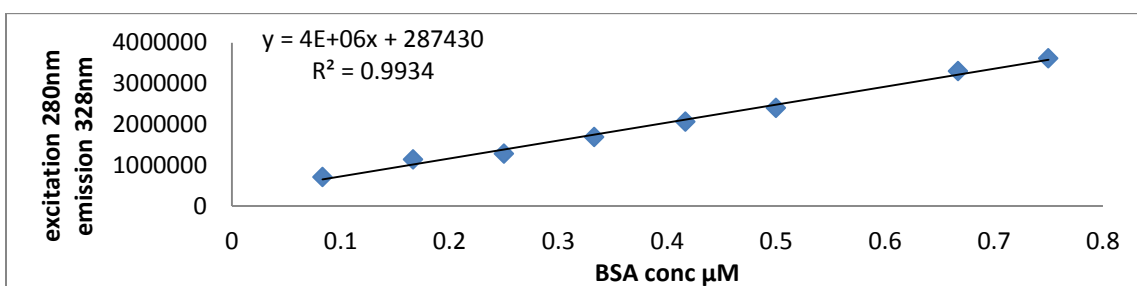


Figure 3-14. Calibration curve of BSA in coac phase of 66.7mMCTAB in 66.7mM NaOH, 25% v/v HFIP simple ATPS

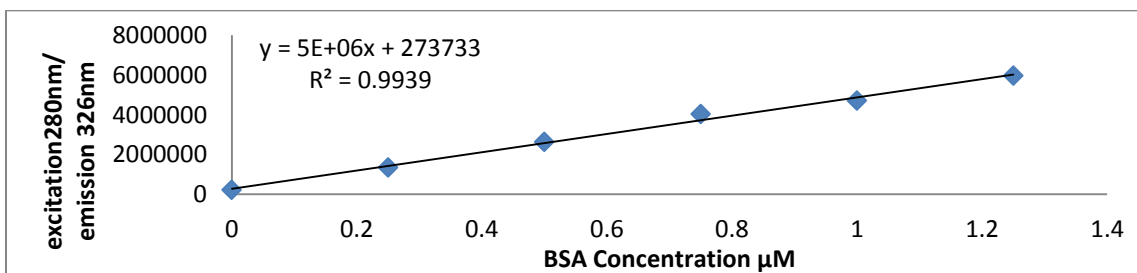


Figure 3-15. Calibration curve of BSA in coacervate phase of 50mM CTAB in 0.195M Tris buffer with 10% v/v HFIP

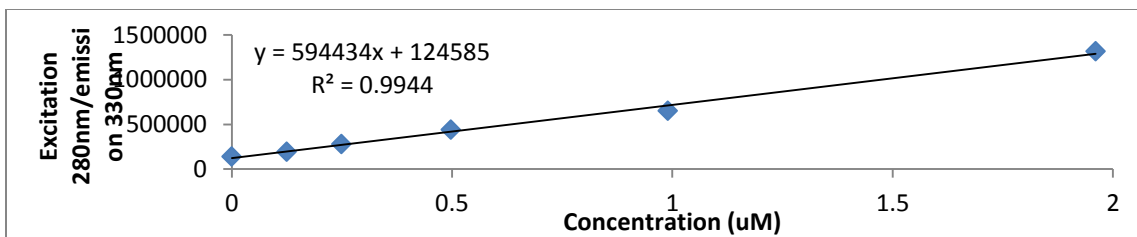


Figure 3-16. Calibration curve of BSA in coacervate phase of 50mM DMMAPS in 10% v/v HFIP

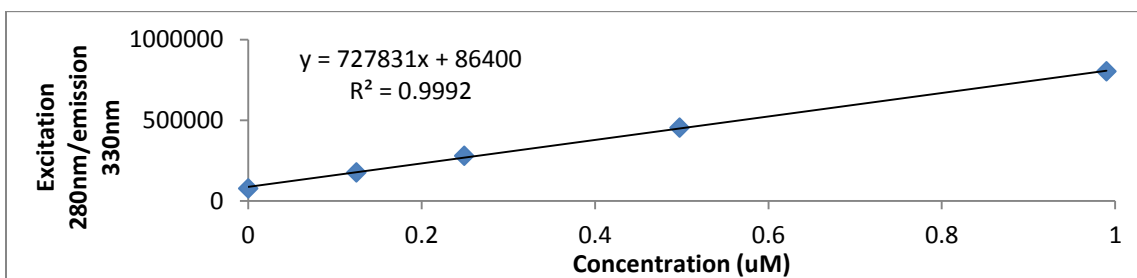


Figure 3-17. Calibration curve of BSA in coacervate phase of 50mM SDS in 4M HCl, 10% v/v HFIP

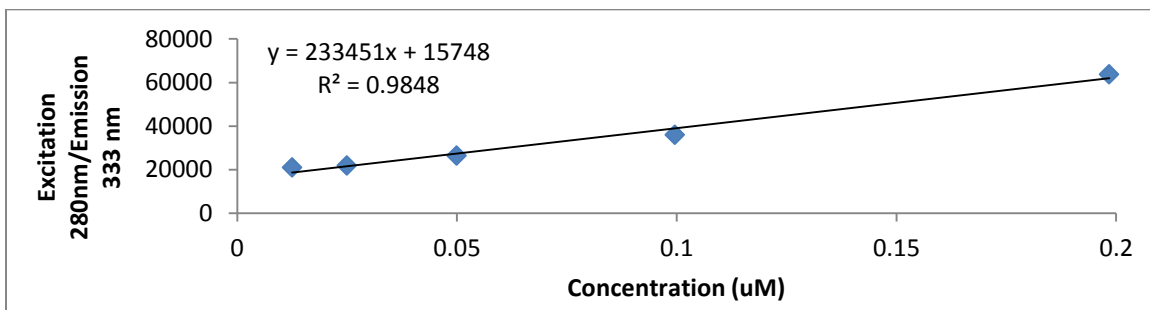


Figure 3-18. Calibration curve of BSA in Aq phase of 50mM SDS in 4M HCl, 10% v/v HFIP

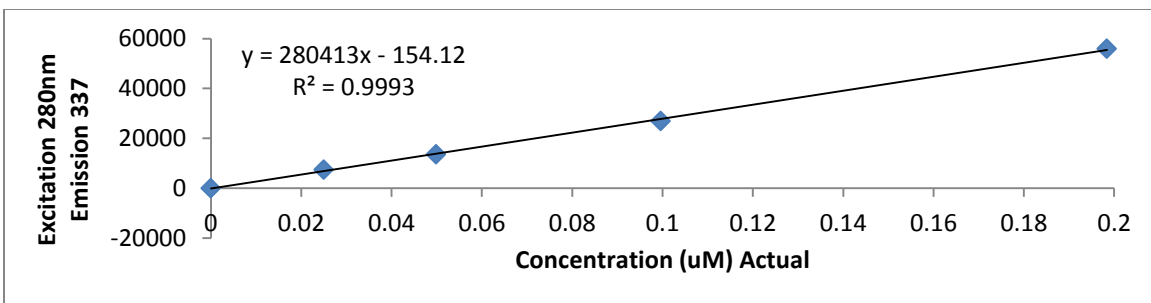


Figure 3-19 Calibration curve of BSA in Aq phase of 0.45M Na₂SO₄ in 10% v/v HFIP

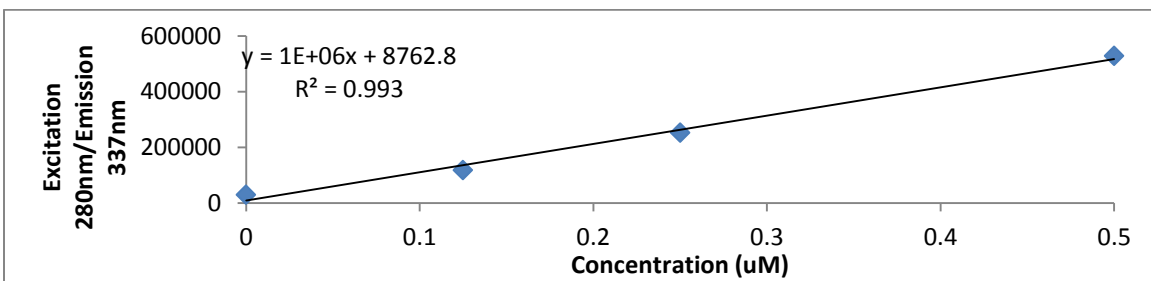


Figure 3-20 Calibration curve of BSA in bottom phase of 0.45M Na₂SO₄ in 10% v/v HFIP

Table 3-3. SDS-HCl-HFIP acid induced cloud point two phase system

HFIP	HCl	phase	HFIP	HCl	phase	HFIP	HCl	phase
10%	1.22	1	11%	1.20	1	12.2%	1.19	1
10%	1.83	1	11%	1.81	1	12.2%	1.79	1
10%	2.135	1	11%	2.11	1	12.2%	2.08	1
10%	2.318	1	11%	2.29	1	12.2%	2.26	1
10%	2.44	1	11%	2.41	1	12.2%	2.38	1
10%	3.05	1	11%	3.01	1	12.2%	2.98	1
10%	3.66	1	11%	3.61	1	12.2%	3.57	1
10%	4.27	1	11%	4.22	1	12.2%	4.17	2
10%	4.88	1	11%	4.82	1	12.2%	4.76	2

Perez-Bendito[20] reported that with HCl(>4M) and SDS(>0.25% w/v), there is liquid-liquid two phase separation under room temperature. However, under our lab room temperature, no phase separation is observed. At 37 degrees in oven, many small oil-drops are formed but they disappear immediately after taken out to get centrifuged. When adding HFIP(15% v/v), SDS-HCl-HFIP has two phase separation. Below is the chart of how concentration of HCl and percentage of HFIP (v/v) make a difference of phase formation. 12% HFIP is a dividing line to have phase separation at lab temperature when concentration of HCl is higher than 4M. SDS concentration is 50mM which is 1.44% w/v. Moreover, 10% HFIP-4.27M HCl-1.44% SDS is clear one phase at lab temperature but is cloudy when heating up to 37 Celsius, and ultimately it forms two liquid phase at higher temperature. 10% HFIP-4.88M HCl-1.44% SDS forms two phases at 37 degrees. It is concluded that SDS-HCl-HFIP is an acid induced cloud point two phase system as well, in which HFIP lowers down the transition temperature and makes it possible to for cloud point separation at lab temperature with HFIP >12.2% & HCl>4M.

Table 3-4. Observation of cytochrome c extraction in SDS/HCl/HFIP system

Cytochrome C (100 μ M)	SDS (100mM)	HCl (12M)	HFIP %	observation
0	100 μ l	20 μ l	20 μ l 14.3%	No phase separation
0	100 μ l	20 μ l	30 μ l 20%	Phase separation
10 μ l	100 μ l	20 μ l	30 μ l 18.75%	No phase separation
10 μ l	100 μ l	30 μ l	30 μ l 17.65%	Phase separation, cytochrome c extracted to bottom phase

Anionic SDS is used to make phase separation with HFIP and HCl and to extract protein. At low pH, positively charged Cytochrome c is added in and red color is observed at bottom phase.

Table 3-5. Observation of cytochrome c extraction in CTAB-HFIP-Tris system

The CTAB/HFIP system could be used to extract protein based on both electrostatic attraction and hydrophobic interaction. Two proteins are selected to do the experiment – BSA (66kDa, pI=4.7) and cytochrome C (12kD, pI=10-10.5).

Protein extracted	composition	Observation
Cytochrome C pI~10 (positively charged at pH6.8)	50mM CTAB, Tris, pH6.8, 10% HFIP	Red color at top phase, cytochrome C not extracted into bottom phase
BSA pI~4.7 (negatively charged at pH6.8)	50mM CTAB, Tris, pH6.8 10%HFIP	87%BSA extracted into bottom phase. BSA is hardly detectable in Aq phase.

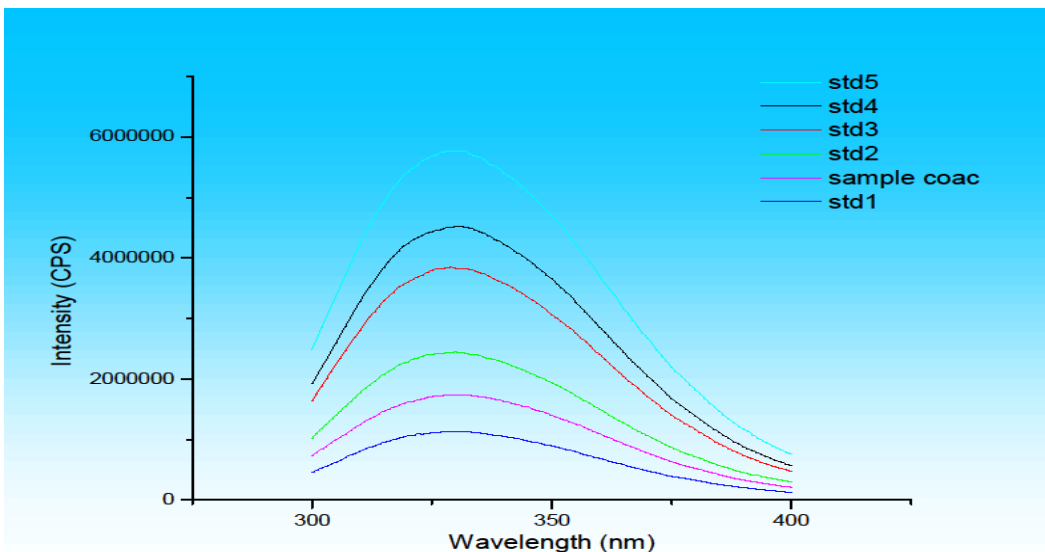


Figure 3-21. Emission Spectrum of BSA in coacervate phase of 50mM CTAB in 0.195M Tris buffer, 10% v/v HFIP. Excitation wavelength is 280nm.

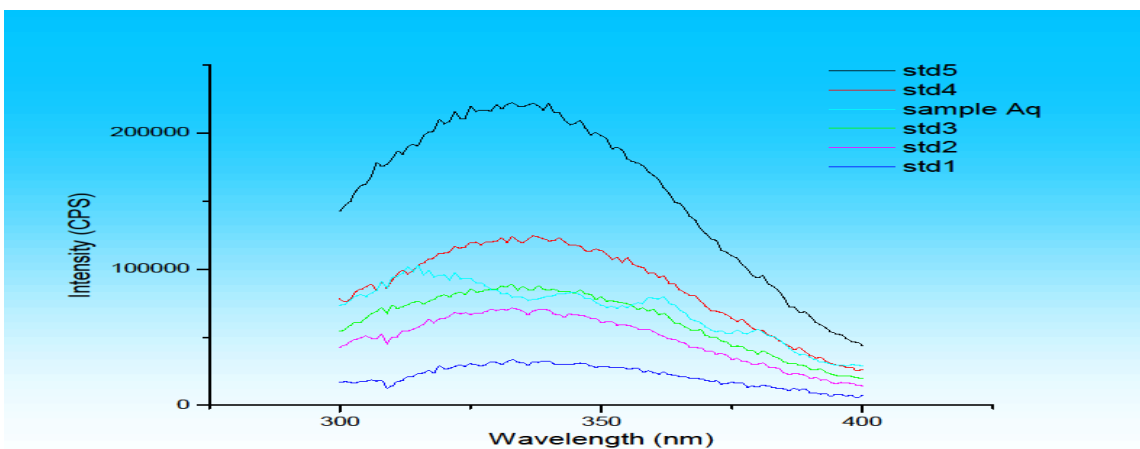


Figure 3-22. Emission spectra of BSA standard solutions in the Aq phase of CTAB-HFIP-NaOH

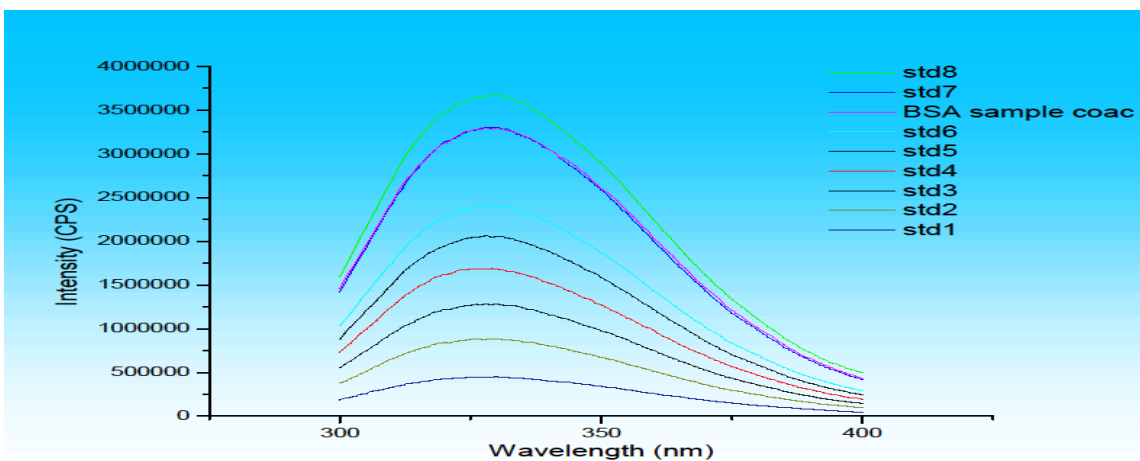


Figure 3-23. Fluorescence spectra of BSA in coacervate sample and standards. The coacervate phase of CTAB-HFIP-NaOH is diluted by 1-propanol with 15 dilution factor. The 8 standards' spectra correspond to 8 standards' points in calibration curve. BSA was excited at 280nm and has maxi emission at 330nm.

Chapter 4

Extraction of Proteins in Perfluorinated Alcohols Induced Coacervates: Strategies for Removal of Surfactants, Gel Electrophoresis, and LC-MS Analysis for Peptide Mapping

Abstract

Aqueous two phase systems (ATPS) which contain a surfactant-rich coacervate phase and a surfactant-lean phase are under investigation for their utility in the extraction and pre-concentration of protein mixtures[1][2][3][4]. In the process of recovering protein mixtures from highly concentrated surfactant-rich phase, different approaches are discussed here such as removal of surfactants using methods such as precipitation of surfactants by removal of fluorinated alcohol from the complex coacervates or lowering the temperature. Another alternative is separating the proteins from the surfactant in the coacervate matrix by gel-electrophoresis or using size-exclusion “spin-columns”, also known as Filter Aided Sample Preparation (FASP) method[5]. . In this chapter, sample treatments before applying to gel electrophoresis or Mass Spectrometry (MS) are discussed. How to introduce coacervate directly to gel electrophoresis is included in discussion. Different sample treatment for simple and complex coacervates are used to remove the surfactants and/or recover the proteins for additional separation and analysis by electrophoresis, LC, and MS. Due to the advantage of hydrophobic environment of coacervates, hydrophobic proteins have higher solubility in coacervate phase which could be used to concentrate and solubilize membrane

proteins. Bacteriorhodopsin is chosen as a sample protein to show some preliminary results in extraction, purification and identification of membrane protein.

Introduction

The word “*Coacervation*” comes from Latin word “*acervus*” with the prefix “*co*” which means heaping together. It was first introduced by Bungenberg de Jong and Kruyt to imply the aggregation of colloidal particles that leads to phase separation in aqueous solutions[6]. The colloidal-rich phase is called coacervate phase. In general, coacervate systems can be classified as Aqueous Two Phase Systems (ATPS) due to presence of high concentrations of water in both the colloidal – rich and colloidal-lean phases [7]. One example of ATPS is simple coacervates made of aqueous solutions of nonionic surfactants above their Cloud Point Temperature (CPT)[8]. Complex coacervates are comprised of two oppositely charged amphiphiles (surfactants, polyelectrolytes, or biopolymers). Another group of ATPS is composed of aqueous solutions of polymers such as dextran and polyethylene glycol (PEG) [9] with each phase containing a different polymer. The formation mechanism of the polymer ATPS is demixing of polymer solutions and is different from coacervation. We have recently reported formation of simple and complex coacervates, and subsequent phase separation in aqueous solutions of a wide variety of amphiphilic molecules containing a small percentage (~1%-10%) of a perfluorinated alcohol or acid. The coacervate phase is rich in amphiphile and has high concentration of the fluoroalcohol. The concentration of water in Perfluorinated

Alcohol Induced Coacervates (PFAIC) is much smaller than other types of ATPS, ~ 5%-35%[10].

The ATPS have been used for extraction of various classes of compounds, especially biomolecules such as proteins. The PFAIC systems provide sites for various types of interaction with solutes such as hydrophobic, electrostatic, hydrogen bonding and dipolar interactions through selection of chemical composition. The PFAIC phases have potentially greater range of extraction selectivity than other types of ATPS.

The presence of the amphiphiles in the coacervate phase can interfere with separation and analytical methodologies such as electrophoresis, HPLC and MS. In this paper, model proteins were extracted into simple and complex PFAIC made of HexaFluoro 2-Propanol (HFIP) and different types of surfactants. Different strategies are examined for removal of surfactants from the coacervates or recovery of proteins through back extraction. For complex coacervates, one strategy involves precipitation of the cationic complex through evaporation of HFIP that has induced the coacervation. Some of the extracted protein(s) that may have precipitated with the cationic complex will then be extracted into a urea solution. A second approach for removing surfactant(s) is through dialysis. Finally, the method known as Filter-Aided Sample Preparation (FASP)[5] can be used. This method involves running the extracted proteins solutions in the coacervate phases through a spin-column and centrifuge to accelerate the filtration of the surfactants and small molecules through the size exclusion gel and recovery of the extracted protein(s) on top of the filter. The use of gel

electrophoresis of proteins extracted into various simple and complex coacervates was also examined.

Materials

Anionic surfactant sodium dodecyl sulfate (SDS, $C_{12}H_{25}OSO_3^-Na^+$) and cationic surfactant cetyltrimethylammonium bromide (CTAB, $CH_3(CH_2)_{15}N^+(CH_3)_3Br^-$) were purchased from Affymetrix USB corporation, "Ultrapure" (Cleveland, OH). Dodecyltrimethyl-ammonium bromide (DTAB, $CH_3(CH_2)_{11}N^+(CH_3)_3Br^-$) $\geq 99\%$ was from sigma. Sodium hexadecyl sulfate (SHS, $C_{16}H_{33}OSO_3^-Na^+$) $\geq 99\%$, sodium octadecyl sulfate (SOS, $C_{18}H_{37}OSO_3^-Na^+$) $\geq 99\%$, and octadecyltrimethylammonium bromide (OTAB, $CH_3(CH_2)_{17}N^+(CH_3)_3Br^-$) $\geq 99\%$, were purchased from Lancaster Synthesis. 1,1,1,3,3,3-hexafluoropropanol(HFIP) $\geq 99\%$, and 2,2,2-Trifluoro ethanol, $\geq 99\%$, were purchased from TCI America. The zwitterionic surfactant 3-(N,N-dimethylmyristylammonio) propane sulfonate (DMMAPS) and sodium sulfate were purchased from Sigma Aldrich. Hydrochloric acid certified ACS plus, was purchased from Fisher Chemicals. Bovine serum albumin, Fraction V was purchased from Sigma. Bacteriorhodopsin from Halobacterium salinarum(lyophilized powder) was purchased from Bras Ded Port S.A., Spain. Gramicidin D was purchased from MP Biomedicals, USA. Tris(hydroxymethyl) aminomethane, 99+% grade for biochemistry, urea(+99%), Triton X-114, acrylamide electrophoresis grade (99+%), biacrylamide (99%), ammonium persulfate(APS, >98% for electrophoresis), N,N,N',N'-tetramethylethylenediamine(TEMED, >99% for electrophoresis) were purchased from sigma-aldrich.

Methods

Gel Preparation for DTAB-PAGE

Stacking gel(4%): 1.537ml H₂O, 0.312ml 0.5M Tris-HCl(pH=10), 25 μ l 10% DTAB(w/v), 0.33ml stock acrylamide (38.96g acrylamide, 1.04g bisacrylamide dissolved in 100ml H₂O), 12 μ l APS(10%), 2.5 μ l TEMED. Resolving gel(12%): 2.54ml H₂O, 1.875ml 1.5M Tris-HCl(pH=8.8), 75 μ l 10% DTAB, 3ml stock acrylamide solution, 37 μ l APS(10%), 5 μ l TEMED. The preparation method was based on CTAB-PAGE protocol[11].

Following the extraction of 2 μ M BSA in the coacervates of in CTAB (42.5mM)-HFIP(15% v/v)-Tris(pH6.8, 0.2M) and DTAB(42.5mM)-HFIP(15% v/v)-Tris(pH6.8, 0.2M), the aqueous top phases of the two PFAIC systems were separated from the corresponding coacervate bottom phases. Detergent-rich bottom phases were dried at 80° C for 6 hours to evaporate HFIP and the remaining solid was diluted in 200 μ l DTAB or CTAB sample buffer for gel running. When running DTAB-PAGE, the polarity of the electrodes was reversed.

Extraction and recovery of BSA from complex coacervate

Three complex PFAIC systems composed of the following oppositely charged surfactants were prepared SDS(12C)-CTAB(16C), SHS(16C)-CTAB(16C), and SDS(12C)-OTAB(18C) to extract BSA. 440 μ l of 100mM of the anionic surfactant (SDS or SHS) in water was mixed with 440 μ l of 100mM the cationic surfactant (CTAB or OTAB) in water and with 100 μ l

HFIP, and 20 μ l of 100 μ M BSA in H₂O with a total volume of 1.0 mL were added into 1.5 mL micro centrifuge tube to form ATPS of 88mM SDS-CTAB, 2 μ M BSA, with 10%v/v HFIP. The liquid-liquid two phase systems were centrifuged at mid-high speed for 15min to facilitate mass transfer and distribution of BSA between two phases equilibrated. The top aqueous phases were removed and 20 μ l, 6M urea was combined with the bottom coacervate phase to back extract the protein into urea. The mixture of urea with the coacervate phase was centrifuged at high speed at 4°C for 10min that resulted in formation in a new liquid-liquid phase with the aqueous urea solution forming the top phase of the SDS/OTAB coacervate system. Upon mixing of urea with the SHS/CTAB, the catanionic complex precipitated and the proteins were extracted into the aqueous urea solution. The top liquid phase for each system was transferred to a new tube for DTAB-PAGE experiments.

Extraction of proteins mixture by different PFAIC systems and examined by SDS-PAGE

Extractions of a proteins mixture were performed in three simple PFAIC systems: CTAB/Tris/HFIP, SDS/HCl/HFIP, and DMMAAPS/HFIP; one complex PFAIC, SDS/CTAB/HFIP a liquid-liquid two phase Aq(Na₂SO₄)/HFIP , and the cloud point system of Triton-X 114 as control system. . The mixture was purchased as protein standard ladder and included proteins with a wide range of MW between 14 kDa and 200 kDa and pI range 4-6.18: A-Lactalbumin (Bovinemild) 14.2kDa (pI 4-5), Trypsin Inhibitor(Soybean), 20.1kDa (pI4.6), Carbonic Anhydrase(Bovie) 29kDa (pI6.18), Ovalbumin(egg) 45ka(pI 4.99),

Albumin(Bovine) 66kDa (pI4.7), Phosphorylaseb(rabbitmuscle), 97.4kDa (pI5.9), β -Galactosidase(E. coli.) 116kDa (pI4.6), and Myosin(rabbit muscle) 205kDa (pI5.0-5.3). SDS-PAGE was run to examine the extraction results. The total volume of each of coacervate is 1ml with 10% HFIP except for Triton X 114 that did not contain any HFIP. The salt concentration in the Aq. (Na₂SO₄)/HFIP system was 0.45M while all the coacervates contained 50mM of surfactants in 1ml. Protein mixtures were first dissolved in pure HFIP and a 100 μ l solution of proteins in HFIP was added to each of the first five systems. To make sure the Triton-X 114 has exactly the same amount of protein as other systems, 100 μ l of HFIP with proteins was added into empty tube first, and then the tube was put into water bath to evaporate all the HFIP. After this, 1ml of 17mM Triton X-114 was added to dissolve proteins. At 37°C, solution of Triton X-114 became cloudy and separated into two phases. All protein samples in the PFAIC systems plus Triton X-114 were equilibrated by rotator for 24 hours at 37°C temperature.

Removal of surfactants from PFAIC phase

Coacervate phase was firstly diluted three-fold by HFIP in each of PFAIC. 50 μ l of the diluted PFAIC phase was diluted another four fold with 150 μ l of 70% 2-propanol+30% 0.1M HCl to flow through the 10kDa size exclusion filters by spinning at 10,000g for 20min. Addition of HCl was to help dissolve coacervate phase in solvent. It worked very well when only 70% 2-propanol cannot dissolve complex coacervate. The multiple times of dilutions were to reduce viscosity and increase fluidity. Otherwise, it would take longer time to spin

the solution down through the filter. Then 200µl of solutions above were added to corresponding size exclusion filters to wash surfactants for three more times. 200µl 0.1M Tris buffer (pH 6.8) was added to wash surfactants for two more times. The flow-through solutions were discarded.

Proteins collection step: 50µl 0.1M Tris buffer (pH=6.8) was added onto the filter and vortexed to dissolve the proteins that remained on the filter into solution. A new tube to collect flow-through was replaced and the filter was reversed quickly so that the solution with proteins could be collected. The filters were spun at 10,000g for 20min. Then the collected proteins solutions were loaded onto SDS-PAGE.

Surfactant Removal for LC-MS Analysis

In order to examine the ability of the FASP method for removal of surfactants for LC-MS analysis in proteomics applications, a sample mixture of bacteriorhodopsin (BR) and BSA was extracted into three different simple PFAIC and binary Aq(salt)/HFIP systems.

Protein Preparation: 670 µg purple membrane (75% bacteriorhodopsin and 25% lipids) was dissolved in 100 µl HFIP which gives 193 µM bacteriorhodopsin in HFIP. 100 µM BSA was prepared in H₂O. 10 µl of BR and 10µl BSA solutions were added respectively into each of the four ATPSs (CTAB/Tris/HFIP, SDS/HCl/HFIP, DMMAPS/HFIP, and Na₂SO₄/HFIP). Thus, the starting materials contained BSA=64 µg=1 nmol, BR=6.7 µg/ µl*10 µl*75%=50.25 µg=1.93nmol.

Composition of ATPSs: 0.4M Na₂SO₄/15%HFIP; 50mM CTAB/0.2mM Tris(pH=6.8) /15% HFIP; 50mM SDS/4M HCl/12.5% HFIP; 50mM DMMAPS/(6%TFE and 1% HFIP). The concentration of TFE and DMMAPS was based on DMMAPS phase diagram reported previously.[12]. Samples were vortexed for 2min and centrifuged for 30min at 10,000 rpm on tabletop centrifuge. For each system, the top aqueous phase was separated from the corresponding coacervate or HFIP bottom phase.

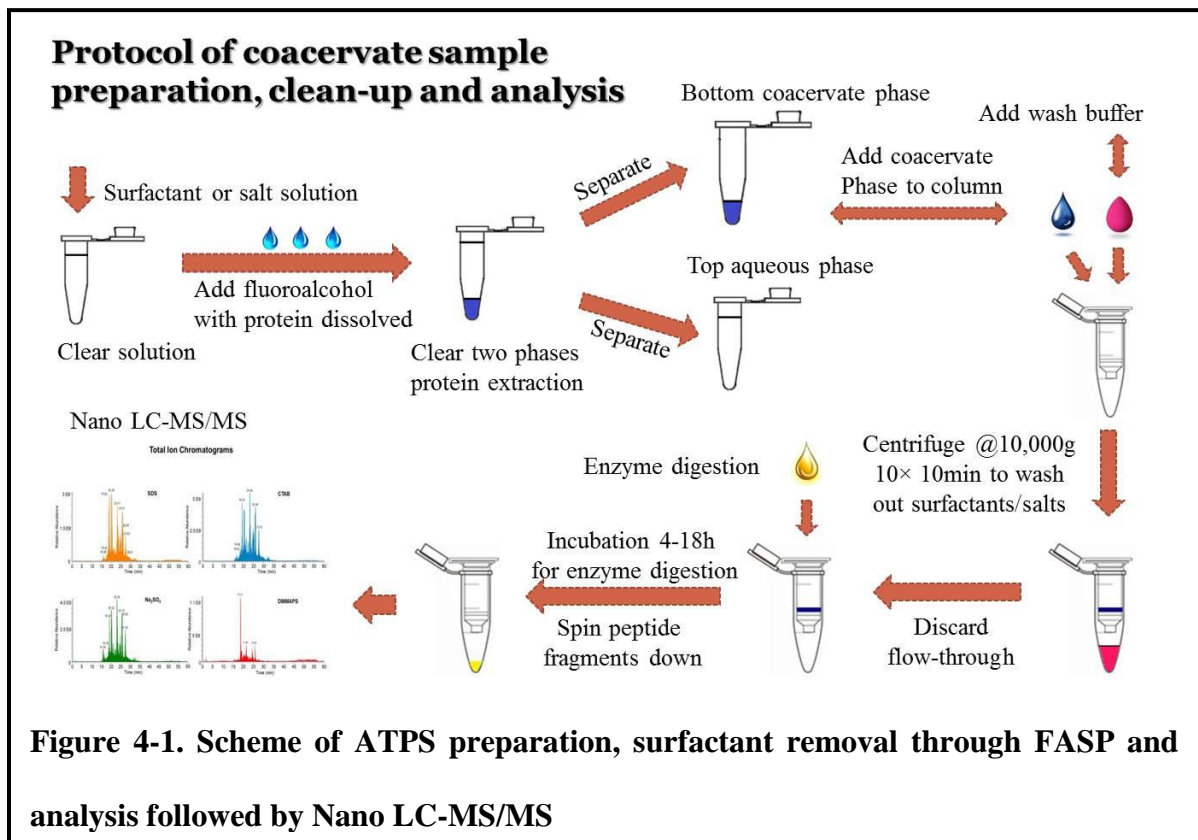


Figure 4-1. Scheme of ATPS preparation, surfactant removal through FASP and analysis followed by Nano LC-MS/MS

The surfactants were removed as described above by FASP method[5]. The remaining proteins on top of size exclusion filter were treated by reduction and alkylation reaction. After that a trypsin digestion of proteins was performed. Reduction: 27 μ l of 0.05M Tris (pH=8) was added onto all four filters with 3 μ l DTT(0.1M). Vortex and store at 56 $^{\circ}$ C for 30min. Alkylation: The solution was spun down after reducing. 100 μ l iodoacetamide (50mM) was added into four filters and incubated in darkness for 20min. 0.01mg/ml trypsin was used to digest protein samples at 37 $^{\circ}$ C for 15.5 hours. Then peptides fragments were dissolved in 50 μ l Tris buffer(pH=8, 0.05M) and spanned down for sample analysis.

Nano LC/MS/MS: Orbit trap Q exactive was used to identify the samples. 10 μ l sample (~200ng) was injected into nano LC-MS/MS, with flow rate of 350nl/min, separated on a C-18 column. Gradient elution was from 5% AcN to 40% AcN in 30min.

Results and Discussion

Direct Introduction of Coacervate Sample in PAGE

In order to separate and characterize proteins extracted into coacervates containing cationic surfactants such as DTAB or CTAB, the usefulness of CTAB-PAGE was investigated. The widely popular SDS-PAGE method is incompatible with direct introduction of samples taken from the coacervate phase containing cationic surfactants. Figure 4-2 shows the gel image when introducing complex coacervate directly SDS-PAGE.

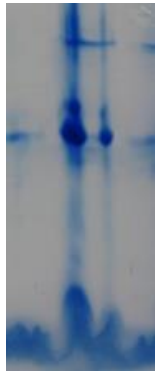


Figure 4-2. SDS-PAGE. BSA extracted into coacervate phase of SDS/CTAB/HFIP

Complex coacervation could precipitate when diluting with sample buffer because of the presence of oppositely charged surfactants. Moreover, the interaction between HFIP and CTAB may cause phase separation at gel running buffer pH. Removal of surfactants is necessary for simple CTAB coacervate to solve this problem. CTAB-PAGE[11] has been reported as a supplement of SDS-PAGE. However, CTAB has a relatively high Krafft point ($\sim 26\text{ }^{\circ}\text{C}$), below which a CTAB micelle solution can transform from liquid to crystalline solid phase. Comparing to CTAB, DTAB has the shorter chain length (C12) and has lower Krafft temperature than CTAB, resulting in larger solubility in water at room temperature. For example, during solution preparation, we observed that a 100mM CTAB solution could go through a phase change from liquid form to crystalline form due to fluctuations in ambient temperature, while 100mM DTAB solution remained stable under the same conditions. Thus, DTAB-PAGE instead of CTAB-PAGE was utilized to run samples containing a cationic

surfactant. Before loading onto a gel, the surfactant-rich phase of a coacervate phase was heated to evaporate HFIP. HFIP must be removed before loading onto gel from sample because it forms phase separation with cationic surfactant DTAB or CTAB at neutral pH. Resolution and band tailing may come from high concentration of DTAB or CTAB in the loading sample which interferes with protein migration. The gels show the possibility of direct introducing CTAB coacervate samples to DTAB-PAGE or CTAB-PAGE. Another possibility is that the overnight heating treatment may have led to degradation of the protein that resulted in protein poor band shape.

SDS-based simple coacervate and salt-based ATPS were investigated for direct application on gel electrophoresis. Thus, we put our emphasis on simpler ATPSs, such as SDS/HCl/HFIP or salt/HFIP or TFE. In Figure 4-4, extraction of BSA as a hydrophilic protein and gramicidin D as a hydrophobic peptide are applied to SDS/HCl/HFIP, Aq(ammonium sulfate)/HFIP, and Aq(ammonium sulfate)/TFE systems. Lane 1 is SDS/HCl/HFIP/BSA extraction samples. BSA is supposed to have a band around 66kDa while in Lane 1 only bands at bottom of the gel are shown in Figure 4-4, which is not the correct position for BSA. It is possible that hydrolysis of amide bonds occurred in the presence of acid as catalyst for hydrolysis reaction. Lane 2 is SDS/HCl/HFIP/Gramicidin D extraction samples. Bands at the bottom of the gel could potentially be gramicidin D which is only 2kD. The ladder could not spread completely either because of the gel length or the high concentration of polyacrylamide which was 15% resolving gel. Lane 3 is ammonium sulfate-HFIP-BSA and Lane 4 is ammonium sulfate-TFE-BSA. Based on observation, $(\text{NH}_4)_2\text{SO}_4/\text{TFE}$ had smaller volume of bottom phase than $(\text{NH}_4)_2\text{SO}_4/\text{HFIP}$. According to gel information, BSA was highly

concentrated in the bottom phase of ammonium sulfate-TFE. So far, we know that SDS/HCl/HFIP extracts both hydrophilic protein and hydrophobic peptide, but we are not sure how much protein will be degraded under such extremely acidic surrounding. 2M $(\text{NH}_4)_2\text{SO}_4$ with 15% v/v HFIP and 2M $(\text{NH}_4)_2\text{SO}_4/15\%$ TFE are practical to extract hydrophilic protein such as BSA. Moreover, $(\text{NH}_4)_2\text{SO}_4/15\%$ TFE shows an extraordinary extracting and pre-concentrating ability comparing to all the others in Figure 4-4.

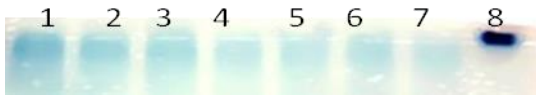


Figure 4-3A. DTAB-HFIP coacervate applied to DTAB-PAGE. DTAB-PAGE to show extraction of 2 μM BSA extraction in bottom phase of DTAB(42.5mM)-HFIP(15% v/v)-Tris(pH6.8, 0.2M) ATPS. Lane1: DTAB coac 1:2 dilution; Lane2: DTAB coac 1:3 dilution; Lane3: DTAB coac 1:4 dilution; Lane4-6(same): DTAB coac 1:5 dilution; Lane7: DTAB coac 1:6 dilution; Lane8: control BSA.

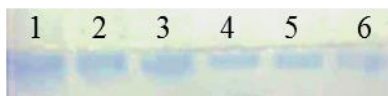


Figure 4-3B. CTAB-HFIP coacervate applied to DTAB-PAGE. DTAB-PAGE for 2 μM BSA extracted into bottom phase of CTAB (42.5mM)-HFIP(15% v/v)-Tris(pH6.8, 0.2M). Lane1: CTAB coac 1:2 dilution; Lane2: CTAB coac 1:3 dilution; Lane3: CTAB coac 1:4 dilution; Lane4: CTAB coac 1:5 dilution; Lane5: CTAB coac 1:6 dilution; Lane6: CTAB coac 1:7 dilution.

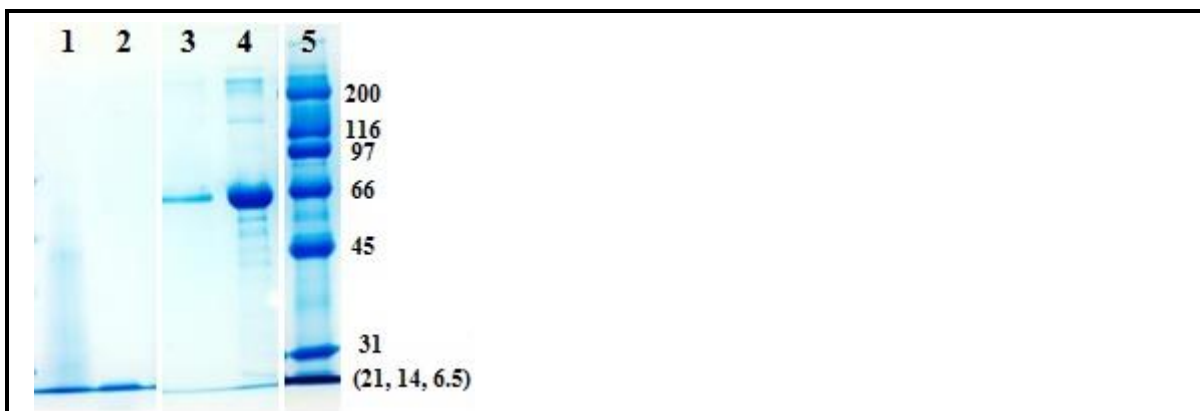


Figure 4-4. SDS-PAGE, extraction of BSA and gramicidin D in ATPSs SDS-HCl-HFIP, HFIP-(NH₄)₂SO₄, TFE-(NH₄)₂SO₄

Lane1: 132µg BSA extracted into 50mM SDS, 4M HCl, 15% HFIP coacervate,; Lane2: 0.5mg gramicidin D extracted 50mM SDS, 4M HCl, 15% HFIP coacervate,; Lane3: 132µg BSA extracted into Aq (2M (NH₄)₂SO₄) / 15% HFIP,; Lane4: 132µg BSA extracted 2M (NH₄)₂SO₄, 15% TFE; Lane5: standard ladder

The effect of HFIP on SDS-PAGE

Figure 4-5 shows the electropherograms for a mixtures of standard proteins with molecular masses of 10 kDa – 250 kDa (lanes 1-2) and BSA (lanes 3-4), where HFIP was added to the samples. The gel image indicates that HFIP doesn't show any effect on SDS gel. Complex coacervates cannot be introduced to SDS-PAGE directly as shown in Figure4-2. The precipitation of cationic complex composed of oppositely charged surfactants and interaction between HFIP and CTAB could cause problems when running gel. Complex coacervate phase itself is not completely miscible in SDS-PAGE buffer and would stay as a

separated viscous phase when loading onto lanes. How to avoid phase separation problem during gel running becomes the first challenge to resolve. Figure5 illustrates that HFIP itself doesn't have negative impact on SDS-PAGE running, which means the combination of HFIP and SDS is not the source of poor band shape problem with complex coacervate samples. Then the cause of broadened band can only be the presence of concentrated CTAB. However, it is not easy to completely remove CTAB from complex coacervates since the coacervate phase is highly viscous and the structure inside the phase is relatively stable. In order to lower the concentration of cationic surfactant, back extraction by 6M urea was applied as shown in Figure6. Meanwhile, the removal of HFIP was also performed to eliminate any potential interaction between HFIP with back extracted CTAB.

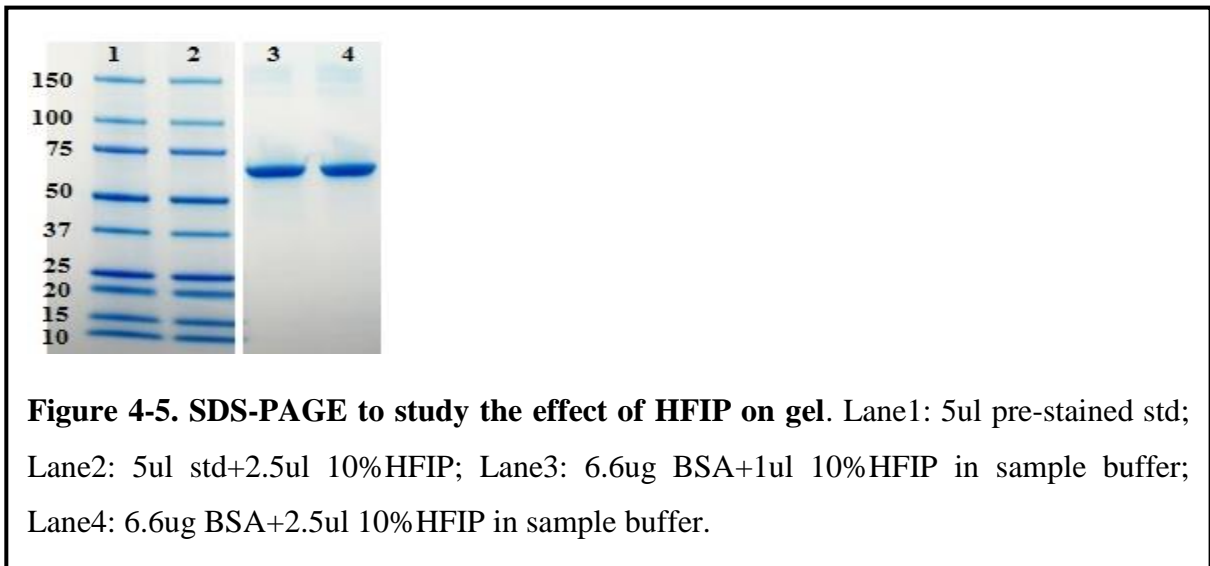
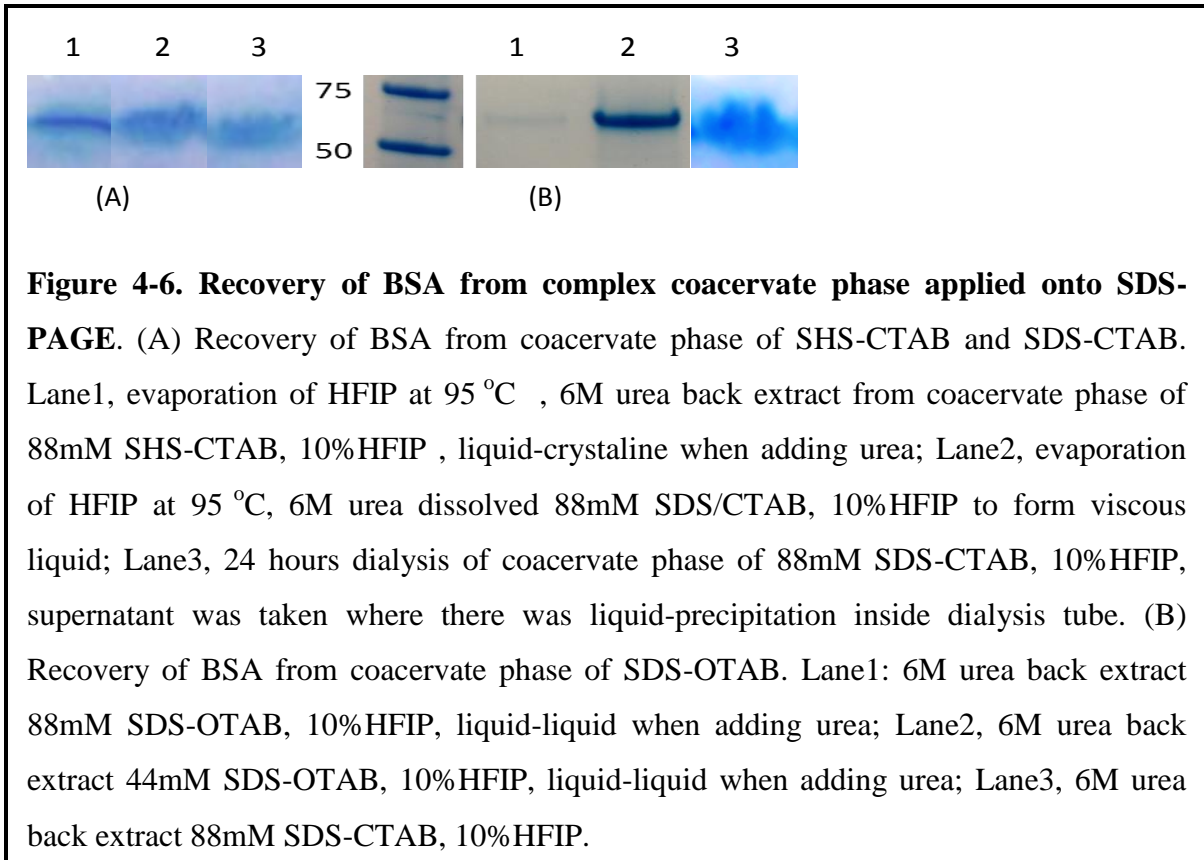


Figure 4-5. SDS-PAGE to study the effect of HFIP on gel. Lane1: 5ul pre-stained std; Lane2: 5ul std+2.5ul 10%HFIP; Lane3: 6.6ug BSA+1ul 10%HFIP in sample buffer; Lane4: 6.6ug BSA+2.5ul 10%HFIP in sample buffer.



As shown in Figure4-6A, SHS/CTAB and SDS/CTAB complex coacervates were compared under treatment of HFIP removal and urea back extraction. Lane1 shows a better band resolution than Lane2 indicating that SHS/CTAB had less CTAB back extracted to urea phase than SDS/CTAB. This may be related to different solubility of between SHS and SDS. SHS/CTAB formed precipitation while SDS/CTAB didn't with addition of urea. The precipitation may also trap CTAB which lowers the concentration of CTAB in urea phase. Lane2 and Lane3 implied little difference between evaporation and dialysis as the method to remove HFIP. Dialysis is a relatively slow process to remove surfactants from complex

coacervate. After 24 hours, there was still precipitation inside dialysis tube, showing that both concentrated SDS and CTAB were still there. In Figure 6-B, lane2 of 44mM SDS/OTAB has a more intense band between 50-75kDa for BSA than lane1 of 88mM SDS/OTAB. Comparing to 88mM SDS/OTAB, 44mM surfactants form smaller coacervate volume which may increase the interacting surface between protein and urea, to help extraction of BSA back to urea upper phase. OTAB is a C18 cationic surfactant which has higher molecular weight and lower Krafft temperature than CTAB. The results surprisingly show that BSA band is very clean and narrow. It looks like that OTAB was not extracted back to urea phase during back extraction. With two liquid phases existing during this process, the mass transfer was mainly about protein. However, it was not the same case for SDS-CTAB back extraction as shown in Figure 4-6B lane3. The band is smeared in lane 3 with poor resolution. It could possibly be caused by CTAB back extracted into urea. Coacervate phase of SDS/CTAB is less viscous than SDS/OTAB, giving a faster mass transfer speed between urea and coacervate phase than SDS/OTAB. Additionally, CTAB is lighter and smaller than OTAB thus easier to go to urea phase. It is also potentially caused by overloading of BSA due to a higher back extraction recovery from SDS/CTAB than SDS/OTAB. Nevertheless, the results provide information about recovery of protein from coacervate phase by back extraction and possibility to apply to gel electrophoresis. SDS/OTAB could potentially be a good system for back extraction like this. Moreover, it shows the evidence that urea as a powerful reagent to denature and solubilize proteins, can be applied as a new second phase to back extract BSA from protein enriched complex coacervate phase.

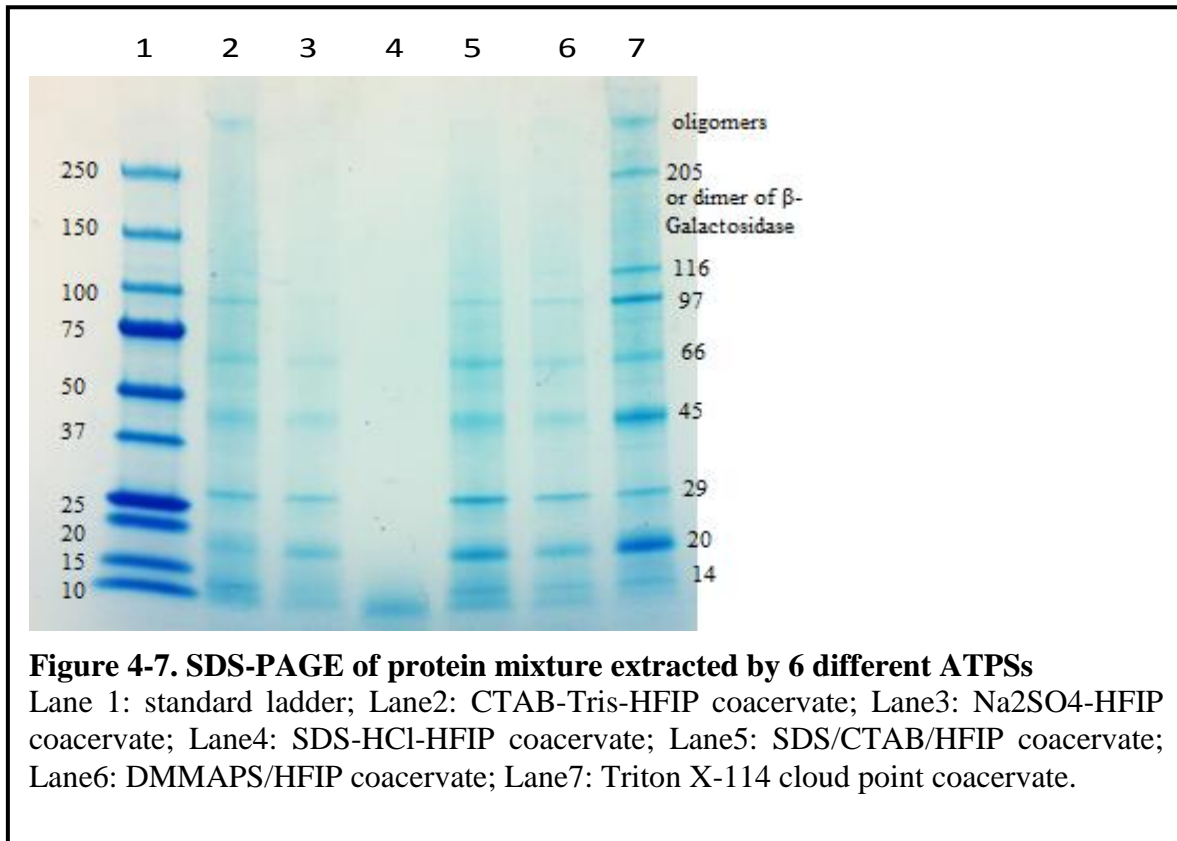
Extraction of protein mixtures in ATPSs followed by FASP clean-up method

The earlier results clearly showed that removal of surfactants from the coacervate phase is necessary prior to running gel electrophoresis. Filter Aided Sample Preparation (FASP) method was used to clean surfactant(s), perfluorinated alcohol and salt in complex and simple aqueous two phase systems. A mixture of sample proteins with different MW and pI was prepared and extracted into six different ATPS with different compositions. The ATPS consisted of four PFAIC systems, an Aq(salt)-HFIP biphasic system, and a CPS made of triton X-114. Following the extraction of the mixture, the surfactants in the coacervate phases were removed by FASP method, the remaining proteins on the filter were dissolved in tris buffer and were run on SDS-PAGE. Figure 4-7 illustrates the eletropherograms of extracted samples and the standard run in aqueous solution. The protein mixture consisted of A-Lactalbumin(Bovinemild) 14.2kDa (pI 4-5), Trypsin Inhibitor(Soybean) 20.1kDa(pI 4.6), Carbonic Anhydrase(Bovie) 29kDa(pI 6.18), Ovalbumin(egg) 45kDa (pI 4.99), Abumin(Bovine) 66kDa (pI 4.7), Phosphorylase(rabbitmuscle) 97.4kDa(pI 5.9), β -Galactosidase(E. coli.) 116kDa (pI 4.6), and Myosin(rabbit muscle) 205kDa (5.0-5.3).

As shown in Figure4-7, Lane7 Triton X-114 cloud point shows extraction of protein mixture with strong intensity of each of the bands comparing to others. However this is not contrast to Bordier's results[13] who reported that the triton phase only extracts membrane proteins and not soluble proteins. This may be because of the method used to induce phase separation was different from Bordier's which was modified by involving multiple extractions with sucrose cushion phase between aqueous phase and detergent phase. In our sample

preparation, one extraction was performed by increasing temperature to cloud point to enrich proteins in small volume detergent-rich phase[14][15]. This is also consistent with sample preparation methods for other ATPSs. Moreover, one more band shows at very top of lane7 with molecular weight higher than 250kDa which could be oligomer of the proteins. The band between 150 and 250 kDa on Lane7 may either be Myosin(205kDa) or dimer of β -Galactosidase(232kDa). ATPS such as CTAB/HFIP, SDS/CTAB/HFIP and DMMAPS/HFIP systems show almost all the proteins except Myosin (rabbit muscle, pI 5.0-5.3) at 205kDa. It seems that surfactants such as SDS, CTAB, and DMMAPS have some limitations in extraction of large proteins such as myosin comparing to nonionic surfactant triton X-114. This could possibly be related to phase viscosity which may limit mass transfer between two phases. There are also other factors such as hydrophobicity difference between two phases. Moreover, it is still unknown about the effect of HFIP in stabilizing the secondary structure that might impact the partitioning behavior in PFAIC systems. Na_2SO_4 /HFIP draws most of the proteins from 14kDa to 66kDa to bottom phase while poorly extracts proteins of large size above 100kDa. However, the bottom phase doesn't have structure like other coacervate phase which may result in different hydrophobicity or charge as a factor to effect extraction. An interesting result is lane4, SDS/HCl/HFIP which barely shows any protein bands from 14 to 200kDa but presents a thick band below 10kDa. The mixture did not include any small MW proteins or peptides under 10kDa. It confirms the assumption that hydrolysis of proteins may have occurred in extreme acidic environment due to the presence of 4M HCl. We are unable to identify the number of proteins that have been extracted into the coacervate phase of SDS/HCl/HFIP using the SDS-PAGE results. Mass spectrometry should be utilized to

identify the peptide fragments. Nevertheless, the results indicate that the FASP method works well in removing surfactant(s) from both complex and simple coacervates, making it practical to separate the mixture by gel electrophoresis.



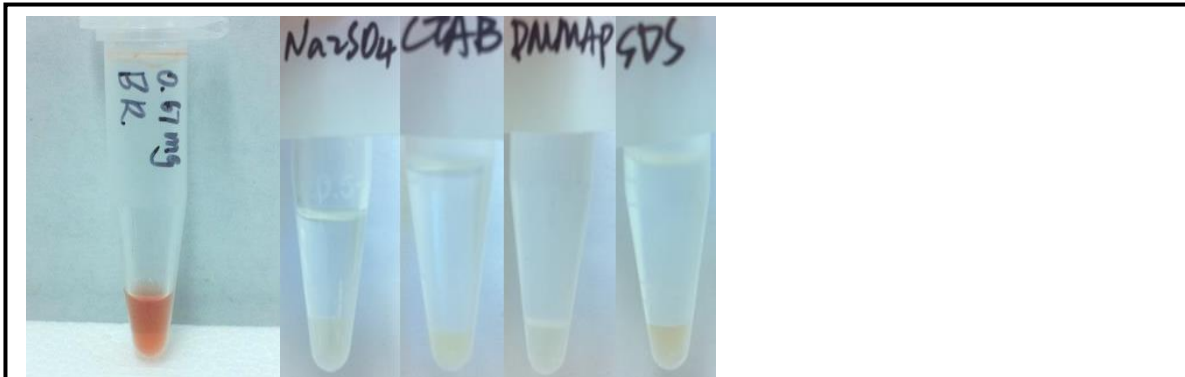
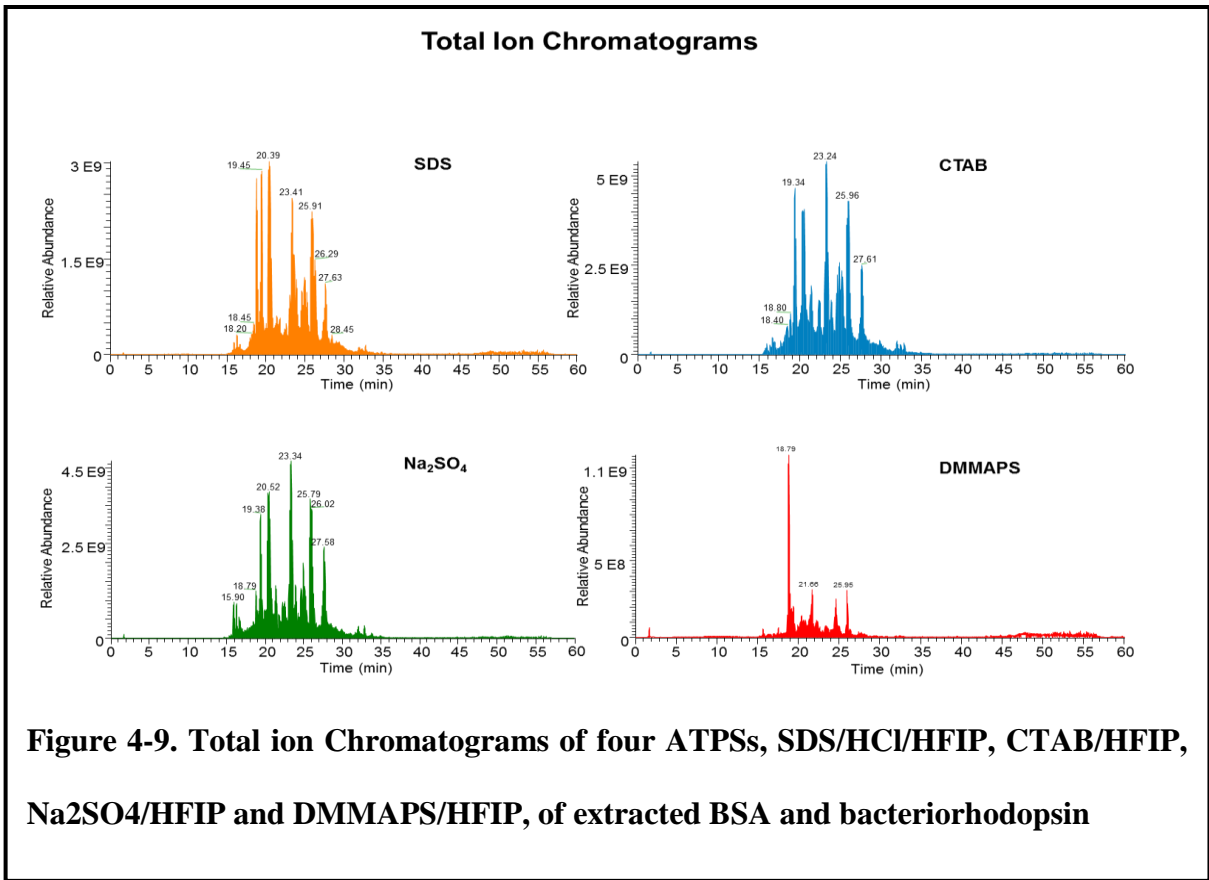


Figure 4-8. Sample images of extracted bacteriorhodopsin in HFIP and four ATPSs

Membrane protein extraction by ATPSs combined with nano LC-MS/MS detection

The surfactants in coacervates could also interfere with LC-MS that is commonly used for analysis and characterization of proteins. Based on the investigation of using FASP method to prepare clean surfactant-rich samples, identification of proteins extracted by ATPSs could be accomplished by mass spectrometry. First we extracted a mixture of 1.93 nmol of bacteriorhodopsin (BR) and 1 nmol Bovine Serum Albumin (BSA), a soluble protein into three different Simple-PFAIC systems with the following compositions: 50mM SDS/4M HCl/15% HFIP; 50mM CTAB/Tris (pH=6.8)/12.5 % HFIP, and 50mM DMMAAPS/6% TFE/1% HFIP.

The three systems contained representative anionic, cationic, and zwitterionic surfactants. The fourth system was made of aqueous kosmotropic salt and HFIP (0.4 M Na₂SO₄/15% HFIP) and was used as control to test the effectiveness of surfactant removal using FASP methodology. Following the extraction, the coacervate phases were separated from the top aqueous phase and were passed through a commercially available polycarbonate size exclusion filter which should retain the proteins mix on the top and passing through the smaller molecules (surfactants and buffers). The proteins were treated according to a protocol for bottom-up proteomic analysis (i.e. washed, reduced, denatured, alkylated, and digested by trypsin). The resultant tryptic peptides were dissolved in Tris buffer, separated, and then sequenced using nano LC-MS/MS. The total ion chromatograms (TIC) for the tryptic digest of the two protein mixture are shown in Fig4-9. As can be seen, the TIC for the three coacervates with different detergents were as clean as the Na₂SO₄ system that did not contain a detergent, which demonstrates the effectiveness of the FASP methodology for removal of surfactants (i.e., all signals were attributed to tryptic peptides of BR and BSA). The presence of detergents would result in loss of MS signal from the peptides and would dominate the TIC. An example of this from a different study where SDS was not removed prior to analysis is shown in Figure10. These experiments were performed in collaboration with Professor Muddiman's group at NCSU.



The clean Total Ion Chromatograms as shown in Figure 4-9 (as compared to Figure 4-10), show that there is no ion suppression due to surfactants. BSA and bacteriorhodopsin peptides were identified by Mascot search engine. BR was identified based on 3 tryptic peptides in MASCOT. The remaining 10 tryptic peptides have either ≤ 5 amino acids (AA) or ≥ 20 AA. MASCOT parameters included cleaving enzyme of trypsin, 5ppm peptide tolerance, 0.02Da fragment ion tolerance. Variable modifications included oxidation of methionine,

deamidation of glutamine and asparagine. Fixed modification was carbamidomethylation of cysteine.

The most abundant peaks identified for bacteriorhodopsin and bovine serum albumin were selected to compare the relative abundance in four ATPSs. For membrane protein bacteriorhodopsin, the peptide K.AESMRPEVASTFK.V with elution time between 18.79-18.80min has the highest abundance. For BSA, the peptide K.LVNELTEFAK.T eluted between 25.75-25.85 shows the strongest signal than other BSA peptides. The initial concentration ratio BR/BSA is 1.93/1. After extraction, the ratio of peak intensity of BR/BSA was different among four systems. As shown in Table4-1, the DMMAPS/HFIP coacervate shows peak intensity ratio of BR/BSA as high as 16.6 while CTAB/HFIP only has 0.09. It suggests that DMMAPS coacervate may have higher selectivity in bacteriorhodopsin than BSA. Based on different hydrophobicity/charge on different proteins, there may be different extracting efficiency and selectivity between ATPSs.

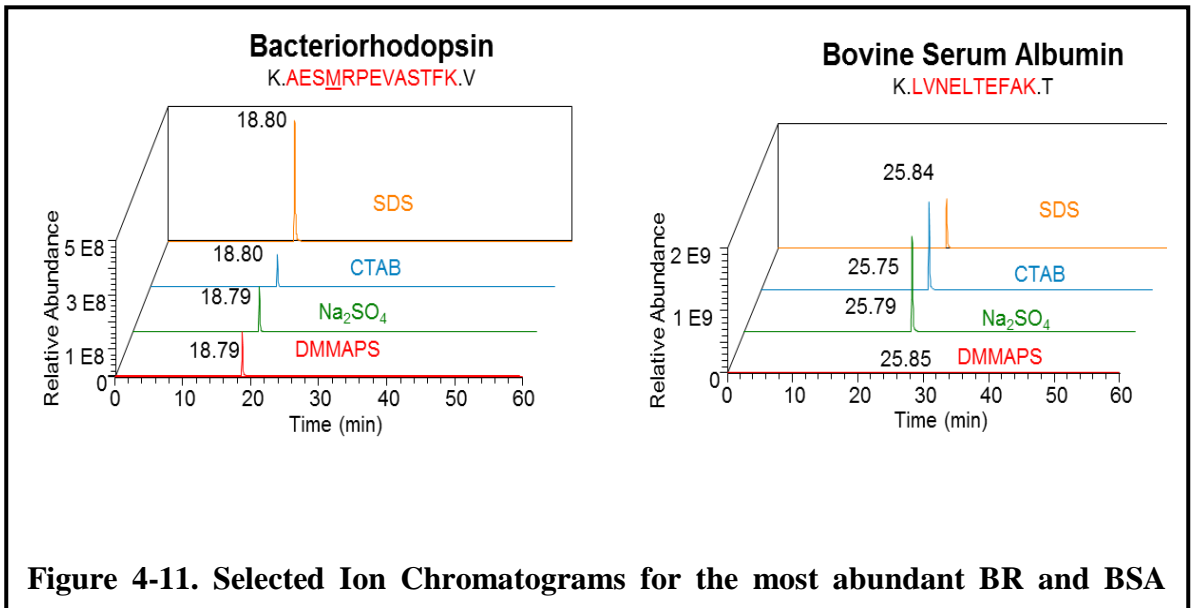
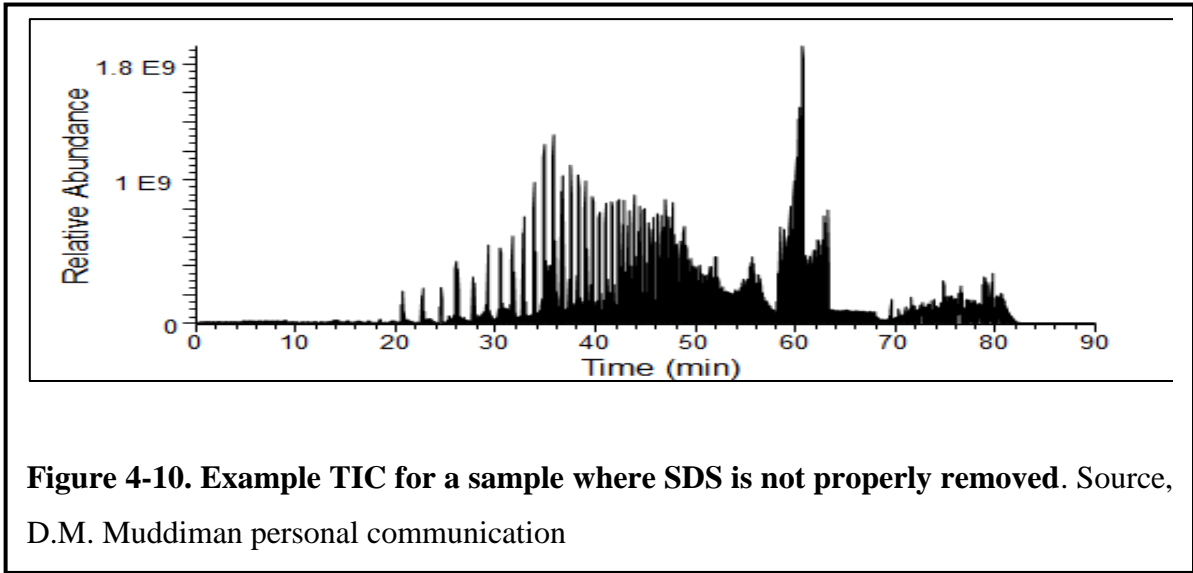


Table 4-1. Abundance ratio between bacteriorhodopsin and BSA calculated from the most abundant peptide peaks for each protein

	BR peak intensity ($\times 10^8$)	BSA peak intensity ($\times 10^8$)	Br/BSA Ratio
SDS	4.54	8.13	0.56
CTAB	1.21	14.2	0.09
Na ₂ SO ₄	1.69	15.3	0.11
DMMAPS	1.66	0.1	16.6

Note that the results presented here can only be interpreted to recognize the general trends and do not show the absolute quantities of the proteins in coacervate phases. This is because the variables during preparation for each of the ATPSs could be different and the amount of sample loss for each system is unknown as well. Moreover, the SDS/HCl/HFIP coacervate shows potential hydrolysis based on SDS-PAGE results in Figure 8. Once the protein is cleaved into small peptide fragments, during FASP clean-up process, those peptides would pass through the filter with washing buffer and be discarded. However, based on MS identified peptide fragments, the same selected ion for BSA were detected between SDS/HCl

coacervate and other ATPSs, suggesting the proteins digestion was done by trypsin instead of hydrolysis. Note that unlike the situation in Fig. 8 where the protein was exposed to strongly acidic condition for 24 hours, the sample preparation in this case done within an hour, so there was little time for hydrolysis during preparation. Moreover the peak intensity varies from different peptides identified in the same protein which suggests different amount of peptides lost during this process. The best way to solve the problem is to use an internal standard such as stable-isotope labeled peptides that would allow absolute quantitation of target proteins from the relative ratio between labeled and unlabeled peptide signals[16]. However, the relative ratio between two proteins in Fig. 4-9 and Table 4-1 still indicates differences in selectivity in partitioning of proteins in different ATPS. DMMAPS/HFIP potentially has higher selectivity for the hydrophobic proteins while CTAB/HFIP and salt/HFIP may attract more hydrophilic or charged proteins into the coacervate phase.

Conclusion

To solve the problems of incompatibility between composition of certain complex and simple PFAIC DTAB-PAGE could be used as an alternative of SDS-PAGE. Cationic surfactant gel works as a supplement to combine with extraction system of CTAB/HFIP or DTAB/HFIP, as well as the ones without anionic surfactant. Back extraction by urea from complex coacervate phase combined with precipitation of surfactants with high Krafft points, provide an alternative way to remove or reduce the amount of surfactants. Dialysis is not the best

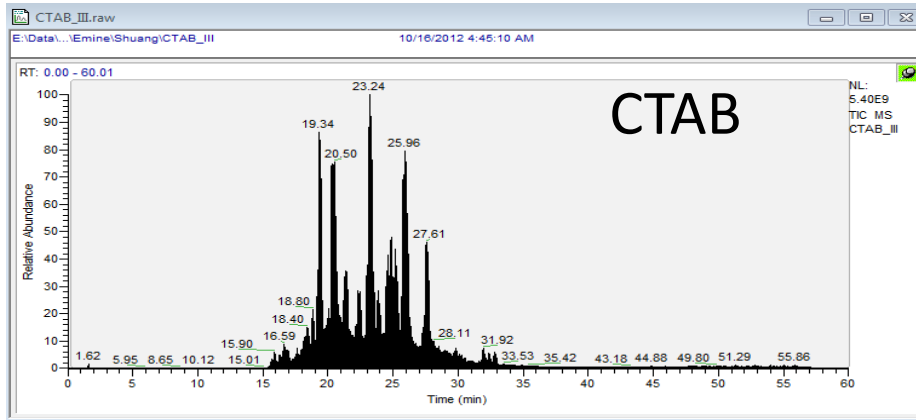
solution to remove both cationic and anionic surfactants from complex coacervate. FASP methods are demonstrated with the capability to clean any type of surfactant(s) from PFAIC. The PFAIC systems offer versatility and flexibility in selection and optimization of the phase chemical composition to enhance extraction selectivity and efficiency for a wide range of proteins.in application of protein identification and quantitation.

References

- [1] J. X. Xiao, U. Sivars, and F. Tjerneld, "Phase behavior and protein partitioning in aqueous two-phase systems of cationic–anionic surfactant mixtures," *J. Chromatogr. B. Biomed. Sci. App.*, vol. 743, no. 1, pp. 327–338, 2000.
- [2] R. Hatti-Kaul, "Aqueous two-phase systems. A general overview," *Mol. Biotechnol.*, vol. 19, no. 3, pp. 269–277, Nov. 2001.
- [3] J. A. Asenjo and B. A. Andrews, "Aqueous two-phase systems for protein separation: A perspective," *J. Chromatogr. A*, vol. 1218, no. 49, pp. 8826–8835, Dec. 2011.
- [4] J. A. Asenjo and B. A. Andrews, "Aqueous two-phase systems for protein separation: Phase separation and applications," *J. Chromatogr. A*, vol. 1238, pp. 1–10, May 2012.
- [5] J. R. Wiśniewski, A. Zougman, N. Nagaraj, and M. Mann, "Universal sample preparation method for proteome analysis," *Nat. Methods*, vol. 6, no. 5, pp. 359–362, Apr. 2009.
- [6] H. G. Bungenberg de Jong and H. R. Kruyt, "Coacervation (Partial Miscibility on Colloid Systems)," *Proc Koninkl Med Akad Wetershap*, vol. 32, pp. 849–856, 1929.
- [7] F. M. Menger, A. V. Peresyphkin, K. L. Caran, and R. P. Apkarian, "A Sponge Morphology in an Elementary Coacervate," *Langmuir*, vol. 16, no. 24, pp. 9113–9116, Nov. 2000.
- [8] W. L. Hinze and E. Pramauro, "A Critical Review of Surfactant-Mediated Phase Separations (Cloud-Point Extractions): Theory and Applications," *Crit. Rev. Anal. Chem.*, vol. 24, no. 2, pp. 133–177, Jan. 1993.

- [9] A. D. Diamond and J. T. Hsu, "Protein partitioning in PEG/dextran aqueous two-phase systems," *Aiche J.*, vol. 36, no. 7, pp. 1017–1024, Jul. 1990.
- [10] M. G. Khaledi, S. I. Jenkins, and S. Liang, "Perfluorinated Alcohols and Acids Induce Coacervation in Aqueous Solutions of Amphiphiles," *Langmuir*, vol. 29, no. 8, pp. 2458–2464, Feb. 2013.
- [11] R. J. Simpson, "CTAB-PAGE," *Cold Spring Harb. Protoc.*, vol. 2010, no. 4, p. pdb.prot5412–pdb.prot5412, Apr. 2010.
- [12] S. I. Jenkins, "Novel Aqueous Two-Phase Systems: Characterization and Applications in Chemical Separation," PhD Dissertation, North Carolina State University, 2011.
- [13] C. Bordier, "Phase separation of integral membrane proteins in Triton X-114 solution," *J. Biol. Chem.*, vol. 256, no. 4, pp. 1604–1607, Feb. 1981.
- [14] L. Koshy, A. H. Saiyad, and A. K. Rakshit, "The effects of various foreign substances on the cloud point of Triton X 100 and Triton X 114," *Colloid Polym. Sci.*, vol. 274, no. 6, pp. 582–587, Jun. 1996.
- [15] W. L. Hinze and E. Pramauro, "A Critical Review of Surfactant-Mediated Phase Separations (Cloud-Point Extractions): Theory and Applications," *Crit. Rev. Anal. Chem.*, vol. 24, no. 2, pp. 133–177, Jan. 1993.
- [16] D. R. Barnidge, G. D. Hall, J. L. Stocker, and D. C. Muddiman, "Evaluation of a cleavable stable isotope labeled synthetic peptide for absolute protein quantification using LC-MS/MS," *J. Proteome Res.*, vol. 3, no. 3, pp. 658–661, Jun. 2004.

Supplemental Data



Protein sequence coverage: 12%

Matched peptides shown in **bold red**.

```
1  MLELLPTAVE  GVSQAQITGR  PEWIWLALGT  ALMGLGTLYF  LVKGMGVSDP
51 DAKKFYAITT  LVPPIAFTMY  LSMLLGYGLT  MVPFGGEQNP  IYWARYADWL
101 FTTPLLLLDL  ALLVDADQGT  ILALVGADGI  MIGTGLVGAL  TKVYSYRFVW
151 WAISTAAMLY  ILYVLFFGFT  SKAESMRPEV ASTFKVLRNV  TVVLWSAYPV
201 VWLIGSEGAG  IVPLNIETLL  FMVLDVSAKV  GFGLILLRSR  AIFGEAEAPE
251 PSAGDAAAAT  SD
```

Unformatted sequence string: [262 residues](#) (for pasting into other applications).

Figure 4-12. Total Ion Chromatogram with bacteriorhodopsin identified in CTAB-HFIP extraction

Sequence Coverage for Br: 12%
 Matched peptides are shown in **bold red**
 Remaining tryptic fragments are highlighted in **blue**

1 MLELLPTAVE GVSQAQITGE PENIWLALGT ALMGLGTLYF LVR **GMGVSDP**
 51 **DAKK** FYAITT LVPPIAFTMY LSMLLGYGLT MVPFGGEQNP IYWAR **FADWL -**
 101 **FTTPLL**LLDL ALLVDADQGT ILALVGADGI NIGTGLVGLL TR **FYSYR** EVW -
 151 **MAI**STAAMLY ILYWLEFGFT **SR** **AESMRPEV** **ASTFK** **WLE**IV **TIW**LNSAYPV -
 201 **VMLIGSE**GAG IVPLNIETLL **FW**LDVSAK **V** **GFGLILLR** **SR** **RI**FGAEAPE -
 251 **PSAGDGA**AT **SD**

Figure 4-13. Matched peptides fragments of bacteriorhodopsin digested by trypsin identified.

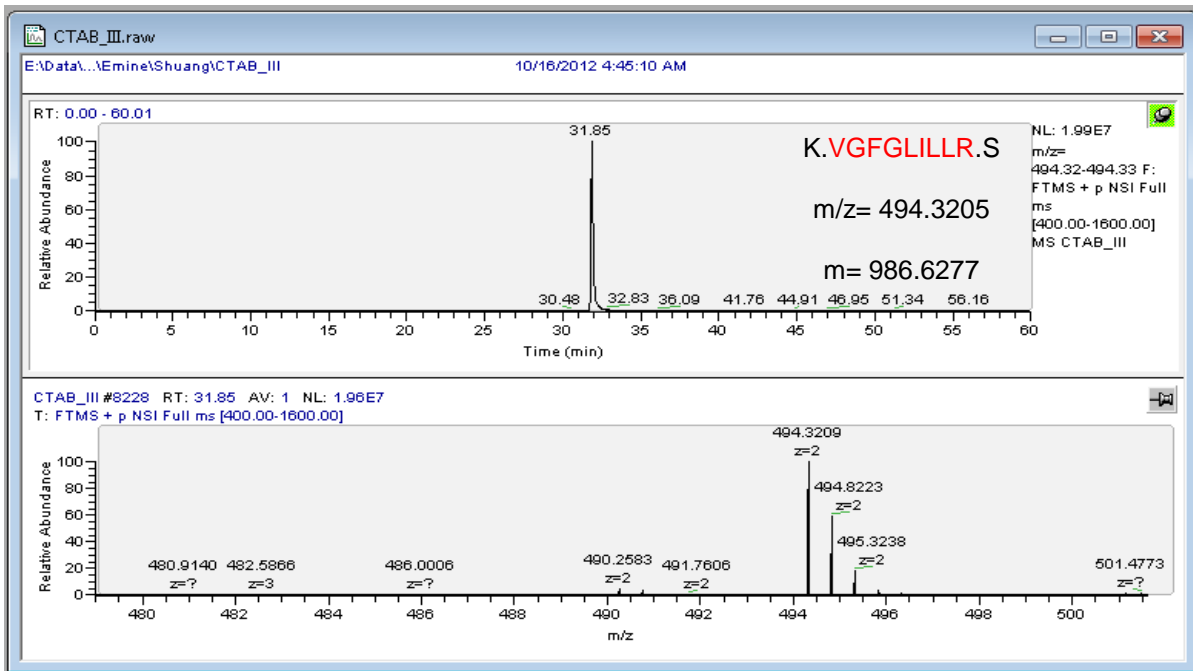


Figure 4-14. Extracted Ion Chromatograms and FTMS spectra for identified BR peptide1 K.VGFGILLR.S

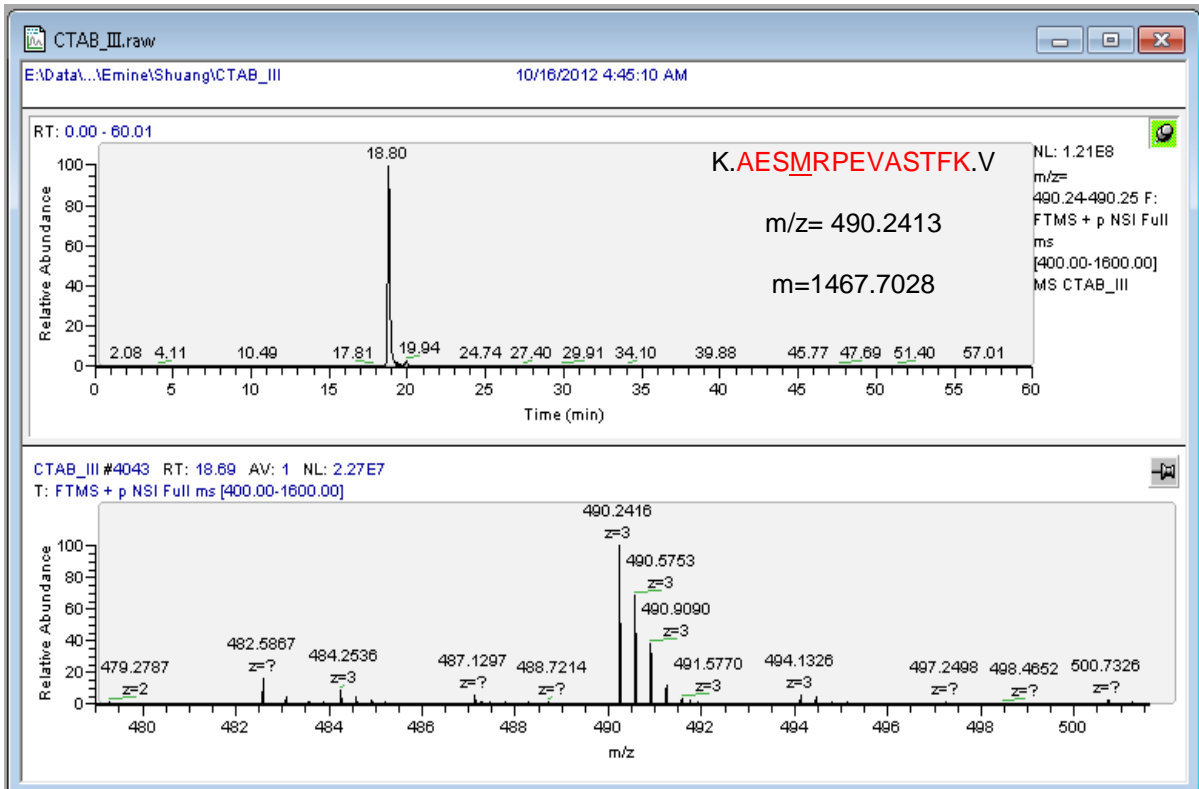


Figure 4-15. Extracted Ion Chromatograms and FTMS spectra for identified BR peptide2 K.AESMRPEVASTFK.V

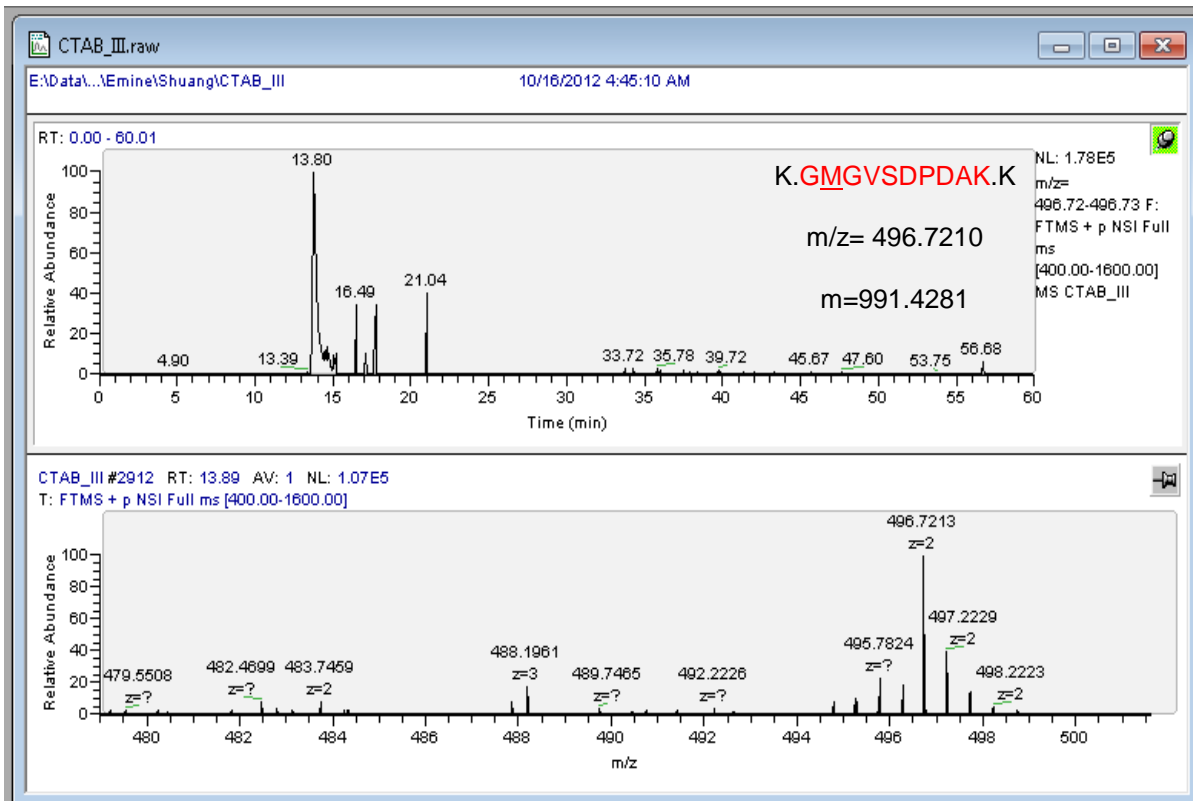


Figure 4-16. Extracted Ion Chromatograms and FTMS spectra for identified BR peptide3 K.GMGVSDPDAK.K